

Novel Low Cost Green Plug Smart Filter Soft Starter (GP-SF-SS) Schemes for Small Horse Power Motorized Loads

Adel M. Sharaf and Adel A.A. El-Gammal
Centre for Energy Studies, University of Trinidad and Tobago (UTT),
Wallerfield, Trinidad and Tobago

Abstract: The study presents a family of novel switched smart filter compensated devices using Green Plug Smart Filter Soft Starter (GP-SF-SS) devices for small single phase induction motors used in air-conditioning, ventilation and water pumping. GP-SF-SS devices are members of a family of smart switched filter capacitor compensation devices developed by Sharaf for energy conservation and enhanced utilization of cyclical and temporal type motorized loads. GP-SF-SS devices are equipped with a dynamic online error driven optimally tuned controller that ensures improved power factor, reduced feeder losses, stabilized voltage, minimal current ripples and efficient energy utilization/conservation with minimal impact on the host electric grid security and reliability. The proposed schemes can enhance the power quality; extend induction motor life span by reducing overheating due to inrush currents and harmonics. They prevent overheating and possible motor damage. The family of GP-SF-SS schemes is intended for use with residential/commercial motor drives used in water pumping, ventilation, air conditioning, compressors, refrigeration applications. The family of Green Energy devices and filters is based on concept of avoiding cyclical variations and transients in voltage and current to ensure uniform quasi steady state power and energy load demand.

Key words: Efficiency optimization, energy conservation, Single-Phase Induction Motors Drives (SPIMs), power quality, switched/modulated power filters, Multi Objective Optimization (MOO), Particle Swarm Optimization (PSO), Genetic Algorithm (GA)

INTRODUCTION

Small scale induction motors drives consume over 50% of the total electrical energy generated in the developed countries (Zahedi and Veaz-Zadeh, 2009). The electric utility industry and consumers of electrical energy around the world are facing new challenges for cutting electric energy cost, improving energy utilization, enhancing energy-efficiency, demand-side management, improving supply waveform-power quality, reducing safety hazards to personnel and protecting sensitive computer and automatic-data processing networks (Mademlis *et al.*, 2005; De Rossiter Correa *et al.*, 2004).

There is a mushrooming use of nonlinear electric loads especially in large motor drives arc furnaces and power electronic converter loads. All these nonlinear loads are byproduct of analog (saturation or limiter type) or digital (converter, solid state switching type) nonlinearities (Shenoy and Nirody, 2006; Neri *et al.*, 2005). Nonlinear type loads cause severe waveform distortion, power quality problems interference and extra feeder losses due to excessive inrush currents and severe voltage sags. The extended use of power electronic

switching converters and devices in motor drives, process-industries: Mining. Oil and Gas Industries and industrial DC and AC arc type furnaces have resulted in a polluted grid and unreliable radial distribution/utilization system with serious inherent voltage and power quality problems (Sharaf *et al.*, 1998, 2000). These non-linear type electric loads are used with ventilation, air conditioning, water pumping and low power factor industries such as sewing, printing, shear and press machinery and food processing plants.

These non-linear loads also fall in the category of inrush or arc type motorized loads and combined with fluorescent lighting can cause waveform distortion, harmonic interference and voltage flickering (Sharaf and Kreidi, 2002; Sharaf and Chalet, 1998). Generally, direct online motor starting is an economical method for starting induction motors. But direct starting will result in severe voltage sags and extra heating.

When starting large induction motors, excessive voltage dips result in overheating and loss of motor life expectancy (Sharaf and Aljankawey, 2006). In the study, a family of novel switched filter devices using Green Plug Smart Filter Soft Starter (GP-SF-SS) devices equipped with

a dynamic online error driven and optimally tuned controllers that can ensure improved power factor, reduced feeder losses, reduced voltage and current ripples, efficient energy utilization/conservation with minimal impact on the electric grid security and supply continuity for single phase induction motor loads. In this study, seven different control strategies were examined and validated, namely: self tuned conventional pid controller, self tuned modified pid controller-I, self tuned modified pid controller-II, self tuned variable structure sliding mode controller vsc/smc/b-b, self tuned zonal activation or target practice controller, self tuned tan-sigmoid incremental integral action controller and self tuned multi-stage incremental action controller.

The need for an on-line gains adaptation or self tunable control mechanism is highly needed in the control of any non-linear systems with un-modeled dynamics. Several AI-related soft computing techniques, such as Genetic Algorithms and Particle Swarm Optimization PSO are emerging as valuable, robust, simple and effective tools in industrial process automation and on-line control adaptation. GA is an iterative search algorithm based on natural selection and genetic search mechanism. However, GA is very fussy; it contains selection, copy, crossover and mutation scenarios and so on. Furthermore, the process of coding and decoding not only impacts its precision but also increases the complexity of the genetic algorithm.

However, Particle Swarm Optimization (PSO) is a novel emerging intelligence which was flexible optimization algorithm proposed in 1995. There are many common characteristics between PSO and GA. First, they are both flexible optimization technologies. Second, they all have strong universal property independent of any gradient information.

However, PSO is much simpler to implement than GA and its operation is more convenient, without selection, copy and crossover. The proposed tri-loop dynamic error driven self tuned controllers are also used to ensure energy efficiency, control loop decoupling, stability and system efficient utilization while maintaining full voltage stability capability. The study presents a novel application of both Multi Objective Particle Swarm Optimization MOPSO and Genetic search Algorithms MOGA optimization and search techniques for online tuning are used to optimally tune the gains of the different controllers.

The smart filter/energy conservation devices ensure for single phase induction motor loads: supply power quality PQ enhancement, enhanced electric energy efficiency, dynamic minimum current ripple tracking, dynamic minimum current level, dynamic minimum power

tracking, dynamic minimum effective power ripple tracking, dynamic minimum RMS source current tracking, dynamic maximum power factor, minimum harmonic ripple content, reduced harmonic ripple content, reduction of voltage sags conditions associated with induction motor starting and inrush currents, extended life span of the induction motor, reduced KWh consumption and electricity billing, minimized switching transients and load excursions, maximized power/energy utilization under unbalanced load conditions, Reduce THD, regulate voltage to be maintained at around 1pu.

MATERIALS AND METHODS

Genetic Algorithm (GA): Genetic algorithm is an optimization method inspired by Darwin's reproduction and survival of the fittest individual (Davis, 1991). This algorithm looks for the fittest individual from a set of candidate solutions called population. The population is exposed to crossover, mutation and selection operators to find the fittest individual. The fitness function assesses the quality of each individual in evaluation process. The selection operator ensures the fittest individuals for the next generation.

The crossover and mutation operators are used for variety of populations. Figure 1 shows the general flow chart of the GA algorithm based on total error iterative minimum search. The steps of genetic algorithm are depicted as follows:

Start: Generate random population of n chromosomes (suitable solutions for the problem).

Fitness: Evaluate the fitness $f(x)$ of each chromosome x in the population.

New population: Create a new population by repeating following steps until the new population is complete:

- Selection: Select two parent chromosomes from a population according to their fitness (the better fitness, the bigger chance to be selected)
- Crossover: With a crossover probability cross over the parents to form a new offspring (children). If no crossover was performed, offspring is an exact copy of parents
- Mutation: With a mutation probability mutate new offspring at each locus (position in chromosome)
- Accepting: Place new offspring in a new population

Replace: Use new generated population for a further run of algorithm.

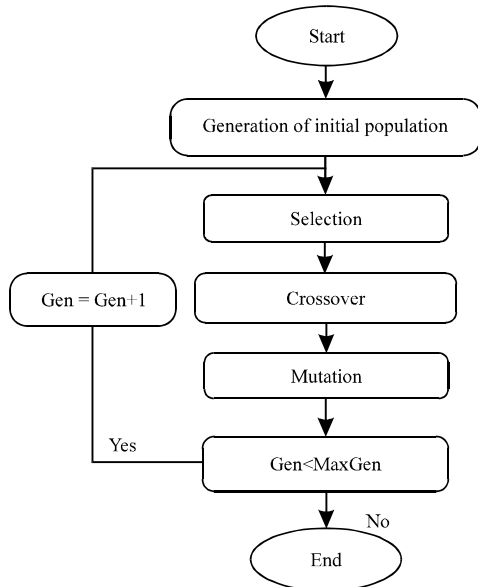


Fig. 1: Flow chart for the GA minimizing search algorithm

Test: If the end condition is satisfied, stop and return the best solution in current population.

Loop: Go to step 2.

Particle swarm optimization: Particle Swarm Optimization (PSO) is an evolutionary computation optimization technique (a search method based on a natural system) developed by Kennedy and Eberhart (1995) and Shi and Eberhart (1999).

The system initially has a population of random selective solutions. Each potential solution is called a particle. Each particle is given a random velocity and is flown through the problem space. The particles have memory and each particle keeps track of its previous best position (called the P_{best}) and its corresponding fitness. There exist a number of P_{best} for the respective particles in the swarm and the particle with greatest fitness is called the global best (G_{best}) of the swarm. The basic concept of the PSO technique lies in accelerating each particle towards its P_{best} and G_{best} locations with a random weighted acceleration at each time step. The main steps in the particle swarm optimization algorithm and selection process are described as follows:

- Step 1: Initialize a population of particles with random positions and velocities in d dimensions of the problem space and fly them
- Step 2: Evaluate the fitness of each particle in the swarm

- Step 3: For every iteration, compare each particle's fitness with its previous best fitness (P_{best}) obtained. If the current value is better than P_{best} , then set P_{best} equal to the current value and the P_{best} location equal to the current location in the d-dimensional space
- Step 4: Compare P_{best} of particles with each other and update the swarm global best location with the greatest fitness (G_{best})
- Step 5: Change the velocity and position of the particle

According to Eq. 1 and 2, respectively

$$V_{id} = \omega \times V_{id} + C_1 \times \text{rand}_1 \times (P_{id} - X_{id}) + C_2 \times \text{rand}_2 \times (P_{gd} - X_{id}) \quad (1)$$

$$X_{id} = X_{id} + V_{id} \quad (2)$$

Where V_{id} and X_{id} represent the velocity and position of the i th particle with d dimensions, respectively. rand_1 and rand_2 are two uniform random functions and ω is the inertia weight which is chosen beforehand.

- Repeat steps 2-5 until convergence is reached based on some desired single or multiple criteria

The PSO optimization search utilized dynamic total error minimization algorithm has many key parameters and these are described as follows: ω is called the inertia weight that controls the exploration and exploitation of the search space because it dynamically adjusts velocity. V_{max} is the maximum allowable velocity for the particles (i.e., in the case where the velocity of the particle exceeds V_{max} then it is limited to V_{max}). Thus, resolution and fitness of search depends on V_{max} . If V_{max} is too high then particles will move beyond a good solution. If V_{max} is too low, particles will be trapped in local minima. The constants C_1 and C_2 in Eq. 1 and 2, termed as cognition and social components, respectively. These are the acceleration constants which changes the velocity of a particle towards P_{best} and G_{best} (generally, somewhere between P_{best} and G_{best}). Figure 2 shows the general flow chart of the PSO algorithm based on total error iterative minimum search. The most striking difference between PSO and the other evolutionary algorithms is that PSO chooses the path of cooperation over competition.

The other optimization algorithms commonly use some form of decimation, survival of the fittest. In contrast, the PSO population is stable and individuals are not destroyed or recreated. Individuals are influenced by the best performance of their neighbors. Individuals eventually converge on optimal points in the problem domain. In addition, the PSO traditionally does not have genetic operators like crossover between individuals and

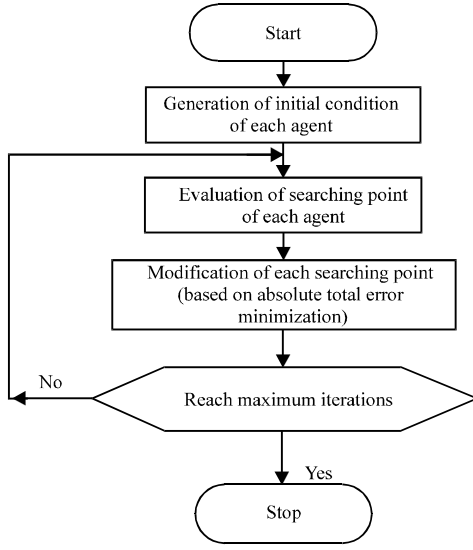


Fig. 2: Flow chart for the PSO minimizing search algorithm

mutation and other individuals never substitute particles during the run. So, in PSO all the particles tend to converge to the best solution quickly, comparing with GA.

Multi objective optimization: The following definitions are used in the proposed Multi Objective Optimization (MOO) search algorithm (Ngatchou *et al.*, 2005; Berizzi *et al.*, 2001; Coello and Lechuga, 2002).

Definition 1: The general MO problem requiring the optimization of N objectives may be formulated as follows:

$$\vec{y} = \vec{F}(\vec{x}) = [f_1(\vec{x}), f_2(\vec{x}), f_3(\vec{x}), \dots, f_N(\vec{x})]^T \quad (3)$$

$$\text{subject to } g_j(\vec{x}) \leq 0 \quad j=1, 2, \dots, M \quad (4)$$

$$\vec{x} = [\vec{x}_1, \vec{x}_2, \dots, \vec{x}_p]^T \in \Omega \quad (5)$$

Where:

\vec{y} = The objective vector

$g_j(\vec{x})$ = Represents the constraints

\vec{x} = P-dimensional vector representing the decision variables within a parameter space Ω

The space spanned by the objective vectors is called the objective space. The subspace of the objective vectors satisfying the constraints is called the feasible space.

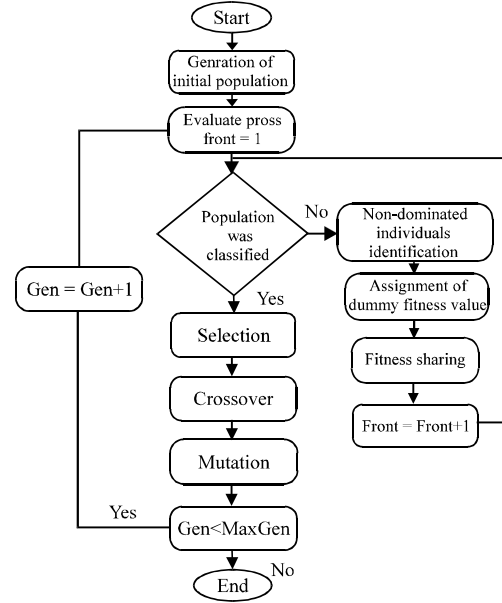


Fig. 3: Flow chart of NSGA

Definition 2: A decision vector $\vec{x}_1 \in \Omega$ is said to dominate the decision vector $\vec{x}_2 \in \Omega$ (denoted by $\vec{x}_1 \prec \vec{x}_2$, if the decision vector \vec{x}_1 is not worse than \vec{x}_2 in all objectives and strictly better than \vec{x}_2 in at least one objective.

Definition 3: A decision vector $\vec{x}_1 \in \Omega$ is called Pareto-optimal, if there does not exist another $\vec{x}_2 \in \Omega$ that dominates it. An objective vector is called Pareto-optimal, if the corresponding decision vector is Pareto-optimal.

Definition 4: The non-dominated set of the entire feasible search space Ω is the Pareto-optimal set. The Pareto-optimal set in the objective space is called Pareto-optimal front.

Multi-objective genetic algorithm: The Non-dominated Sorting Genetic Algorithm (NSGA) is a multi-objective genetic algorithm that was developed by Deb *et al.* (2002). This algorithm has been chosen over a conventional genetic algorithm for three principal reasons: no need to specify a sharing parameter, a strong tendency to find a diverse set of solutions along the Pareto optimal front and the ability to specify multiple objectives without the need to combine them using a weighted sum. The basic idea behind NSGA is the ranking process executed before the selection operation, as shown in Fig. 3. This process identifies non dominated solutions in the population, at each generation to form non dominated fronts (Srinivas and Deb, 1994), after this the selection, crossover and mutation usual operators are performed. In the ranking

procedure, the non dominated individuals in the current population are first identified. Then, these individuals are assumed to constitute the first non dominated front with a large dummy fitness value (Srinivas and Deb, 1994).

The same fitness value is assigned to all of them. In order to maintain diversity in the population, a sharing method is then applied. Afterwards, the individuals of the first front are ignored temporarily and the rest of population is processed in the same way to identify individuals for the second non dominated front.

A dummy fitness value that is kept smaller than the minimum shared dummy fitness of the previous front is assigned to all individuals belonging to the new front. This process continues until the whole population is classified into non dominated fronts. Since the non dominated fronts are defined, the population is then reproduced according to the dummy fitness values.

Multi-objective particle swarm optimization: In MOPSO (Ngatchou *et al.*, 2005; Berizzi *et al.*, 2001; Coello and Lechuga, 2002), a set of particles are initialized in the decision space at random. For each particle i , a position x_i in the decision space and a velocity v_i are assigned. The particles change their positions and move towards the so far best-found solutions.

The non-dominated solutions from the last generations are kept in the archive. The archive is an external population in which the so far found non-dominated solutions are kept. Moving towards the optima is done in the calculations of the velocities as follows:

$$V_{id} = \omega \times V_{id} + C_1 \times \text{rand}_1 \times (P_{pd} - X_{id}) + C_2 \times \text{rand}_2 \times (P_{rd} - X_{id}) \quad (6)$$

Where:

- $P_{r,d}, P_{p,d}$ = Randomly chosen from a single global Pareto archive
- ω = Inertia factor influencing the local and global abilities of the algorithm
- $V_{i,d}$ = The velocity of the particle i in the d th dimension
- c_1 and c_2 = Weights affecting the cognitive and social factors, respectively
- r_1 and r_2 = Uniform random functions in the range (Zahedi and Veaz-Zadeh, 2009)

According to Eq. 6, each particle has to change its position $X_{i,d}$ towards the position of the two guides $P_{r,d}, P_{p,d}$ which must be selected from the updated set of non-dominated solutions stored in the archive. The particles change their positions during generations until a termination criterion is met. Finding a relatively large set

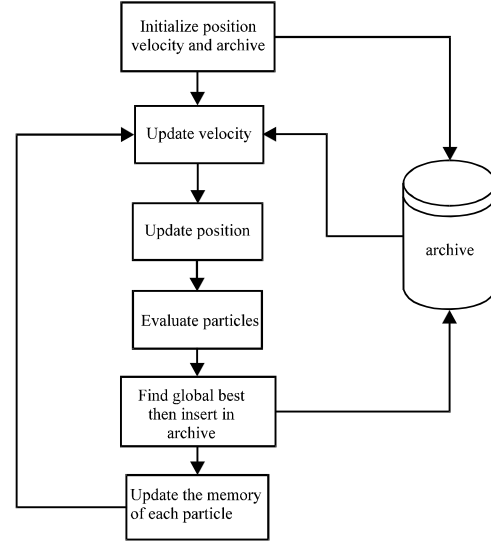


Fig. 4: Flow chart of the MOPSO optimization search algorithm

of Pareto-optimal trade-off solutions is possible by running the MOPSO for many generations. Figure 4 shows the flow chart of the Multi-Objective Particle Swarm Optimization MOPSO.

RESULTS AND DISCUSSION

PSO and other Evolutionary Computation (EC) techniques: A comparison between conventional optimization techniques and evolutionary algorithms (like genetic algorithm and PSO) is shown in Table 1 (Poirier *et al.*, 2001). The most striking difference between PSO and the other evolutionary algorithms is that PSO chooses the path of co-operation over competition.

The other algorithms commonly use some form of decimation, survival of the fittest. In contrast, the PSO population is stable and individuals are not destroyed or created. Individuals are influenced by the best performance of their neighbors. Individuals eventually converge on optimal points in the problem domain. In addition, the PSO traditionally does not have genetic operators like crossover between individuals and mutation and other individuals never substitute particles during the run. Instead the PSO refines its search by attracting the particles to positions with good solutions. Moreover, compared with genetic algorithms (GAs), the information sharing mechanism in PSO is significantly different. In GAs, chromosomes share information with each other. So the whole population moves like a one group towards an optimal area. In PSO, only Gbest (or Pbest) gives out the information to others. It is a one-way information sharing mechanism. The evolution only looks

Table 1: comparison between conventional optimization procedures and evolutionary algorithms

| Property | Evolutionary | Traditional |
|------------------|---|--|
| Search space | Population of potential solutions | Trajectory by a single point |
| Motivation | Natural selection and social adaptation | Mathematical properties (gradient, Hessian) |
| Applicability | Domain independent, applicable to variety of problems | Applicable to a specific problem domain |
| Point transition | Probabilistic | Deterministic |
| Prerequisites | An objective function to be optimised | Auxiliary knowledge such as gradient vectors |
| Initial guess | Automatically generated by the algorithm | Provided by user |
| Flow of control | Mostly parallel | Mostly serial |
| CPU time | Large | Small |
| Results | Global optimum more probable | Local optimum, dependant of initial guess |
| Advantages | Global search, parallel, speed | Convergence proof |
| Drawbacks | No general formal convergence proof | Locality, computational cost |

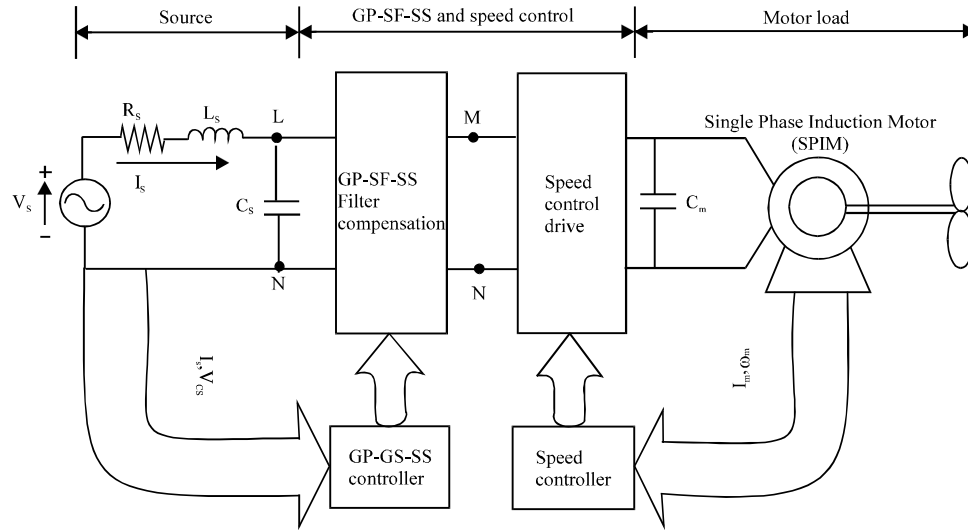


Fig. 5: The proposed Green Plug-Smart Filter-Soft Starter (GP-SF-SS) for Single Phase Induction Motor (SPIM) drive system

for the best solution. In PSO all the particles tend to converge to the best solution quickly, comparing with GA, even in the local version in most cases.

Sample study motorized system: Figure 5 shows the block diagram of the utilization Single-phase Induction Motor (SPIM) and the connection of the Green Plug-Smart Filter-Soft Starter (GP-SF-SS) and the speed control drive system to the SPIM load. Figure 6 and 7 show the proposed tri-loop dynamic tracking controller to ensure both objectives of (energy/power) saving as well as power quality enhancement of the supply system current and load bus voltage.

The novel PSO and GA self tuned multi regulators and coordinated controller are used for the following purposes: Green Plug Filter Compensator GPFC-SPWM regulator for pulse width switching scheme to regulate the DC bus voltage and minimize inrush current transients and load excursions and the SPIM drive with the speed

regulator that ensure speed reference tracking with minimum inrush conditions and ensure reduced voltage transients and improved energy utilization. Figure 8 and 15 show the proposed family of Green Plug-Smart Filter-Soft Starter (GP-SF-SS) schemes.

Figure 8 shows a hybrid series, parallel filter compensator scheme acting as a series/parallel capacitor and or parallel tuned arm filter. Figure 9 shows a switched capacitor compensator scheme with combined parallel tuned arm filter.

Figure 10 shows a hybrid switched series/parallel capacitor compensation scheme which acts with AC source and SPIM inductances as a blocking tuned arm filter. Figure 11 shows a combined capacitor compensator or tuned arm filter.

Figure 12 shows a switched series and/or parallel capacitor compensator for series compensation and power factor correction. Figure 13 shows a switched doubly tuned arm filter at two separate tuned frequencies. Figure

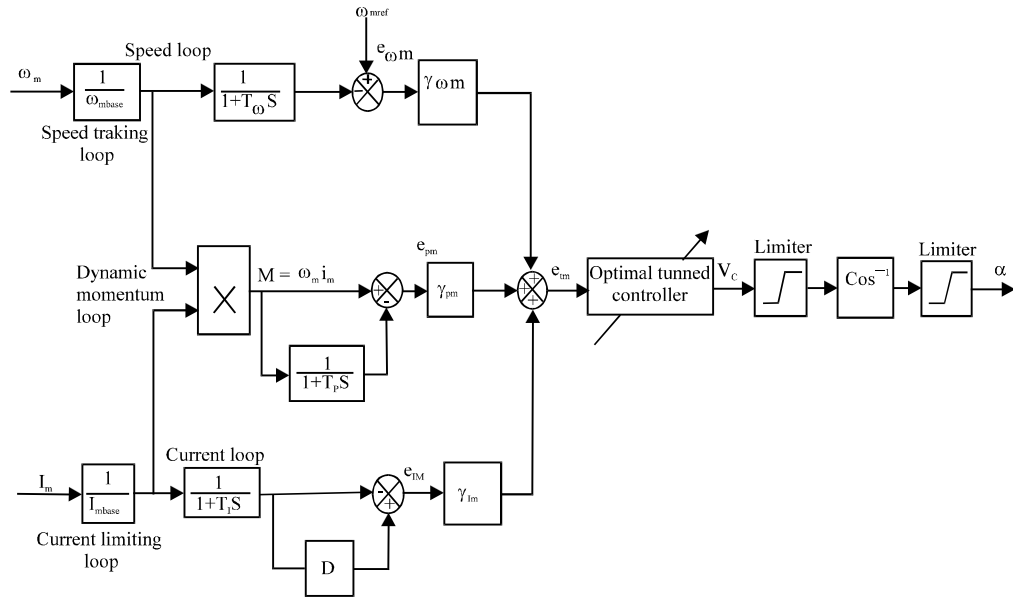


Fig. 6: Tri-loop error driven self regulating dynamic controller for control of Single Phase Induction Motor (SPIM) drive

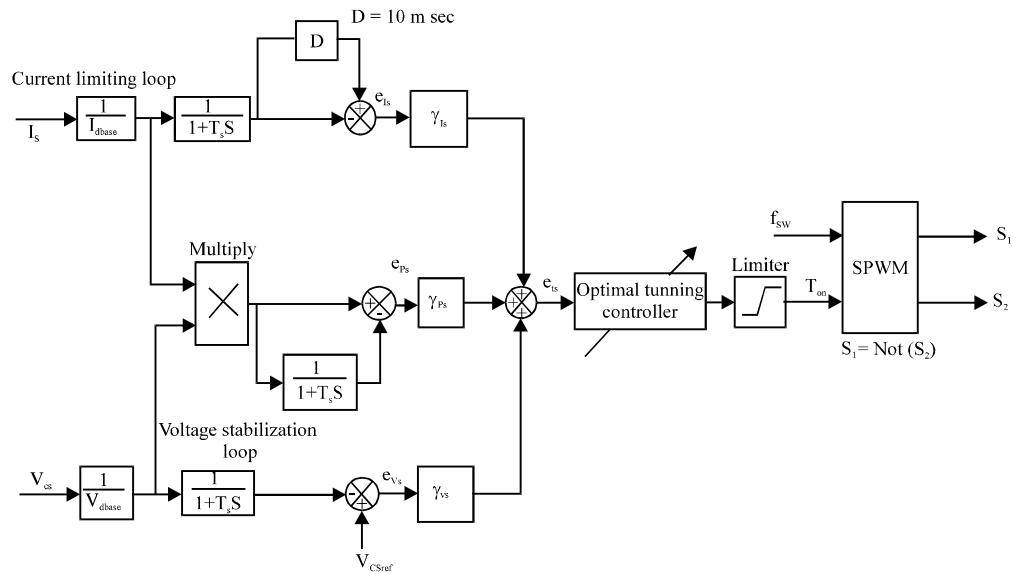


Fig. 7: Tri-loop error driven self regulating dynamic controller for the Green Plug-Smart Filter-Soft Starter (GP-SF-SS) scheme

14 shows a switched tuned arm filter using a low cost triac. Finally, Fig. 15 shows a switched C-type damped power filter capable of providing a low impedance path to all harmonics. It can utilize a triac or a fast MOSFET switch in slow and fast dynamic loads.

All filters objectives can be either: harmonic reduction and Power Quality (PQ) enhancement or electric power/energy savings and dynamic reactive

compensation for the single phase induction motor loads. The proposed utilization scheme is fully validated using the Matlab/Simulink software environment under normal conditions, load excursion, SPIM motor torque changes to assess the control system robustness, effective energy utilization and speed reference tracking. The common concerns of power quality are the long duration voltage variations (overvoltage, under-voltage and sustained

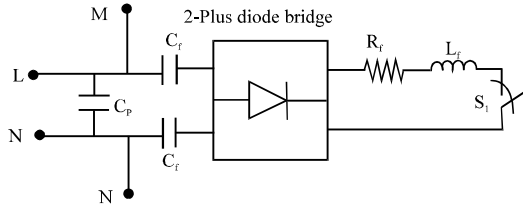


Fig. 8: Economic tuned-arm power filter and capacitor compensator scheme-A

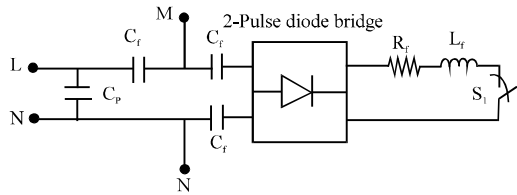


Fig. 9: Low cost tuned-arm power filter/capacitor compensator scheme-B

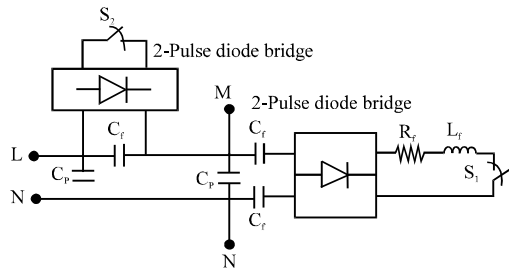


Fig. 10: Low cost tuned-arm power filter and capacitor compensation scheme-C

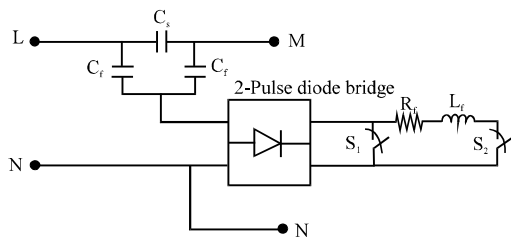


Fig. 11: Low cost tuned-arm power filter/capacitor compensator scheme-D

interruptions), short duration voltage variations (interruption, sags and swells), voltage imbalance (voltage unbalance), waveform distortion (DC offset, harmonics, inter-harmonics, notching and noise), voltage fluctuation (voltage flicker) and power frequency variations. To prevent the undesirable states and to reduce the power consumption, a GPF scheme is used to stabilize system.

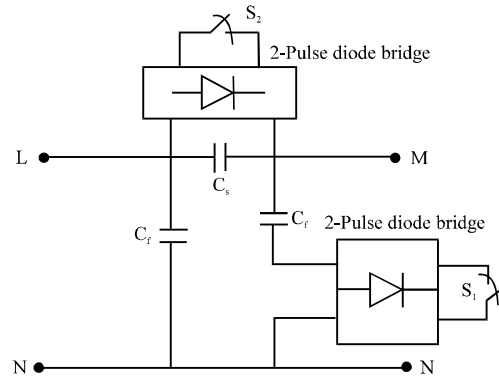


Fig. 12: Switched series parallel capacitor compensator scheme-E

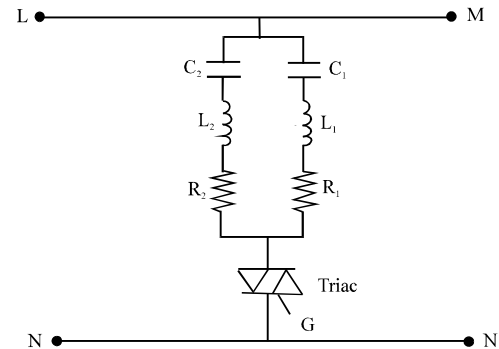


Fig. 13: Dual-tuned-arm filter compensator scheme-F

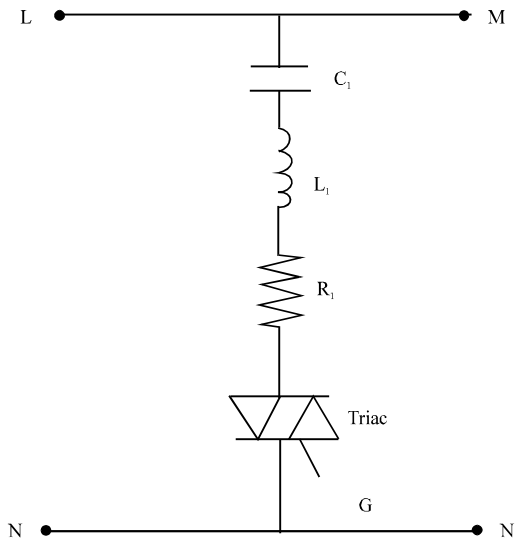


Fig. 14: Low cost Tuned-Arm Power Filter (TAF) compensator scheme-G

Dynamic error driven control: The proposed control system comprises two sub-regulators or controllers

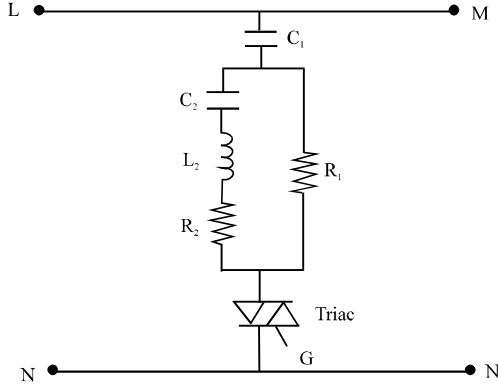


Fig. 15: Low cost switched C-type power filter compensator scheme-H

named as DC side Green Plug Filter Compensator GPFC-SPWM regulator and the SPIM drive speed controller. Figure 6 and 7 depict the proposed multi-loop dynamic self regulating controllers based on multi objective optimization search and optimization technique based on soft computing PSO and GA.

The global error is the summation of the three loop individual errors including voltage stability, current limiting and synthesize dynamic power loops. Each multi loop dynamic control scheme is used to reduce a global error based on a tri-loop dynamic error summation signal and to mainly track a given speed reference trajectory loop error in addition to other supplementary motor current limiting and dynamic power loops are used as auxiliary loops to generate a dynamic global total error signal that consists of not only the main loop speed error but also the current ripple, over current limit and dynamic over load power conditions.

The global error signal is input to the self tuned controllers shown in Fig 6. The (per-unit) three dimensional-error vector (e_{vs} , e_{is} , e_{ps}) of the electric source controller scheme is governed by the following equations:

$$e_{vs}(k) = V_s(k) \left(\frac{1}{1+ST_s} \right) \left(\frac{1}{1+SD} \right) - V_s(k) \left(\frac{1}{1+ST_s} \right) \quad (7)$$

$$e_{is}(k) = I_s(k) \left(\frac{1}{1+ST_s} \right) \left(\frac{1}{1+SD} \right) - I_s(k) \left(\frac{1}{1+ST_s} \right) \quad (8)$$

$$e_{ps}(k) = I_s(k) \times V_s(k) \left(\frac{1}{1+ST_s} \right) \left(\frac{1}{1+SD} \right) - I_s(k) \times V_s(k) \left(\frac{1}{1+ST_g} \right) \quad (9)$$

The total or global error $e_{is}(k)$ for the GP-SF-SS side scheme at a time instant:

$$e_{is}(k) = \gamma_{vs} e_{vs}(k) + \gamma_{is} e_{is}(k) + \gamma_{ps} e_{ps}(k) \quad (10)$$

In the same manner, the (per-unit) three dimensional-error vector (e_{ω_m} , e_{im} , e_{pm}) of the SPIM motor scheme is governed by the following equations:

$$e_{\omega_m}(k) = \omega_m(k) \left(\frac{1}{1+ST_m} \right) \left(\frac{1}{1+SD} \right) - \omega_m(k) \left(\frac{1}{1+ST_m} \right) \quad (11)$$

$$e_{im}(k) = I_m(k) \left(\frac{1}{1+ST_m} \right) \left(\frac{1}{1+SD} \right) - I_m(k) \left(\frac{1}{1+ST_m} \right) \quad (12)$$

$$e_{pm}(k) = I_m(k) \times \omega_m(k) \left(\frac{1}{1+ST_m} \right) \left(\frac{1}{1+SD} \right) - I_m(k) \times \omega_m(k) \left(\frac{1}{1+ST_m} \right) \quad (13)$$

And the total or global error $e_{tm}(k)$ for the MPFC scheme at a time instant:

$$e_{tm}(k) = \gamma_{\omega_m} e_{\omega_m}(k) + \gamma_{im} e_{im}(k) + \gamma_{pm} e_{pm}(k) \quad (14)$$

A number of conflicting objective functions are selected to optimize using the PSO algorithm. These functions are defined by the following:

- J1 = Minimize the Total Harmonic Distortion of the load current (THDi)
- J2 = Minimize the Total Harmonic Distortion of the load Voltage (THDv)
- J3 = Maximize the electric energy efficiency
- J4 = Maximize the power factor
- J5 = Minimize the KWh consumption

In general, to solve this complex optimality search problem, there are two possible optimization techniques based on Particle Swarm Optimization (PSO): Single aggregate selected Objective Optimization (SOO) which is explained and Multi Objective Optimization (MOO). The main procedure of the SOO is based on selecting a single

aggregate objective function with weighted single objective parameters scaled by a number of weighting factors. The objective function is optimized (either minimized or maximized) using either Genetic Algorithm (GA) or Particle Swarm Optimization search algorithm (PSO) methods to obtain a single global or near optimal solution. On the other hand, the main objective of the Multi Objective (MO) problem is finding the set of acceptable (trade-off) optimal solutions. This set of accepted solutions is called Pareto front.

These acceptable trade-off multi level solutions give more ability to the user to make an informed decision by seeing a wide range of near optimal selected solutions that are feasible and acceptable from an overall standpoint. Single Objective (SO) optimization may ignore this trade-off viewpoint which is crucial.

The main advantages of the proposed MOO method are: It doesn't require a priori knowledge of the relative importance of the objective functions and it provides a set of acceptable trade-off near optimal solutions. This set is called Pareto front or optimality trade-off surfaces. Both SOO and MOO searching algorithms are tested, validated and compared.

The dynamic error driven controller regulates the controllers' gains using the Particle Swarm Optimization (PSO) and GA to minimize the system total error and the selected objective functions. The proposed dynamic tri loop error driven controller, developed by Sharaf which is a novel advanced regulation concept that operates as an adaptive dynamic type multi-purpose controller capable of handling sudden parametric changes, load and/or source excursions.

By using the tri loop error driven controller, it is expected to have a smoother, less dynamic overshoot, fast and more robust controller when compared to those of classical control schemes. Seven different control structures were examined and validated, for speed trajectories tracking: tuned conventional PID controller, tuned modified PID controller-I, tuned modified PID controller-II, tuned variable structure sliding mode controller VSC/SMC/B-B, tuned zonal activation or target practice controller, tuned tan-sigmoid incremental integral action controller and tuned multi-stage incremental action controller.

Self tuned conventional PID controller: Fundamentally, the conventional PID controller comprises three basic control actions. They are simple to implement and they provide good performance. The tuning process of the gains of PID controllers can be complex because is iterative: first, it is necessary to tune the proportional

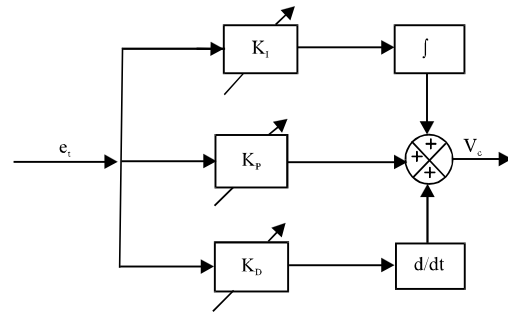


Fig. 16: Optimally tuned conventional PID controller block diagram

mode, then the integral and then add the derivative mode to stabilize the overshoot then add more proportional and so on. The PID controller has the following form in the time domain as shown in Fig. 16:

$$u(t) = K_p e(t) + K_i \int_0^t e(t) dt + K_d \frac{de(t)}{dt} \quad (15)$$

Where:

$e(t)$ = The selected system error

$u(t)$ = The control variable

K_p = The proportional gain

K_i = The integral gain

K_d = The derivative gain

Each coefficient of the PID controller adds some special characteristics to the output response of the system. Because of this choosing the right parameters becomes a crucial decision. In this scheme, the tri loop error driven controller is utilized with traditional PID controller. PID controller gains (K_p , K_i , K_d) are dynamically self tuned using the PSO and GA dynamic search and optimization criterion based on total error minimization, steady state error, maximum overshoot, settling time and rising time.

Self tuned modified PID controller-I: In the tuned modified PID controller- I proposed controller scheme, an optimally tuned modified PID controller for the SPIM motor drive systems is developed using the Particle Swarm Optimization technique (PSO) and the Genetic Algorithm GA, where the additional integral of the squared system error is implemented in this modified PID controller as shown in Fig. 17.

$$u(t) = K_p e(t) + K_i \int_0^t e(t) dt + K_d \frac{de(t)}{dt} + K_e (e(t))^2 \quad (16)$$

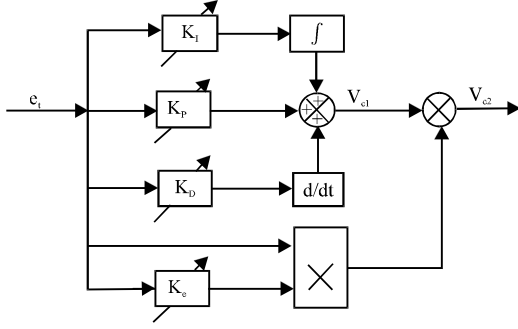


Fig 17: Optimally Tuned modified PID controller-I block diagram

The modified PID controller gains (K_p , K_i , K_d and K_e) are tuned using the PSO searching algorithm to minimize the selected objective functions (J_1 - J_5).

Self tuned modified PID controller-II: The tuned modified PID controller-II proposed control scheme is shown in Fig. 18. The resultant control voltage has the form in the time domain as:

$$u(t) = \left(K_p e(t) + K_i \int_0^t e(t) dt + K_d \frac{de(t)}{dt} \right) \times K_e e(t)^2 \quad (17)$$

Self tuned Variable Structure Sliding Mode Bang-Bang (VSC/SMC/B-B) controller: In the variable structure sliding mode controller scheme, an optimally adaptive and self tuned variable structure sliding mode controller for SPIM motor drive systems using Particle Swarm Optimization technique (PSO) and Genetic Algorithm (GA) as shown in Fig 19. The slope of the sliding surface is designed as:

$$\sigma = \beta e_t + K_\alpha \frac{de_t}{dt} \quad (18)$$

With adaptive term:

$$\beta = \beta_0 + \beta_1 |e_t| \quad (19)$$

Where;

$$|e_t| = \sqrt{(\gamma_i e_t)^2 + (\gamma_\omega e_\omega)^2 + (\gamma_v e_v)^2 + (\gamma_P \gamma_P)^2} \quad (20)$$

The system control voltage has the following form in the time domain (Srinivas and Deb, 1994), the control is an on-off logic that is when $\sigma > 0$, $V_c = 1$ and when $\sigma < 0$, $V_c = -1$.

The PSO and GA optimization and parameters searching algorithms are implemented for tuning the gains β_0 , β_1 and α to minimize the selected objective functions (J_1 - J_5).

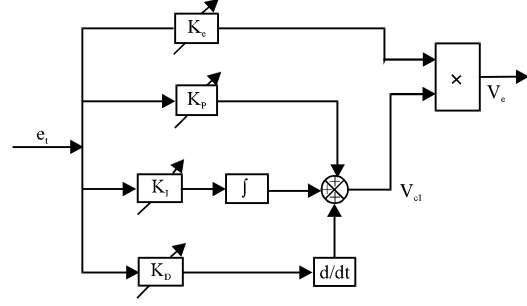


Fig. 18: Optimally tuned modified PID controller-II block diagram

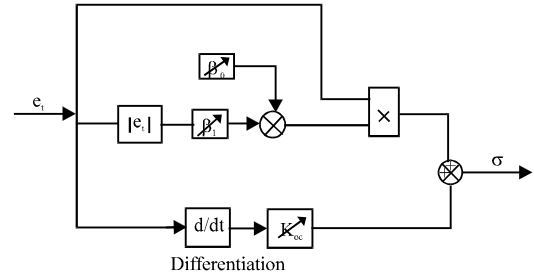


Fig. 19: Optimally tuned VSC/SMC/B-B controller block diagram

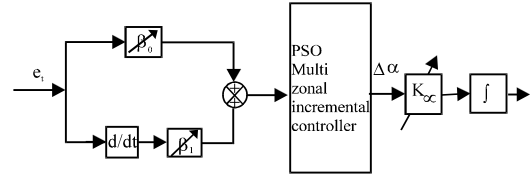


Fig. 20: Optimally tuned zonal activation or target Practice controller block diagram

Self tuned zonal activation or target practice controller:

Figure 20 shows the proposed zonal activation or target practice controller scheme. In this strategy, the tri loop error driven controller is utilized with zonal activation or target practice controller which is dynamically self tuned using the PSO and GA search and optimization criterion based on total error minimization, steady state error, maximum overshoot and settling and rising time. The dynamic supplementary control loops utilizes speed, current, ripples and dynamic momentum excursion errors. Zonal Activation Target Practice Controller is composed from concentric circles representative zones, each circle has a radius depends on the values of the total error and the first derivative of the total error as shown in Fig 21:

$$R = \beta_1 e(t) + \beta_0 \frac{de(t)}{dt} \quad (21)$$

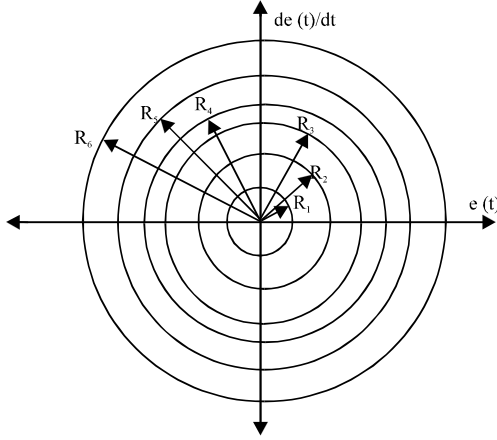


Fig. 21: Zonal activation target practice controller boundaries

Table 2: Zonal activation controller boundaries *number of zones can be selected for best performance

| Zone no. | Zone boundary (PU) | $\Delta\alpha$ (deg) |
|----------|----------------------------|----------------------|
| 1 | $0 \leq R_1 \leq 0.025$ | 2.5 |
| 2 | $0.025 \leq R_2 \leq 0.05$ | 5.0 |
| 3 | $0.05 \leq R_3 \leq 0.1$ | 10.0 |
| 4 | $0.1 \leq R_4 \leq 0.2$ | 20.0 |
| 5 | $0.2 \leq R_5 \leq 0.4$ | 30.0 |
| 6 | $0.4 \leq R_6 \leq 0.5$ | 40.0 |

Zonal activation target Practice controller determines the value of boundaries $\Delta\alpha$ which assigned to each zone according to the values of the total error and the first derivative of the total error as shown in Table 2 and Fig. 20. Then the value of the controlling firing angle α is determined using the following form:

$$\alpha = \int K_{\alpha} d\alpha \quad (22)$$

Where $0.01 \leq K_{\alpha} \leq 1.0$, β_0 and β_1 are an optimization parameter which is tuned using MOPSO and MOGA to minimize the selected objective functions.

Self tuned tan-sigmoid incremental controller: Figure 22 shows the Tan-sigmoid self adjusting multi loop controller. The change in the control voltage ΔV_c is defined as:

$$\Delta V_c = k_0 R_e \left(\frac{1 - e^{-\beta_0 e(t)}}{1 + e^{-\beta_0 e(t)}} \right) \quad (23)$$

Where:

$$R = \sqrt{\left(e(t) \right)^2 + \left(\frac{d}{dt} e(t) \right)^2} \quad (24)$$

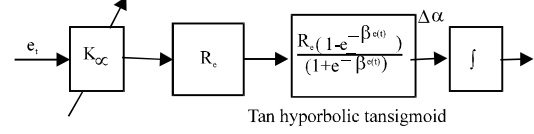


Fig 22: Optimally tuned tan-sigmoid incremental integral action controller

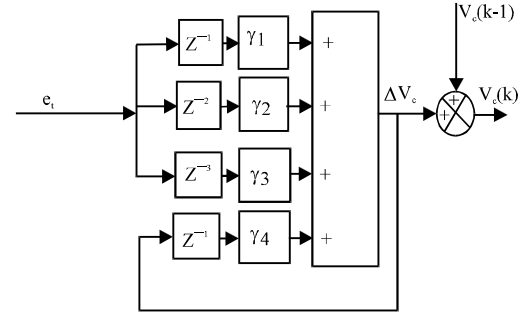


Fig 23: Tuned multi-Stage incremental action regression based controller block diagram

and: $50 \leq K_0 \leq 200.0$, $1 \leq \beta \leq 5$ are optimization parameters which are tuned using MOPSO and MOGA to minimize the selected objective functions. The system control voltage has the following form in the time domain:

$$V_c = \int_0^t \Delta V_c dt \quad (25)$$

Self tuned multi-loop incremental controller: Figure 23 shows the change in the control voltage ΔV_c of the Multi-loop incremental controller that is defined as:

$$\Delta V_c(k) = \gamma_1 e(k-1) + \gamma_2 e(k-2) + \gamma_3 e(k-3) + \gamma_4 e(k-4) + \gamma_5 \Delta V_c \quad (26)$$

$$V_c(k) = \Delta V_c(k) + V_c(k-1) \quad (27)$$

In this strategy, the PSO and GA searching algorithms are implemented for tuning the gains (γ_1 - γ_4) minimize the selected objective functions (J_1 - J_5).

Self tuned Artificial Neural Network controller (ANN): The neural network used in this study is the simplest one that uses three layers which is widely used in the control of the electrical machines. Each layer is composed of neurons. Each neuron is connected via weights to the previous layer. The first layer is connected to the input variables. The second one is connected via weights to all the neurons of the previous layer and the last one is composed of one neuron given the output value. The weights and the biases of the ANN network's are updated

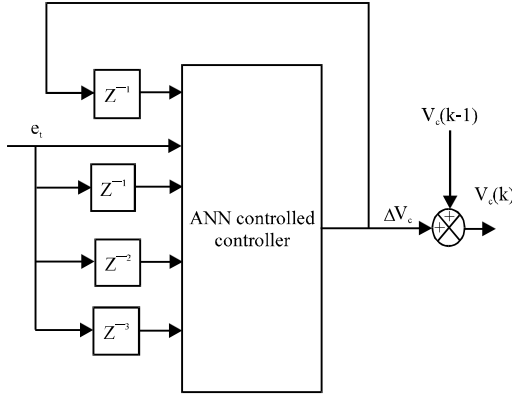


Fig. 24: ANN incremental controlled controller block diagram

to provide that the global error of the system is minimized. The proposed ANN regulator is tuned on-line using the back-propagation algorithm. The on-line ANN rule-based algorithm is used to update the ANN network weights and biases to ensure continuous effective dynamic response while keeping the motor inrush current under specified tolerable limits. The input vector with 3 layer ANN as shown in Fig. 24 is:

$$\bar{X} = \{e_i(k-1), e_i(k-2), e_i(k-3), \Delta V_c(k-1)\} \quad (28)$$

Self tuned Fuzzy Logic Controller (FLC): As shown in Fig. 25, the FLC system consists of three subsystems which are the fuzzification, rule base and defuzzification. Fuzzification subsystem converts the exact inputs to fuzzy values using five membership functions: Positive Big (PB), Positive Small (PS), Zero (ZZ), Negative Small (NS) and Negative Big (NB). The rule base unit processes these fuzzy values with fuzzy rules.

The defuzzification unit converts the fuzzy results to exact values. The FLCs input values are the global error e_i and change in global error, de_i . According to these variables, a rule table is produced in the FLCs rule base unit as shown in Table 3.

Digital simulation results: The GP-SF-SS devices system performance is compared for two cases; without (as shown in Table 4) and with the GP-SF-SS devices, the second case is studied with fixed and self tuned type controllers using either GA or PSO. In addition, the second case is studied to compare the performance with Artificial Neural Network (ANN) controller (Table 5) and Fuzzy Logic Controller FLC (Table 6) with the self tuned type controllers using either GA

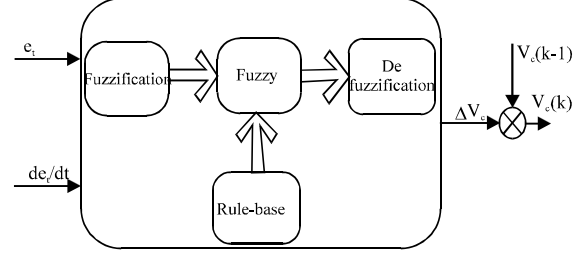


Fig. 25: Main structure of the FLC-incremental controller

Table 3: Fuzzy rules decision table

| e_i | de_i | | | | |
|-------|--------|----|----|----|----|
| | NB | NS | ZZ | PS | PB |
| NB | NB | NB | NS | NS | ZZ |
| NS | NB | NS | NS | ZZ | PS |
| ZZ | NS | NS | ZZ | PS | PS |
| PS | NS | ZZ | PS | PS | PB |
| PB | ZZ | PS | PS | PB | PB |

Table 4: System behavior without (GP-SF-SS) schemes

| Items | Without (GP-SF-SS) | RMS |
|---|--------------------|--------|
| RMS motor voltage (PU) | | 0.8782 |
| RMS motor current (PU) | | 0.8576 |
| Maximum transient voltage over/under shoot (PU) | | 0.1597 |
| Maximum transient current-over/under shoot (PU) | | 0.1775 |
| System efficiency | | 0.8145 |
| NMSE_V | | 0.3293 |
| NMSE_ω _m | | 0.5093 |
| NMSE_I | | 0.2398 |
| THDv_bus L (%) | | 17.486 |
| THDi_bus L (%) | | 19.475 |
| THDv_bus M (%) | | 16.456 |
| THDi_bus M (%) | | 18.465 |
| Motor power factor | | 0.7516 |

or PSO. The seven self tuned type controllers based either GA or PSO are tuned conventional PID controller, tuned modified PID controller-I, Tuned modified PID controller-II, tuned variable structure sliding mode controller VSC/SMC/B-B, tuned zonal ctivation or target practice controller, tuned tan-sigmoid incremental integral action controller and tuned multi-stage incremental action controller.

All of the controllers discussed in the study have been applied to the speed tracking control of the same system parameters for performance comparison. Matlab-Simulink Software was used to design, test and validate the effectiveness of the GP-SF-SS devices for small motors used in household appliances, washers, dryers, fans, water pumps, ventilation systems, air-conditions and other applications in dispersing machines, actuators and small converters with induction motor size up to 5-25 KVA. The digital dynamic simulation model using Matlab/Simulink software environment allows for low cost

Table 5: System dynamic behavior comparison using ANN controller

| Items | GP-SF-SS scheme A | GP-SF-SS scheme B | GP-SF-SS scheme C | GP-SF-SS scheme D | GP-SF-SS scheme E | GP-SF-SS scheme F | GP-SF-SS scheme G | GP-SF-SS scheme H |
|---|----------------------|----------------------|----------------------|----------------------|----------------------|----------------------|----------------------|----------------------|
| RMS motor voltage (PU) | 0.9520 | 0.9389 | 0.9414 | 0.9542 | 0.9485 | 0.9407 | 0.9524 | 0.9261 |
| RMS motor current (PU) | 0.7269 | 0.6943 | 0.7509 | 0.6576 | 0.7081 | 0.6807 | 0.7401 | 0.6853 |
| Maximum Transient | 0.0866 | 0.0951 | 0.0878 | 0.0862 | 0.0938 | 0.0916 | 0.0888 | 0.0898 |
| Voltage over/under shoot (PU) | | | | | | | | |
| Maximum transient | 0.0859 | 0.0955 | 0.0952 | 0.0886 | 0.0920 | 0.0875 | 0.0923 | 0.0894 |
| Current over/under Shoot (PU) | | | | | | | | |
| System efficiency | 0.9012 | 0.8527 | 0.8905 | 0.8908 | 0.8555 | 0.8942 | 0.8759 | 0.8630 |
| NMSE _V ×10 ⁻¹ | 0.3378 | 0.5472 | 0.5005 | 0.8032 | 0.5105 | 0.5542 | 0.2851 | 0.6072 |
| NMSE _{ω_m} ×10 ⁻¹ | 0.6218 | 0.6720 | 0.6079 | 0.7635 | 0.2514 | 0.8283 | 0.9618 | 0.6750 |
| NMSE _I ×10 ⁻¹ | 0.2170 | 0.6127 | 0.2366 | 0.9221 | 0.7448 | 0.8563 | 0.2523 | 0.5160 |
| THD _v _bus L (%) | 8.0866 | 8.8861 | 7.9180 | 7.1127 | 8.9779 | 7.0492 | 8.1413 | 8.9164 |
| THDi _{bus} L (%) | 8.8441 | 8.2750 | 8.4412 | 8.9262 | 7.9386 | 7.3801 | 8.2725 | 8.0730 |
| THD _v _bus M (%) | 7.7610 | 8.5900 | 8.7014 | 7.6675 | 8.2304 | 8.6072 | 7.0900 | 8.7596 |
| THDi _{bus} M (%) | 8.4061 | 8.6479 | 8.8828 | 7.8089 | 7.9789 | 7.2004 | 8.8978 | 8.3977 |
| Motor power factor | 0.8909 | 0.8825 | 0.8938 | 0.8563 | 0.8718 | 0.8625 | 0.8862 | 0.8584 |
| Reduction in | 12.6386 | 12.7662 | 12.0525 | 12.6566 | 13.8291 | 12.4920 | 13.1753 | 13.0346 |
| KWh consumption (%) | | | | | | | | |

Table 6: System dynamic behavior comparison using the FLC controller

| Items | GP-SF-SS scheme A | GP-SF-SS scheme B | GP-SF-SS scheme C | GP-SF-SS scheme D | GP-SF-SS scheme E | GP-SF-SS scheme F | GP-SF-SS scheme G | GP-SF-SS scheme H |
|---|----------------------|----------------------|----------------------|----------------------|----------------------|----------------------|----------------------|----------------------|
| RMS motor voltage (PU) | 0.9443 | 0.9517 | 0.9419 | 0.9525 | 0.9403 | 0.9593 | 0.9356 | 0.9493 |
| RMS motor current (PU) | 0.7443 | 0.7292 | 0.7331 | 0.7356 | 0.7204 | 0.6711 | 0.6787 | 0.7158 |
| Maximum transient | 0.0930 | 0.0952 | 0.0920 | 0.0965 | 0.0944 | 0.0875 | 0.0949 | 0.0879 |
| Voltage over/under shoot (PU) | | | | | | | | |
| Maximum transient current | 0.0928 | 0.0931 | 0.0942 | 0.0899 | 0.0906 | 0.0911 | 0.0924 | 0.0877 |
| Over/under shoot (PU) | | | | | | | | |
| System efficiency | 0.8788 | 0.8575 | 0.8534 | 0.8545 | 0.8616 | 0.8789 | 0.8863 | 0.8789 |
| NMSE _V ×10 ⁻¹ | 0.4076 | 0.3662 | 0.1461 | 0.4374 | 0.2244 | 0.2338 | 0.4377 | 0.6551 |
| NMSE _{ω_m} ×10 ⁻¹ | 0.7776 | 0.4769 | 0.2580 | 0.4247 | 0.9460 | 0.5037 | 0.8576 | 0.2416 |
| NMSE _I ×10 ⁻¹ | 0.4893 | 0.8974 | 0.9482 | 0.5073 | 0.4057 | 0.2905 | 0.3816 | 0.8778 |
| THD _v _bus L (%) | 8.4756 | 9.8340 | 7.9340 | 7.6680 | 9.1958 | 6.4685 | 8.3135 | 6.8687 |
| THDi _{bus} L (%) | 7.5479 | 7.1746 | 8.4469 | 9.6391 | 6.0443 | 9.1476 | 8.6664 | 9.7769 |
| THD _v _bus M (%) | 6.2888 | 6.1939 | 8.8543 | 9.1573 | 7.0203 | 8.7167 | 7.1567 | 6.3369 |
| THDi _{bus} M (%) | 9.3727 | 6.3183 | 8.8582 | 6.5006 | 7.7203 | 8.2898 | 8.4577 | 8.0611 |
| Motor power factor | 0.8837 | 0.8697 | 0.8903 | 0.8581 | 0.8795 | 0.9047 | 0.8685 | 0.8787 |
| Reduction in | 13.2319 | 12.6070 | 13.7407 | 12.1542 | 13.9029 | 12.2293 | 13.2564 | 12.3885 |
| KWh consumption (%) | | | | | | | | |

assessment and prototyping, system parameters selection and optimization of control settings. The use of GA and PSO-search algorithm is used in online gain adjusting to minimize controller absolute value of total error. This is required before full scale prototyping which is both expensive and time consuming. The effectiveness of dynamic simulators brings on detailed sub-models selections and tested sub-models Matlab library of power system components already tested and validated. The dynamic simulation conditions are identical for all tuned controllers. To compare the global performances of all controllers, the Normalised Mean Square Error (NMSE) deviations between output plant variables and desired values and is defined as:

$$NMSE_{VS} = \frac{\sum (V_s - V_{s-ref})^2}{\sum (V_{s-ref})^2} \quad (29)$$

$$NMSE_{\omega_m} = \frac{\sum (\omega_m - \omega_{m-ref})^2}{\sum (\omega_{m-ref})^2} \quad (30)$$

$$NMSE_{I_s} = \frac{\sum (I_s - I_{s-ref})^2}{\sum (I_{s-ref})^2} \quad (31)$$

The control system comprises the three dynamic multi-loop error driven regulator is co-ordinated to minimize the selected objective functions. SOO obtains a single global or near optimal solution based on a single weighted objective function. The weighted single objective function combines several objective functions using specified or selected weighting factors as follows:

$$= \alpha_1 J_1 + \alpha_2 J_2 + \alpha_3 J_3 + \alpha_4 J_4 + \alpha_5 J_5 \quad (32)$$

Where $\alpha_1 = 0.20$, $\alpha_2 = 0.20$, $\alpha_3 = 0.20$, $\alpha_4 = 0.20$, $\alpha_5 = 0.20$ are selected weighting factors. J_1 , J_2 , J_3 , J_4 and J_5 are the selected objective functions. On the other hand, the MO finds the set of acceptable (trade-off) optimal solutions. This set of accepted solutions is called Pareto front. These acceptable trade-off multi level solutions give more ability to the user to make an informed decision by seeing a wide range of near optimal selected solutions.

Self tuned conventional PID controller: Table 7 shows the system behavior using traditional controllers with constant controller gains for the (GP-SF-SS) eight schemes. In addition, Table 8 shows system behavior comparison using the SOGA based Tuned conventional PID controller and Table 9 shows the system behavior comparison using the MOGA based Tuned conventional PID controller.

Finally, Table 10 and 11 show system behavior comparison using the SOPSO and MOPSO, respectively based tuned conventional PID controller. Comparing the system dynamic response results of the two study cases, with GA and PSO tuning algorithms and traditional controllers with constant controller gains results, ANN controller and FLC, it is quite apparent that the GA and PSO tuning algorithms highly improved the system dynamic performance from a general power quality point of view. The GA and PSO tuning algorithms had a great impact on Motor RMS voltage (PU) is improved from

0.8782 (without the (GP-SF-SS) device), 0.9500 (constant gains controller), 0.9414 (ANN controller) and 0.9525 (FLC) to around 0.9675 (SOGA based tuned controller), 0.9785 (MOGA based tuned controller), 0.9627 (SOPSO) based tuned controller and 0.9735 (MOPSO based tuned controller).

Motor RMS current (PU) is reduced from 0.8576 (without the (GP-SF-SS) device), 0.7064 (constant gains controller), 0.7269 (ANN controller) and 0.7158 (FLC) to around 0.6376 (SOGA based tuned controller), 0.6453 (MOGA based tuned controller), 0.6606 (SOPSO) based tuned controller and 0.5824 (MOPSO based tuned controller). Maximum Transient Motor Voltage Over/Under Shoot (PU) is reduced from 0.1597 (without the (GP-SF-SS) device), 0.0858 (constant gains controller), 0.0888 (ANN controller) and 0.0949 (FLC) to around 0.0240 (SOGA based tuned controller), 0.0469 (MOGA based tuned controller), 0.0321 (SOPSO) based tuned controller and 0.0483 (MOPSO based tuned controller).

Table 7: System dynamic behavior comparison using the constant parameters conventional PID controller

| Items | GP-SF-SS scheme A | GP-SF-SS scheme B | GP-SF-SS scheme C | GP-SF-SS scheme D | GP-SF-SS scheme E | GP-SF-SS scheme F | GP-SF-SS scheme G | GP-SF-SS scheme H |
|--|----------------------|----------------------|----------------------|----------------------|----------------------|----------------------|----------------------|----------------------|
| RMS motor voltage (PU) | 0.9500 | 0.9496 | 0.9586 | 0.9285 | 0.9462 | 0.9538 | 0.9256 | 0.9546 |
| RMS motor current (PU) | 0.7064 | 0.6562 | 0.6593 | 0.6785 | 0.6930 | 0.6998 | 0.7454 | 0.7126 |
| Maximum transient voltage over/under shoot (PU) | 0.0858 | 0.0944 | 0.0914 | 0.0881 | 0.0869 | 0.0875 | 0.0902 | 0.0902 |
| Maximum transient current over/under shoot (PU) | 0.0864 | 0.0961 | 0.0874 | 0.0900 | 0.0892 | 0.0876 | 0.0956 | 0.0893 |
| System efficiency | 0.8954 | 0.8677 | 0.8895 | 0.8980 | 0.8867 | 0.8976 | 0.9011 | 0.9017 |
| NMSE _V ×10 ⁻¹ | 0.1721 | 0.3234 | 0.1288 | 0.9623 | 0.1973 | 0.8957 | 0.2262 | 0.2868 |
| NMSE _{ω_m} ×10 ⁻¹ | 0.2519 | 0.7748 | 0.5897 | 0.6793 | 0.8571 | 0.6321 | 0.9128 | 0.3555 |
| NMSE _I ×10 ⁻¹ | 0.7644 | 0.2392 | 0.6403 | 0.6435 | 0.8015 | 0.3830 | 0.4092 | 0.3282 |
| THD _{v_bus L} (%) | 6.8208 | 8.6008 | 6.9478 | 8.7799 | 7.5528 | 7.5302 | 7.5970 | 6.5950 |
| THD _{i_bus L} (%) | 9.3836 | 6.1051 | 9.5581 | 8.4434 | 6.2780 | 8.4436 | 8.9070 | 8.9680 |
| THD _{v_bus M} (%) | 9.1149 | 8.1016 | 7.8787 | 7.7108 | 8.4200 | 6.3196 | 8.1044 | 6.8222 |
| THD _{i_bus M} (%) | 7.0554 | 7.1384 | 9.1692 | 7.5970 | 8.0389 | 9.5442 | 7.4731 | 8.4674 |
| Motor power factor | 0.8872 | 0.8836 | 0.8733 | 0.8590 | 0.8679 | 0.8763 | 0.8786 | 0.8924 |
| Reduction in KWh consumption (%) | 13.6978 | 12.7728 | 12.2793 | 12.3231 | 13.2706 | 13.8245 | 13.9720 | 12.2578 |

Table 8: System dynamic behavior comparison using the SOGA based tuned conventional PID controller

| Items | GP-SF-SS scheme A | GP-SF-SS scheme B | GP-SF-SS scheme C | GP-SF-SS scheme D | GP-SF-SS scheme E | GP-SF-SS scheme F | GP-SF-SS scheme G | GP-SF-SS scheme H |
|--|----------------------|----------------------|----------------------|----------------------|----------------------|----------------------|----------------------|----------------------|
| RMS motor voltage (PU) | 0.9675 | 0.9698 | 0.9697 | 0.9842 | 0.9723 | 0.9697 | 0.9630 | 0.9894 |
| RMS motor current (PU) | 0.6376 | 0.6007 | 0.6413 | 0.6399 | 0.5921 | 0.5820 | 0.6036 | 0.5905 |
| Maximum transient voltage over/under shoot (PU) | 0.0240 | 0.0419 | 0.0431 | 0.0402 | 0.0444 | 0.0323 | 0.0304 | 0.0322 |
| Maximum transient current over/under shoot (PU) | 0.0415 | 0.0265 | 0.0445 | 0.0348 | 0.0419 | 0.0495 | 0.0319 | 0.0422 |
| System efficiency | 0.9167 | 0.9350 | 0.9163 | 0.9413 | 0.9128 | 0.9461 | 0.9327 | 0.9292 |
| NMSE _V ×10 ⁻² | 0.8980 | 0.7120 | 0.7143 | 0.2404 | 0.7122 | 0.1748 | 0.1567 | 0.5586 |
| NMSE _{ω_m} ×10 ⁻² | 0.6660 | 0.3110 | 0.2314 | 0.3145 | 0.8576 | 0.8462 | 0.6678 | 0.8576 |
| NMSE _I ×10 ⁻² | 0.9340 | 0.9194 | 0.8680 | 0.5706 | 0.8056 | 0.3187 | 0.4223 | 0.6899 |
| THD _{v_bus L} (%) | 3.6738 | 4.7325 | 3.1557 | 5.1047 | 4.4011 | 5.8094 | 5.7888 | 3.4243 |
| THD _{i_bus L} (%) | 3.3040 | 5.0623 | 5.4013 | 5.3442 | 4.5590 | 4.0523 | 4.4384 | 3.9562 |
| THD _{v_bus M} (%) | 5.5256 | 3.2876 | 5.7117 | 4.7700 | 5.1726 | 4.7771 | 4.6598 | 3.8161 |
| THD _{i_bus M} (%) | 5.1057 | 4.4888 | 5.5620 | 5.0211 | 4.1383 | 4.8379 | 3.8825 | 3.2618 |
| Motor power factor | 0.9444 | 0.9193 | 0.9231 | 0.9644 | 0.9294 | 0.9345 | 0.9196 | 0.9408 |
| Reduction in KWh consumption (%) | 16.9568 | 16.9499 | 16.9364 | 16.8586 | 17.8487 | 16.0359 | 16.6263 | 16.1241 |

Table 9: System dynamic behavior comparison using a selected solution from the MOGA Pareto front based tuned conventional PID controller

| Items | GP-SF-SS scheme A | GP-SF-SS scheme B | GP-SF-SS scheme C | GP-SF-SS scheme D | GP-SF-SS scheme E | GP-SF-SS scheme F | GP-SF-SS scheme G | GP-SF-SS scheme H |
|--|----------------------|----------------------|----------------------|----------------------|----------------------|----------------------|----------------------|----------------------|
| RMS motor voltage (PU) | 0.9785 | 0.9960 | 0.9793 | 0.9776 | 0.9930 | 0.9814 | 0.9698 | 0.9867 |
| RMS motor current (PU) | 0.6453 | 0.6159 | 0.6123 | 0.6057 | 0.6582 | 0.6364 | 0.6017 | 0.6680 |
| Maximum transient voltage over/under shoot (PU) | 0.0469 | 0.0266 | 0.0231 | 0.0352 | 0.0245 | 0.0399 | 0.0483 | 0.0346 |
| Maximum transient current over/under shoot (PU) | 0.0368 | 0.0237 | 0.0356 | 0.0335 | 0.0300 | 0.0299 | 0.0428 | 0.0246 |
| System efficiency | 0.9581 | 0.9580 | 0.9400 | 0.9628 | 0.9432 | 0.9131 | 0.9215 | 0.9367 |
| NMSE _V $\times 10^{-2}$ | 0.2800 | 0.2778 | 0.5814 | 0.1275 | 0.2492 | 0.5684 | 0.4771 | 0.4592 |
| NMSE _{ω_m} $\times 10^{-2}$ | 0.8219 | 0.2763 | 0.6919 | 0.8953 | 0.1513 | 0.8633 | 0.4722 | 0.5006 |
| NMSE _I $\times 10^{-2}$ | 0.6386 | 0.7455 | 0.9615 | 0.9035 | 0.1282 | 0.4371 | 0.6723 | 0.1359 |
| THDv _{bus L} (%) | 4.1615 | 3.4530 | 5.2564 | 3.5833 | 4.4201 | 3.8794 | 3.4402 | 5.7479 |
| THDi _{bus L} (%) | 3.6622 | 3.4313 | 3.2843 | 5.0090 | 4.9482 | 4.3160 | 4.5272 | 3.8655 |
| THDv _{bus M} (%) | 4.2924 | 5.7835 | 5.7618 | 4.8466 | 3.2841 | 5.2050 | 4.1642 | 3.8128 |
| THDi _{bus M} (%) | 3.4825 | 4.9829 | 4.4900 | 5.2857 | 5.2231 | 5.6462 | 5.0755 | 3.2916 |
| Motor power factor | 0.9425 | 0.9482 | 0.9287 | 0.9390 | 0.9355 | 0.9395 | 0.9313 | 0.9465 |
| Reduction in KWh consumption (%) | 16.7249 | 16.3605 | 16.3394 | 16.4113 | 16.8793 | 17.7564 | 17.0165 | 17.6754 |

Table 10: System dynamic behavior comparison using the SOPSO based tuned conventional PID controller

| Items | GP-SF-SS scheme A | GP-SF-SS scheme B | GP-SF-SS scheme C | GP-SF-SS scheme D | GP-SF-SS scheme E | GP-SF-SS scheme F | GP-SF-SS scheme G | GP-SF-SS scheme H |
|--|----------------------|----------------------|----------------------|----------------------|----------------------|----------------------|----------------------|----------------------|
| RMS motor voltage (PU) | 0.9627 | 0.9632 | 0.9570 | 0.9762 | 0.9624 | 0.9606 | 0.9680 | 0.9679 |
| RMS motor current (PU) | 0.6606 | 0.6648 | 0.6102 | 0.6194 | 0.6224 | 0.5934 | 0.5922 | 0.6279 |
| Maximum transient voltage over/under shoot (PU) | 0.0321 | 0.0310 | 0.0434 | 0.0301 | 0.0268 | 0.0411 | 0.0292 | 0.0346 |
| Maximum transient current over/under shoot (PU) | 0.0453 | 0.0464 | 0.0413 | 0.0429 | 0.0490 | 0.0330 | 0.0255 | 0.0420 |
| System efficiency | 0.9132 | 0.9571 | 0.9253 | 0.9328 | 0.9484 | 0.9581 | 0.9480 | 0.9193 |
| NMSE _V $\times 10^{-2}$ | 0.6336 | 0.5588 | 0.6433 | 0.2308 | 0.4968 | 0.4609 | 0.8873 | 0.4541 |
| NMSE _{ω_m} $\times 10^{-2}$ | 0.2746 | 0.8085 | 0.4723 | 0.4410 | 0.7228 | 0.6282 | 0.1817 | 0.2231 |
| NMSE _I $\times 10^{-2}$ | 0.4257 | 0.5897 | 0.7433 | 0.9500 | 0.5263 | 0.1122 | 0.7787 | 0.4080 |
| THDv _{bus L} (%) | 4.0891 | 5.3808 | 4.9636 | 4.5919 | 3.2655 | 4.5906 | 4.9431 | 4.2308 |
| THDi _{bus L} (%) | 4.8129 | 3.1381 | 3.0904 | 5.0628 | 5.5267 | 5.6720 | 5.6368 | 5.1606 |
| THDv _{bus M} (%) | 5.7222 | 4.0662 | 3.2181 | 5.4751 | 3.8551 | 4.5867 | 5.2337 | 3.2203 |
| THDi _{bus M} (%) | 4.2410 | 5.4517 | 4.3424 | 3.8313 | 3.2064 | 4.8798 | 4.8041 | 5.0905 |
| Motor power factor | 0.9225 | 0.9638 | 0.9449 | 0.9148 | 0.9194 | 0.9335 | 0.9532 | 0.9205 |
| Reduction in KWh consumption (%) | 17.7855 | 16.0447 | 16.3018 | 17.6811 | 16.8949 | 17.8259 | 17.5114 | 17.4152 |

Table 11: System dynamic behavior comparison using a selected solution from the MOPSO Pareto front based tuned conventional PID controller

| Items | GP-SF-SS scheme A | GP-SF-SS scheme B | GP-SF-SS scheme C | GP-SF-SS scheme D | GP-SF-SS scheme E | GP-SF-SS scheme F | GP-SF-SS scheme G | GP-SF-SS scheme H |
|--|----------------------|----------------------|----------------------|----------------------|----------------------|----------------------|----------------------|----------------------|
| RMS Motor voltage (PU) | 0.9735 | 0.9693 | 0.9695 | 0.9871 | 0.9734 | 0.9820 | 0.9879 | 0.9876 |
| RMS motor current (PU) | 0.5824 | 0.6268 | 0.5973 | 0.6444 | 0.6026 | 0.6640 | 0.5923 | 0.6269 |
| Maximum transient Voltage over/under Shoot (PU) | 0.0483 | 0.0291 | 0.0362 | 0.0396 | 0.0330 | 0.0354 | 0.0427 | 0.0254 |
| Maximum transient current Over/under shoot (PU) | 0.0231 | 0.0322 | 0.0411 | 0.0479 | 0.0351 | 0.0254 | 0.0353 | 0.0482 |
| System efficiency | 0.9449 | 0.9642 | 0.9457 | 0.9242 | 0.9535 | 0.9120 | 0.9542 | 0.9229 |
| NMSE _V $\times 10^{-2}$ | 0.3643 | 0.8212 | 0.1954 | 0.4308 | 0.6581 | 0.1409 | 0.3843 | 0.9323 |
| NMSE _{ω_m} $\times 10^{-2}$ | 0.6804 | 0.1856 | 0.3299 | 0.2336 | 0.3484 | 0.7742 | 0.7158 | 0.6262 |
| NMSE _I $\times 10^{-2}$ | 0.1455 | 0.8333 | 0.3079 | 0.5342 | 0.1375 | 0.6646 | 0.4535 | 0.7666 |
| THDv _{bus L} (%) | 3.8768 | 4.8055 | 4.5045 | 3.8953 | 4.3314 | 3.3968 | 5.1739 | 3.4034 |
| THDi _{bus L} (%) | 3.7437 | 4.4955 | 3.9741 | 4.8774 | 4.1384 | 3.3065 | 4.3281 | 4.5951 |
| THDv _{bus M} (%) | 4.2724 | 3.9660 | 3.7755 | 5.1568 | 4.1991 | 5.7096 | 5.3875 | 5.5552 |
| THDi _{bus M} (%) | 3.4044 | 3.0848 | 5.4816 | 4.7585 | 3.9809 | 4.9608 | 3.6366 | 3.6763 |
| Motor power factor | 0.9544 | 0.9203 | 0.9203 | 0.9206 | 0.9604 | 0.9530 | 0.9347 | 0.9256 |
| Reduction in KWh consumption (%) | 17.9147 | 16.5596 | 16.3489 | 17.7905 | 16.5059 | 17.3312 | 17.9808 | 17.3699 |

Maximum Transient Motor Current-Over/Under Shoot (PU) is reduced from 0.1775 (without the GP-SF-SS device), 0.0864 (constant gains controller), 0.0859 (ANN controller) and 0.0928 (FLC) to around 0.0415 (SOGA

based tuned controller), 0.0368 (MOGA based tuned controller), 0.0453 (SOPSO based tuned controller and 0.0231 (MOPSO based tuned controller). The system efficiency is improved from 0.8145 (without the GP-SF-SS

device), 0.8954 (constant gains controller), 0.9012 (ANN controller) and 0.8788 (FLC) to around 0.9167 (SOGA based tuned controller), 0.9581 (MOGA based tuned controller), 0.9132 (SOPSO) based tuned controller and 0.9449 (MOPSO based tuned controller). Moreover, the Normalized Mean Square Error (NMSE-V) of the Motor voltage is reduced from 0.3293 (without the GP-SF-SS device), 0.01721 (constant gains controller), 0.03378 (ANN controller) and 0.04076 (FLC) to around 0.008980 (SOGA based tuned controller), 0.002800 (MOGA based tuned controller), 0.006336 (SOPSO) based tuned controller and 0.003643 (MOPSO based tuned controller). In addition the (NMSE- ω_m) of the SPIM motor is reduced from 0.5093 (without the GP-SF-SS device), 0.02519 (constant gains controller), 0.06218 (ANN controller) and 0.07776 (FLC) to around 0.006660 (SOGA based tuned controller), 0.008219 (MOGA based tuned controller), 0.002746 (SOPSO) based tuned controller and 0.006804 (MOPSO based tuned controller).

The (NMSE-I) of the Motor current is reduced from 0.2398 (without the GP-SF-SS device), 0.07644 (constant gains controller), 0.02170 (ANN controller) and 0.04893 (FLC) to around 0.009340 (SOGA based tuned controller), 0.006386 (MOGA based tuned controller), 0.004257 (SOPSO) based tuned controller and 0.1455 (MOPSO based tuned controller). Total Harmonic Distortion THD (%) of the supply voltage is reduced from 17.486 (without the GP-SF-SS device), 6.8208 (constant gains controller), 8.0866 (ANN controller) and 8.4756 (FLC) to around 3.6738 (SOGA based tuned controller), 4.1615 (MOGA based tuned controller), 4.0891 (SOPSO) based tuned controller and 3.8768 (MOPSO based tuned controller).

THD (%) of the supply current is reduced from 19.475 (without the GP-SF-SS device), 9.3836 (constant gains controller), 8.8441 (ANN controller) and 7.5479 (FLC) to around 3.3040 (SOGA based tuned controller), 3.6622 (MOGA based tuned controller), 4.8129 (SOPSO) based tuned controller and 3.7437 (MOPSO based tuned controller). THD (%) of the motor voltage is reduced from 16.456 (without the GP-SF-SS device), 9.1149 (constant gains controller), 7.7610 (ANN controller) and 6.2888 (FLC) to around 5.5256 (SOGA based tuned controller), 4.2924 (MOGA based tuned controller), 5.7222 (SOPSO) based tuned controller and 4.2724 (MOPSO based tuned controller).

THD (%) of the motor current is reduced from 18.465 (without the GP-SF-SS device), 7.0554 (constant gains controller), 8.4061 (ANN controller) and 9.3727 (FLC) to around 5.1057 (SOGA based tuned controller), 3.4825 (MOGA based tuned controller), 4.2410 (SOPSO) based tuned controller and 3.4044 (MOPSO based tuned controller). Motor power factor is improved from 0.7516

(without the GP-SF-SS device), 0.8872 (constant gains controller), 0.8909 (ANN controller) and 0.8837 (FLC) to around 0.9444 (SOGA based tuned controller), 0.9425 (MOGA based tuned controller), 0.9225 (SOPSO) based tuned controller and 0.9544 (MOPSO based tuned controller). Reduction in KWh Consumption (%) is reduced from 0.000 (without the (GP-SF-SS) device), 12.6978 (constant gains controller), 13.6386 (ANN controller) and 13.2319 (FLC) to around 16.4767 (SOGA based tuned controller), 16.3532 (MOGA based tuned controller), 16.4862 (SOPSO) based tuned controller and 17.8901 (MOPSO based tuned controller).

Self tuned modified PID controller-I: Table 12 shows the system behavior using traditional controllers with constant controller gains for the (GP-SF-SS) eight schemes. In addition, Table 13 shows system behavior comparison using the SOGA based tuned modified PID controller-I and Table 14 shows the system behavior comparison using the MOGA based tuned modified PID controller-I.

Finally, Tables 15 and 16 show system behavior comparison using the SOPSO and MOPSO, respectively based Tuned modified PID controller-I. Comparing the system dynamic response results of the two study cases, with GA and PSO tuning algorithms and traditional controllers with constant controller gains results, ANN controller and FLC, it is quite apparent that the GA and PSO tuning algorithms highly improved the system dynamic performance from a general power quality point of view.

The GA and PSO tuning algorithms had a great impact on Motor RMS voltage (PU) is improved from 0.8782 (without the GP-SF-SS device), 0.9448 (constant gains controller), 0.9414 (ANN controller) and 0.9525 (FLC) to around 0.9851 (SOGA based tuned controller), 0.9917 (MOGA based tuned controller), 0.9669 (SOPSO) based tuned controller and 0.9737 (MOPSO based tuned controller). Motor RMS current (PU) is reduced from 0.8576 (without the GP-SF-SS device), 0.6845 (constant gains controller), 0.7269 (ANN controller) and 0.7158 (FLC) to around 0.6406 (SOGA based tuned controller), 0.6239 (MOGA based tuned controller), 0.6566 (SOPSO) based tuned controller and 0.6479 (MOPSO based tuned controller).

Maximum transient motor voltage over/under shoot (PU) is reduced from 0.1597 without the (GP-SF-SS device), 0.0938 (constant gains controller), 0.0888 (ANN controller) and 0.0949 (FLC) to around 0.0469 (SOGA based tuned controller), 0.0427 (MOGA based tuned controller), 0.0448 (SOPSO) based tuned controller and 0.0463 (MOPSO based tuned controller). Maximum

Table 12: System dynamic behavior comparison using the constant parameters modified PID controller-I

| Items | GP-SF-SS scheme A | GP-SF-SS scheme B | GP-SF-SS scheme C | GP-SF-SS scheme D | GP-SF-SS scheme E | GP-SF-SS scheme F | GP-SF-SS scheme G | GP-SF-SS scheme H |
|--|----------------------|----------------------|----------------------|----------------------|----------------------|----------------------|----------------------|----------------------|
| RMS motor voltage (PU) | 0.9448 | 0.9353 | 0.9337 | 0.9352 | 0.9410 | 0.9468 | 0.9343 | 0.9495 |
| RMS motor current (PU) | 0.6845 | 0.7002 | 0.7127 | 0.6670 | 0.7371 | 0.7504 | 0.7125 | 0.6530 |
| Maximum transient voltage over/under shoot (PU) | 0.0938 | 0.0903 | 0.0902 | 0.0913 | 0.0876 | 0.0915 | 0.0928 | 0.0860 |
| Maximum transient current over/under shoot (PU) | 0.0949 | 0.0946 | 0.0934 | 0.0908 | 0.0867 | 0.0947 | 0.0879 | 0.0907 |
| System efficiency | 0.9020 | 0.8864 | 0.9021 | 0.8765 | 0.8663 | 0.8555 | 0.8618 | 0.8704 |
| NMSE_V $\times 10^{-1}$ | 0.4393 | 0.8723 | 0.4597 | 0.4333 | 0.1873 | 0.9501 | 0.8982 | 0.5059 |
| NMSE_ $\omega_m \times 10^{-1}$ | 0.5909 | 0.5328 | 0.9598 | 0.1338 | 0.3333 | 0.3910 | 0.2167 | 0.7482 |
| NMSE_I $\times 10^{-1}$ | 0.6488 | 0.2796 | 0.5075 | 0.3387 | 0.1149 | 0.2106 | 0.5887 | 0.8731 |
| THDv_bus L (%) | 6.6869 | 9.0298 | 7.4214 | 8.9958 | 7.3315 | 8.9853 | 6.5877 | 6.5893 |
| THDi_bus L (%) | 8.4680 | 6.3793 | 9.5771 | 7.8789 | 6.6467 | 7.0796 | 6.5232 | 6.1107 |
| THDv_bus M (%) | 6.9072 | 9.2573 | 8.8022 | 8.6810 | 7.4883 | 7.8586 | 9.7237 | 9.0211 |
| THDi_bus M (%) | 7.5903 | 9.6865 | 6.7759 | 8.0481 | 7.9518 | 7.8722 | 7.4673 | 8.0112 |
| Motor power factor | 0.9004 | 0.8526 | 0.9043 | 0.8611 | 0.8733 | 0.8731 | 0.8936 | 0.8787 |
| Reduction in KWh consumption (%) | 13.0035 | 12.8073 | 12.9952 | 13.2836 | 13.7859 | 13.5407 | 12.7883 | 12.2191 |

Table 13: System dynamic behavior comparison using the SOGA based tuned modified PID controller-I

| Items | GP-SF-SS scheme A | GP-SF-SS scheme B | GP-SF-SS scheme C | GP-SF-SS scheme D | GP-SF-SS scheme E | GP-SF-SS scheme F | GP-SF-SS scheme G | GP-SF-SS scheme H |
|--|----------------------|----------------------|----------------------|----------------------|----------------------|----------------------|----------------------|----------------------|
| RMS motor voltage (PU) | 0.9851 | 0.9933 | 0.9714 | 0.9894 | 0.9537 | 0.9945 | 0.9587 | 0.9577 |
| RMS motor current (PU) | 0.6406 | 0.6662 | 0.5973 | 0.5900 | 0.6309 | 0.6672 | 0.5821 | 0.6583 |
| Maximum transient voltage over/under shoot (PU) | 0.0469 | 0.0270 | 0.0321 | 0.0474 | 0.0362 | 0.0244 | 0.0423 | 0.0220 |
| Maximum transient current over/under shoot (PU) | 0.0386 | 0.0485 | 0.0329 | 0.0422 | 0.0409 | 0.0491 | 0.0275 | 0.0384 |
| System efficiency | 0.9377 | 0.9301 | 0.9341 | 0.9182 | 0.9394 | 0.9635 | 0.9293 | 0.9299 |
| NMSE_V $\times 10^{-2}$ | 0.8807 | 0.7089 | 0.3113 | 0.5636 | 0.7984 | 0.7089 | 0.1122 | 0.3551 |
| NMSE_ $\omega_m \times 10^{-2}$ | 0.2576 | 0.2852 | 0.1926 | 0.1449 | 0.4474 | 0.3110 | 0.2079 | 0.4817 |
| NMSE_I $\times 10^{-2}$ | 0.3525 | 0.8410 | 0.1416 | 0.9499 | 0.9267 | 0.9517 | 0.8104 | 0.1488 |
| THDv_bus L (%) | 5.1191 | 3.5982 | 3.6842 | 5.5626 | 5.2495 | 3.5393 | 4.4520 | 3.1943 |
| THDi_bus L (%) | 3.6054 | 5.6580 | 4.1341 | 3.1982 | 3.1457 | 3.0392 | 5.3325 | 5.6098 |
| THDv_bus M (%) | 4.3007 | 3.4859 | 4.3528 | 5.3505 | 5.4255 | 5.7485 | 5.3200 | 3.7695 |
| THDi_bus M (%) | 4.4072 | 3.4605 | 4.8632 | 5.0777 | 3.0322 | 5.5927 | 4.8935 | 3.1622 |
| Motor power factor | 0.9354 | 0.9250 | 0.9199 | 0.9228 | 0.9604 | 0.9428 | 0.9487 | 0.9573 |
| Reduction in KWh consumption (%) | 16.6603 | 16.7632 | 16.8202 | 17.2214 | 16.2669 | 16.1018 | 16.9524 | 17.7845KWh |

Table 14: System dynamic behavior comparison using a selected solution from the MOGA pareto front based tuned modified PID controller-I

| Items | GP-SF-SS scheme A | GP-SF-SS scheme B | GP-SF-SS scheme C | GP-SF-SS scheme D | GP-SF-SS scheme E | GP-SF-SS scheme F | GP-SF-SS scheme G | GP-SF-SS scheme H |
|--|----------------------|----------------------|----------------------|----------------------|----------------------|----------------------|----------------------|----------------------|
| RMS motor voltage (PU) | 0.9917 | 0.9875 | 0.9692 | 0.9654 | 0.9923 | 0.9711 | 0.9741 | 0.9852 |
| RMS motor current (PU) | 0.6239 | 0.6693 | 0.6136 | 0.6278 | 0.5963 | 0.6252 | 0.6180 | 0.6394 |
| Maximum transient Voltage over/under shoot (PU) | 0.0427 | 0.0323 | 0.0345 | 0.0229 | 0.0375 | 0.0322 | 0.0439 | 0.0440 |
| Maximum transient current Over/under shoot (PU) | 0.0325 | 0.0289 | 0.0314 | 0.0488 | 0.0352 | 0.0321 | 0.0431 | 0.0323 |
| System efficiency | 0.9325 | 0.9373 | 0.9441 | 0.9465 | 0.9524 | 0.9356 | 0.9460 | 0.9268 |
| NMSE_V $\times 10^{-2}$ | 0.3610 | 0.7281 | 0.2009 | 0.9099 | 0.5032 | 0.9540 | 0.4650 | 0.8030 |
| NMSE_ $\omega_m \times 10^{-2}$ | 0.1543 | 0.6375 | 0.4557 | 0.6252 | 0.3093 | 0.8199 | 0.1710 | 0.3102 |
| NMSE_I $\times 10^{-2}$ | 0.5272 | 0.9220 | 0.1698 | 0.4907 | 0.2897 | 0.8010 | 0.5422 | 0.7674 |
| THDv_bus L (%) | 5.7369 | 4.2281 | 3.5144 | 4.1456 | 4.9191 | 4.3935 | 4.1038 | 4.6154 |
| THDi_bus L (%) | 5.3255 | 4.3269 | 5.5917 | 5.5565 | 3.6072 | 5.4936 | 3.6929 | 4.9569 |
| THDv_bus M (%) | 3.4279 | 5.2190 | 4.2872 | 3.4898 | 3.7474 | 5.0843 | 3.1952 | 3.3422 |
| THDi_bus M (%) | 5.1945 | 5.8020 | 3.6985 | 4.3412 | 3.1218 | 5.1064 | 5.4246 | 4.4830 |
| Motor power factor | 0.9350 | 0.9283 | 0.9556 | 0.9484 | 0.9400 | 0.9213 | 0.9595 | 0.9549 |
| Reduction in KWh consumption (%) | 17.3211 | 16.4108 | 17.7319 | 16.3764 | 16.3702 | 18.0362 | 16.9144 | 16.7126 |

transient motor current-over/under shoot (PU) is reduced from 0.1775 (without the (GP-SF-SS) device), 0.0949 (constant gains controller), 0.0859 (ANN controller) and 0.0928 (FLC) to around 0.0386 (SOGA based tuned controller), 0.0325 (MOGA based tuned controller), 0.0333

(SOPSO) based tuned controller and 0.0298 (MOPSO based tuned controller). The system efficiency is improved from 0.8145 (without the (GP-SF-SS) device), 0.9020 (constant gains controller), 0.9012 (ANN controller) and 0.8788 (FLC) to around 0.9377 (SOGA based tuned

Table 15: System dynamic behavior comparison using the SOPSO based tuned modified PID controller-I

| Items | GP-SF-SS scheme A | GP-SF-SS scheme B | GP-SF-SS scheme C | GP-SF-SS scheme D | GP-SF-SS scheme E | GP-SF-SS scheme F | GP-SF-SS scheme G | GP-SF-SS scheme H |
|---------------------------------|----------------------|----------------------|----------------------|----------------------|----------------------|----------------------|----------------------|----------------------|
| RMS motor voltage (PU) | 0.9669 | 0.9564 | 0.9743 | 0.9834 | 0.9718 | 0.9773 | 0.9556 | 0.9642 |
| RMS motor current (PU) | 0.6566 | 0.6106 | 0.6220 | 0.6622 | 0.6006 | 0.6576 | 0.6391 | 0.6602 |
| Maximum transient | 0.0448 | 0.0256 | 0.0465 | 0.0362 | 0.0487 | 0.0252 | 0.0232 | 0.0324 |
| Voltage over/under shoot (PU) | | | | | | | | |
| Maximum transient current | 0.0333 | 0.0330 | 0.0336 | 0.0323 | 0.0471 | 0.0405 | 0.0486 | 0.0264 |
| Over/under shoot (PU) | | | | | | | | |
| System efficiency | 0.9274 | 0.9347 | 0.9491 | 0.9124 | 0.9244 | 0.9332 | 0.9165 | 0.9588 |
| NMSE_V $\times 10^{-2}$ | 0.3016 | 0.7941 | 0.1445 | 0.7363 | 0.9266 | 0.3960 | 0.3912 | 0.5889 |
| NMSE_ $\omega_m \times 10^{-2}$ | 0.7334 | 0.3718 | 0.8095 | 0.8041 | 0.5268 | 0.4805 | 0.2317 | 0.6028 |
| NMSE_I $\times 10^{-2}$ | 0.2851 | 0.4681 | 0.2859 | 0.6967 | 0.8208 | 0.3545 | 0.4293 | 0.5868 |
| THDv_bus L (%) | 5.5613 | 4.9424 | 3.3938 | 4.3591 | 5.7576 | 4.4323 | 4.1447 | 5.8164 |
| THDi_bus L (%) | 5.5307 | 3.5468 | 3.7122 | 3.7200 | 3.5134 | 3.9672 | 4.1706 | 4.7858 |
| THDv_bus M (%) | 5.0449 | 5.4019 | 5.2373 | 5.8435 | 4.6793 | 4.0421 | 4.0792 | 5.8135 |
| THDi_bus M (%) | 4.1944 | 3.2169 | 5.5222 | 5.3746 | 3.9132 | 5.5614 | 5.1515 | 3.4532 |
| Motor power factor | 0.9616 | 0.9558 | 0.9146 | 0.9558 | 0.9325 | 0.9355 | 0.9123 | 0.9267 |
| Reduction in | 17.7759 | 16.4947 | 17.6530 | 17.8624 | 16.4938 | 16.5088 | 16.1253 | 16.1832 |
| KWh consumption (%) | | | | | | | | |

Table 16: System dynamic behavior comparison using a selected solution from the MOPSO Pareto front based tuned modified PID controller-I

| Items | GP-SF-SS scheme A | GP-SF-SS scheme B | GP-SF-SS scheme C | GP-SF-SS scheme D | GP-SF-SS scheme E | GP-SF-SS scheme F | GP-SF-SS scheme G | GP-SF-SS scheme H |
|---------------------------------|----------------------|----------------------|----------------------|----------------------|----------------------|----------------------|----------------------|----------------------|
| RMS motor voltage (PU) | 0.9737 | 0.9793 | 0.9670 | 0.9951 | 0.9828 | 0.9779 | 0.9807 | 0.9752 |
| RMS motor current (PU) | 0.6479 | 0.6397 | 0.6595 | 0.6045 | 0.6177 | 0.5992 | 0.5832 | 0.5873 |
| Maximum transient | 0.0463 | 0.0397 | 0.0441 | 0.0340 | 0.0491 | 0.0245 | 0.0365 | 0.0370 |
| voltage over/under shoot (PU) | | | | | | | | |
| Maximum transient current | 0.0298 | 0.0322 | 0.0237 | 0.0370 | 0.0451 | 0.0259 | 0.0266 | 0.0238 |
| over/under shoot (PU) | | | | | | | | |
| System efficiency | 0.9262 | 0.9615 | 0.9236 | 0.9219 | 0.9268 | 0.9477 | 0.9436 | 0.9325 |
| NMSE_V $\times 10^{-2}$ | 0.4001 | 0.8822 | 0.3119 | 0.4564 | 0.3901 | 0.4490 | 0.3510 | 0.6597 |
| NMSE_ $\omega_m \times 10^{-2}$ | 0.3602 | 0.9359 | 0.4579 | 0.2908 | 0.1323 | 0.7642 | 0.4883 | 0.1928 |
| NMSE_I $\times 10^{-2}$ | 0.1147 | 0.2940 | 0.7839 | 0.8108 | 0.2384 | 0.6547 | 0.6095 | 0.2877 |
| THDv_bus L (%) | 3.0994 | 3.9875 | 5.7828 | 4.6533 | 5.2011 | 4.7932 | 5.0948 | 3.4442 |
| THDi_bus L (%) | 4.7972 | 4.5219 | 5.8193 | 3.8786 | 3.5328 | 4.6316 | 4.3412 | 4.1310 |
| THDv_bus M (%) | 4.3214 | 5.1195 | 4.9136 | 3.1056 | 4.0126 | 3.2539 | 3.1939 | 5.1713 |
| THDi_bus M (%) | 5.7553 | 4.4751 | 5.4657 | 3.6590 | 3.7103 | 5.5636 | 5.0273 | 5.7794 |
| Motor power factor | 0.9259 | 0.9521 | 0.9350 | 0.9388 | 0.9381 | 0.9169 | 0.9634 | 0.9344 |
| Reduction in | 16.9925 | 17.1471 | 16.2695 | 16.9366 | 17.4730 | 17.8310 | 16.5771 | 16.5401 |
| KWh consumption (%) | | | | | | | | |

controller), 0.9325 (MOGA based tuned controller), 0.9274 (SOPSO) based tuned controller and 0.9262 (MOPSO based tuned controller). Moreover, the Normalized Mean Square Error (NMSE-V) of the Motor voltage is reduced from 0.3293 (without the (GP-SF-SS) device), 0.04393 (constant gains controller), 0.03378 (ANN controller) and 0.04076 (FLC) to around 0.008807 (SOGA based tuned controller), 0.003610 (MOGA based tuned controller), 0.003016 (SOPSO) based tuned controller and 0.004001 (MOPSO based tuned controller).

In addition the (NMSE- ω_m) of the SPIM motor is reduced from 0.5093 (without the (GP-SF-SS) device), 0.05909 (constant gains controller), 0.06218 (ANN controller) and 0.07776 (FLC) to around 0.002576 (SOGA based tuned controller), 0.001543 (MOGA based tuned controller), 0.007334 (SOPSO) based tuned controller and 0.003602 (MOPSO based tuned controller). The (NMSE-I) of the Motor current is reduced from 0.2398 (without the GP-SF-SS device), 0.06488 (constant gains controller), 0.02170 (ANN controller) and 0.04893 (FLC) to around

0.003525 (SOGA based tuned controller), 0.005272 (MOGA based tuned controller), 0.002851 (SOPSO) based tuned controller and 0.001147 (MOPSO based tuned controller). Total Harmonic Distortion THD (%) of the supply voltage is reduced from 17.486 (without the (GP-SF-SS) device), 6.6869 (constant gains controller), 8.0866 (ANN controller) and 8.4756 (FLC) to around 5.1191 (SOGA based tuned controller), 5.7369 (MOGA based tuned controller), 5.5613 (SOPSO) based tuned controller and 3.0994 (MOPSO based tuned controller).

THD (%) of the supply current is reduced from 19.475 (without the GP-SF-SS device), 8.4680 (constant gains controller), 8.8441 (ANN controller) and 7.5479 (FLC) to around 3.6054 (SOGA based tuned controller), 5.3255 (MOGA based tuned controller), 5.5307 (SOPSO) based tuned controller and 4.7972 (MOPSO based tuned controller). THD (%) of the motor voltage is reduced from 16.456 (without the GP-SF-SS device), 6.9072 (constant gains controller), 7.7610 (ANN controller) and 6.2888 (FLC) to around 4.3007 (SOGA based tuned controller),

3.4279 (MOGA based tuned controller), 5.0449 (SOPSO based tuned controller and 4.3214 (MOPSO based tuned controller). THD (%) of the motor current is reduced from 18.465 (without the GP-SF-SS device), 7.5903 (constant gains controller), 8.4061 (ANN controller) and 9.3727 (FLC) to around 4.4072 (SOGA based tuned controller), 5.1945 (MOGA based tuned controller), 4.1944 (SOPSO based tuned controller and 5.7553 (MOPSO based tuned controller).

Motor power factor is improved from 0.7516 (without the GP-SF-SS device), 0.9004 (constant gains controller), 0.8909 (ANN controller) and 0.8837 (FLC) to around 0.9354 (SOGA based tuned controller), 0.9350 (MOGA based tuned controller), 0.9616 (SOPSO based tuned controller and 0.9259 (MOPSO based tuned controller). Reduction in KWh Consumption (%) is reduced from 0.000 (without the GP-SF-SS device), 13.0035 (constant gains controller), 14.6386 (ANN controller) and 14.2319 (FLC) to around 17.8021 (SOGA based tuned controller), 17.9411 (MOGA based tuned controller), 17.3185 (SOPSO based tuned controller and 17.7769 (MOPSO based tuned controller).

Self tuned modified PID controller- II: Table 17 shows the system behavior using traditional controllers with constant controller gains for the (GP-SF-SS) eight schemes. In addition, Table 18 shows system behavior comparison using the SOGA based Tuned modified PID controller-II and Table 19 shows the system behavior comparison using the MOGA based Tuned modified PID controller-II. Finally, Table 20 and 21 show system behavior comparison using the SOPSO and MOPSO respectively based tuned modified PID controller-II. Comparing the system dynamic response results of the two study cases with GA and PSO tuning algorithms and traditional controllers with constant controller gains

results, ANN controller and FLC, it is quite apparent that the GA and PSO tuning algorithms highly improved the system dynamic performance from a general power quality point of view.

The GA and PSO tuning algorithms had a great impact on Motor RMS voltage (PU) is improved from 0.8782 (without the (GP-SF-SS) device), 0.9494 (constant gains controller), 0.9414 (ANN controller) and 0.9525 (FLC) to around 0.9728 (SOGA based tuned controller), 0.9877 (MOGA based tuned controller), 0.9691 (SOPSO based tuned controller and 0.9658 (MOPSO based tuned controller). Motor RMS current (PU) is reduced from 0.8576 (without the GP-SF-SS device), 0.7353 (constant gains controller), 0.7269 (ANN controller) and 0.7158 (FLC) to around 0.5902 (SOGA based tuned controller), 0.6494 (MOGA based tuned controller), 0.6212 (SOPSO based tuned controller and 0.6077 (MOPSO based tuned controller).

Maximum Transient Motor Voltage Over/Under Shoot (PU) is reduced from 0.1597 (without the GP-SF-SS device), 0.0859 (constant gains controller), 0.0888 (ANN controller) and 0.0949 (FLC) to around 0.0274 (SOGA based tuned controller), 0.0453 (MOGA based tuned controller), 0.0464 (SOPSO based tuned controller and 0.0356 (MOPSO based tuned controller). Maximum Transient Motor Current-Over/Under Shoot (PU) is reduced from 0.1775 (without the GP-SF-SS device), 0.0925 (constant gains controller), 0.0859 (ANN controller) and 0.0928 (FLC) to around 0.0245 (SOGA based tuned controller), 0.0334 (MOGA based tuned controller), 0.0488 (SOPSO based tuned controller and 0.0453 (MOPSO based tuned controller). The system efficiency is improved from 0.8145 (without the GP-SF-SS device), 0.8817 (constant gains controller), 0.9012 (ANN controller) and 0.8788 (FLC) to around

Table 17: System dynamic behavior comparison using the constant parameters modified PID controller-II

| Items | GP-SF-SS scheme A | GP-SF-SS scheme B | GP-SF-SS scheme C | GP-SF-SS scheme D | GP-SF-SS scheme E | GP-SF-SS scheme F | GP-SF-SS scheme G | GP-SF-SS scheme H |
|--|----------------------|----------------------|----------------------|----------------------|----------------------|----------------------|----------------------|----------------------|
| RMS motor voltage (PU) | 0.9494 | 0.9482 | 0.9542 | 0.9452 | 0.9531 | 0.9552 | 0.9554 | 0.9533 |
| RMS motor current (PU) | 0.7353 | 0.7141 | 0.7237 | 0.6597 | 0.6946 | 0.6894 | 0.6674 | 0.7375 |
| Maximum transient Voltage over/under shoot (PU) | 0.0859 | 0.0892 | 0.0953 | 0.0949 | 0.0894 | 0.0954 | 0.0910 | 0.0919 |
| Maximum transient current Over/under shoot (PU) | 0.0925 | 0.0930 | 0.0925 | 0.0933 | 0.0914 | 0.0936 | 0.0914 | 0.0924 |
| System efficiency | 0.8817 | 0.8891 | 0.8670 | 0.9043 | 0.8638 | 0.8785 | 0.8747 | 0.8793 |
| NMSE _V $\times 10^{-1}$ | 0.7137 | 0.9628 | 0.8147 | 0.7674 | 0.4440 | 0.1155 | 0.4782 | 0.3914 |
| NMSE _{ω_m} $\times 10^{-1}$ | 0.7818 | 0.4832 | 0.7179 | 0.9230 | 0.7152 | 0.2297 | 0.3882 | 0.7849 |
| NMSE _I $\times 10^{-1}$ | 0.3573 | 0.7925 | 0.2951 | 0.4407 | 0.9076 | 0.9509 | 0.7527 | 0.6405 |
| THD _v bus L (%) | 9.1445 | 6.8204 | 7.5101 | 6.1985 | 7.1886 | 9.1371 | 8.6328 | 9.3997 |
| THD _i bus L (%) | 6.3350 | 7.9160 | 7.6691 | 7.3442 | 9.5192 | 6.6350 | 7.5065 | 9.7242 |
| THD _v bus M (%) | 6.2773 | 7.2342 | 6.5069 | 6.4651 | 6.6510 | 6.3815 | 8.0588 | 8.9402 |
| THD _i bus M (%) | 7.6200 | 9.2201 | 9.1022 | 6.0570 | 8.4897 | 6.4519 | 6.8475 | 9.5024 |
| Motor power factor | 0.8543 | 0.9031 | 0.8554 | 0.8789 | 0.8893 | 0.8850 | 0.8639 | 0.8854 |
| Reduction in KWh consumption (%) | 12.6287 | 13.8898 | 13.7387 | 12.9955 | 12.6808 | 13.3602 | 13.9421 | 13.9100 |

Table 18: System dynamic behavior comparison using the SOGA based tuned modified PID controller-II

| Items | GP-SF-SS scheme A | GP-SF-SS scheme B | GP-SF-SS scheme C | GP-SF-SS scheme D | GP-SF-SS scheme E | GP-SF-SS scheme F | GP-SF-SS scheme G | GP-SF-SS scheme H |
|--|----------------------|----------------------|----------------------|----------------------|----------------------|----------------------|----------------------|----------------------|
| RMS motor voltage (PU) | 0.9728 | 0.9752 | 0.9637 | 0.9811 | 0.9680 | 0.9939 | 0.9844 | 0.9717 |
| RMS motor current (PU) | 0.5902 | 0.6531 | 0.6617 | 0.5941 | 0.5910 | 0.6486 | 0.6450 | 0.6386 |
| Maximum transient voltage over/under shoot (PU) | 0.0274 | 0.0243 | 0.0478 | 0.0291 | 0.0275 | 0.0232 | 0.0387 | 0.0371 |
| Maximum transient current over/under shoot (PU) | 0.0245 | 0.0396 | 0.0342 | 0.0237 | 0.0323 | 0.0288 | 0.0476 | 0.0394 |
| System efficiency | 0.9280 | 0.9420 | 0.9233 | 0.9190 | 0.9638 | 0.9232 | 0.9191 | 0.9147 |
| NMSE _V $\times 10^{-2}$ | 0.1593 | 0.4007 | 0.3164 | 0.5676 | 0.6894 | 0.2995 | 0.6774 | 0.2137 |
| NMSE _{ω_m} $\times 10^{-2}$ | 0.8402 | 0.2551 | 0.6361 | 0.6549 | 0.7682 | 0.5775 | 0.4595 | 0.2931 |
| NMSE _I $\times 10^{-2}$ | 0.6472 | 0.8215 | 0.7625 | 0.7631 | 0.7102 | 0.8097 | 0.2721 | 0.2798 |
| THDv _{bus L} (%) | 3.5030 | 3.7920 | 5.3193 | 4.1622 | 4.8884 | 3.8308 | 5.7405 | 4.6522 |
| THDi _{bus L} (%) | 3.7712 | 4.7880 | 4.9456 | 5.1057 | 5.6602 | 4.7600 | 5.1096 | 4.8218 |
| THDv _{bus M} (%) | 5.7026 | 4.5343 | 5.5958 | 3.8965 | 5.0717 | 4.1062 | 5.5637 | 3.2154 |
| THDi _{bus M} (%) | 5.1524 | 5.7183 | 4.1171 | 3.1807 | 4.0832 | 4.8812 | 5.0063 | 3.2784 |
| Motor power factor | 0.9538 | 0.9596 | 0.9120 | 0.9393 | 0.9450 | 0.9259 | 0.9330 | 0.9638 |
| Reduction in KWh consumption (%) | 16.1947 | 16.9438 | 16.9185 | 16.7393 | 16.3354 | 17.3915 | 17.4392 | 17.4965 |

Table 19: System dynamic behavior comparison using a selected solution from the MOGA Pareto front based tuned modified PID controller-II

| Items | GP-SF-SS scheme A | GP-SF-SS scheme B | GP-SF-SS scheme C | GP-SF-SS scheme D | GP-SF-SS scheme E | GP-SF-SS scheme F | GP-SF-SS scheme G | GP-SF-SS scheme H |
|--|----------------------|----------------------|----------------------|----------------------|----------------------|----------------------|----------------------|----------------------|
| RMS motor voltage (PU) | 0.9877 | 0.9732 | 0.9784 | 0.9935 | 0.9858 | 0.9715 | 0.9906 | 0.9842 |
| RMS motor current (PU) | 0.6494 | 0.6083 | 0.6374 | 0.6688 | 0.6253 | 0.6653 | 0.6545 | 0.6626 |
| Maximum transient voltage over/under shoot (PU) | 0.0453 | 0.0443 | 0.0457 | 0.0388 | 0.0376 | 0.0389 | 0.0247 | 0.0263 |
| Maximum transient current over/under shoot (PU) | 0.0334 | 0.0374 | 0.0293 | 0.0437 | 0.0326 | 0.0227 | 0.0381 | 0.0374 |
| System efficiency | 0.9451 | 0.9231 | 0.9605 | 0.9190 | 0.9633 | 0.9448 | 0.9459 | 0.9126 |
| NMSE _V $\times 10^{-2}$ | 0.2924 | 0.7655 | 0.8916 | 0.3088 | 0.4079 | 0.7081 | 0.1263 | 0.5883 |
| NMSE _{ω_m} $\times 10^{-2}$ | 0.6290 | 0.4958 | 0.1378 | 0.9557 | 0.1469 | 0.1525 | 0.2091 | 0.3759 |
| NMSE _I $\times 10^{-2}$ | 0.7173 | 0.2170 | 0.5490 | 0.1939 | 0.7036 | 0.3465 | 0.5061 | 0.6605 |
| THDv _{bus L} (%) | 3.7913 | 3.7029 | 4.2263 | 4.7116 | 4.2097 | 5.1923 | 3.0945 | 4.9809 |
| THDi _{bus L} (%) | 4.2106 | 5.5442 | 3.9993 | 5.3079 | 5.8335 | 5.2306 | 5.4306 | 4.8899 |
| THDv _{bus M} (%) | 4.9854 | 4.7610 | 4.7671 | 5.3682 | 5.7911 | 4.2588 | 5.4148 | 4.1447 |
| THDi _{bus M} (%) | 4.5770 | 3.1418 | 3.6778 | 4.1496 | 3.3631 | 4.2735 | 3.1674 | 5.8402 |
| Motor power factor | 0.9456 | 0.9393 | 0.9395 | 0.9451 | 0.9623 | 0.9237 | 0.9647 | 0.9585 |
| Reduction in KWh consumption (%) | 16.0577 | 16.4092 | 17.2120 | 16.1411 | 16.7683 | 17.3021 | 17.4765 | 17.4260 |

Table 20: System dynamic behavior comparison using the SOPSO based tuned modified PID controller-II

| Items | GP-SF-SS scheme A | GP-SF-SS scheme B | GP-SF-SS scheme C | GP-SF-SS scheme D | GP-SF-SS scheme E | GP-SF-SS scheme F | GP-SF-SS scheme G | GP-SF-SS scheme H |
|--|----------------------|----------------------|----------------------|----------------------|----------------------|----------------------|----------------------|----------------------|
| RMS motor voltage (PU) | 0.9691 | 0.9713 | 0.9835 | 0.9842 | 0.9763 | 0.9825 | 0.9788 | 0.9663 |
| RMS motor current (PU) | 0.6212 | 0.6433 | 0.6324 | 0.6258 | 0.5867 | 0.5974 | 0.6142 | 0.6049 |
| Maximum transient voltage over/under shoot (PU) | 0.0464 | 0.0346 | 0.0441 | 0.0256 | 0.0237 | 0.0323 | 0.0322 | 0.0353 |
| Maximum transient current over/under shoot (PU) | 0.0488 | 0.0314 | 0.0289 | 0.0381 | 0.0364 | 0.0264 | 0.0354 | 0.0357 |
| System efficiency | 0.9210 | 0.9353 | 0.9518 | 0.9445 | 0.9254 | 0.9305 | 0.9444 | 0.9298 |
| NMSE _V $\times 10^{-2}$ | 0.1438 | 0.8751 | 0.9360 | 0.2779 | 0.2432 | 0.2977 | 0.5851 | 0.8705 |
| NMSE _{ω_m} $\times 10^{-2}$ | 0.3834 | 0.4972 | 0.4976 | 0.6141 | 0.7204 | 0.7205 | 0.3294 | 0.2099 |
| NMSE _I $\times 10^{-2}$ | 0.2045 | 0.2107 | 0.4115 | 0.7322 | 0.4376 | 0.7131 | 0.4177 | 0.1244 |
| THDv _{bus L} (%) | 4.4817 | 5.7854 | 3.7209 | 4.9114 | 3.4368 | 4.1675 | 3.4236 | 3.9953 |
| THDi _{bus L} (%) | 4.3172 | 3.7147 | 5.3702 | 3.8792 | 3.1158 | 5.8145 | 4.3786 | 4.7285 |
| THDv _{bus M} (%) | 3.3625 | 4.4435 | 3.8304 | 3.3385 | 4.4359 | 4.0905 | 3.7869 | 5.7272 |
| THDi _{bus M} (%) | 4.7629 | 4.3552 | 4.4650 | 3.9976 | 3.2615 | 3.7452 | 4.5081 | 3.4193 |
| Motor power factor | 0.9202 | 0.9640 | 0.9277 | 0.9201 | 0.9616 | 0.9476 | 0.9346 | 0.9561 |
| Reduction in KWh consumption (%) | 16.0506 | 16.8014 | 17.4067 | 16.2125 | 16.0961 | 17.2636 | 17.2558 | 16.0565 |

0.9280 (SOGA based tuned controller), 0.9451 (MOGA based tuned controller), 0.9210 (SOPSO) based tuned controller and 0.9388 (MOPSO based tuned controller). Moreover, the Normalized Mean Square Error (NMSE-V)

of the Motor voltage is reduced from 0.3293 (without the GP-SF-SS device), 0.07137 (constant gains controller), 0.03378 (ANN controller) and 0.04076 (FLC) to around 0.001593 (SOGA based tuned controller), 0.002924 (MOGA

Table 21: System dynamic behavior comparison using a selected solution from the MOPSO Pareto front based tuned modified PID controller-II

| Items | GP-SF-SS scheme A | GP-SF-SS scheme B | GP-SF-SS scheme C | GP-SF-SS scheme D | GP-SF-SS scheme E | GP-SF-SS scheme F | GP-SF-SS scheme G | GP-SF-SS scheme H |
|--|----------------------|----------------------|----------------------|----------------------|----------------------|----------------------|----------------------|----------------------|
| RMS motor voltage (PU) | 0.9658 | 0.9745 | 0.9654 | 0.9767 | 0.9858 | 0.9678 | 0.9661 | 0.9837 |
| RMS motor current (PU) | 0.6077 | 0.6634 | 0.6411 | 0.5867 | 0.5864 | 0.5811 | 0.6004 | 0.6265 |
| Maximum transient voltage over/under shoot (PU) | 0.0356 | 0.0229 | 0.0282 | 0.0310 | 0.0469 | 0.0306 | 0.0289 | 0.0339 |
| Maximum transient current over/under shoot (PU) | 0.0453 | 0.0270 | 0.0360 | 0.0344 | 0.0309 | 0.0324 | 0.0465 | 0.0430 |
| System efficiency | 0.9388 | 0.9367 | 0.9249 | 0.9419 | 0.9523 | 0.9302 | 0.9356 | 0.9393 |
| NMSE _V $\times 10^{-2}$ | 0.2527 | 0.8499 | 0.5878 | 0.1414 | 0.2545 | 0.2573 | 0.1942 | 0.7567 |
| NMSE _{ω_m} $\times 10^{-2}$ | 0.3195 | 0.7626 | 0.5715 | 0.9205 | 0.9568 | 0.1509 | 0.9511 | 0.3834 |
| NMSE _I $\times 10^{-2}$ | 0.4985 | 0.7233 | 0.9082 | 0.5814 | 0.2122 | 0.5592 | 0.5918 | 0.2730 |
| THD _{bus L} (%) | 4.5813 | 3.0403 | 3.3773 | 3.1796 | 5.1786 | 3.2238 | 5.0529 | 3.4189 |
| THD _{bus M} (%) | 3.0598 | 3.0348 | 5.8151 | 5.3175 | 5.2004 | 5.5762 | 3.3719 | 3.2936 |
| THD _{bus M} (%) | 5.5529 | 5.8125 | 5.6285 | 4.1372 | 4.8947 | 4.5492 | 3.6188 | 3.8853 |
| THD _{bus M} (%) | 3.8990 | 3.9833 | 5.3316 | 3.0342 | 4.4183 | 4.7566 | 4.0797 | 3.5826 |
| Motor power factor | 0.9213 | 0.9406 | 0.9369 | 0.9508 | 0.9639 | 0.9473 | 0.9481 | 0.9583 |
| Reduction in KWh consumption (%) | 17.2531 | 17.2990 | 16.7742 | 17.1882 | 16.9379 | 16.1134 | 16.0796 | 16.6572 |

based tuned controller), 0.001438 (SOPSO) based tuned controller and 0.002527 (MOPSO based tuned controller). In addition the (NMSE- ω_m) of the SPIM motor is reduced from 0.5093 (without the GP-SF-SS device), 0.07818 (constant gains controller), 0.06218 (ANN controller) and 0.07776 (FLC) to around 0.008402 (SOGA based tuned controller), 0.006290 (MOGA based tuned controller), 0.003834 (SOPSO) based tuned controller and 0.003195 (MOPSO based tuned controller).

The (NMSE-I) of the motor current is reduced from 0.2398 (without the GP-SF-SS device), 0.03573 (constant gains controller), 0.02170 (ANN controller) and 0.04893 (FLC) to around 0.006472 (SOGA based tuned controller), 0.007173 (MOGA based tuned controller), 0.002045 (SOPSO) based tuned controller and 0.004985 (MOPSO based tuned controller).

Total Harmonic Distortion THD (%) of the supply voltage is reduced from 17.486 (without the GP-SF-SS device), 9.1445 (constant gains controller), 8.0866 (ANN controller) and 8.4756 (FLC) to around 3.5030 (SOGA based tuned controller), 3.7913 (MOGA based tuned controller), 4.4817 (SOPSO) based tuned controller and 4.5813 (MOPSO based tuned controller).

THD (%) of the supply current is reduced from 19.475 (without the GP-SF-SS device), 6.3350 (constant gains controller), 8.8441 (ANN controller) and 7.5479 (FLC) to around 3.7712 (SOGA based tuned controller), 4.2106 (MOGA based tuned controller), 4.3172 (SOPSO) based tuned controller and 3.0598 (MOPSO based tuned controller). THD (%) of the motor voltage is reduced from 16.456 (without the GP-SF-SS device), 6.2773 (constant gains controller), 7.7610 (ANN controller) and 6.2888 (FLC) to around 5.7026 (SOGA based tuned controller), 4.9854 (MOGA based tuned controller), 3.3625 (SOPSO) based tuned controller and 5.5529 (MOPSO based tuned controller).

THD (%) of the motor current is reduced from 18.465 (without the GP-SF-SS device), 7.6200 (constant gains controller), 8.4061 (ANN controller) and 9.3727 (FLC) to around 5.1524 (SOGA based tuned controller), 4.5770 (MOGA based tuned controller), 4.7629 (SOPSO) based tuned controller and 3.8990 (MOPSO based tuned controller). Motor power factor is improved from 0.7516 (without the GP-SF-SS device), 0.8543 (constant gains controller), 0.8909 (ANN controller) and 0.8837 (FLC) to around 0.9538 (SOGA based tuned controller), 0.9456 (MOGA based tuned controller), 0.9202 (SOPSO) based tuned controller and 0.9213 (MOPSO based tuned controller). Reduction in KWh Consumption (%) is reduced from 0.000 (without the GP-SF-SS device), 12.6287 (constant gains controller), 12.6386 (ANN controller) and 12.2319 (FLC) to around 16.5828 (SOGA based tuned controller), 17.1336 (MOGA based tuned controller), 16.0191 (SOPSO) based tuned controller and 17.4657 (MOPSO based tuned controller).

Self tuned Variable Structure Sliding Mode Controller (VSC/SMC/B-B): Table 22 shows the system behavior using traditional controllers with constant controller gains for the (GP-SF-SS) eight schemes.

Table 23 shows system behavior comparison using the SOGA based the self tuned variable structure sliding mode controller and Table 24 shows the system behavior comparison using the MOGA based the self tuned variable structure sliding mode controller.

Finally, Table 25 and 26 show system behavior comparison using the SOPSO and MOPSO, respectively based the self tuned variable structure sliding mode controller. Comparing the system dynamic response results of the two study cases, with GA and PSO tuning

Table 22: System dynamic behavior comparison using the constant parameters variable structure sliding mode controller

| Items | GP-SF-SS scheme A | GP-SF-SS scheme B | GP-SF-SS scheme C | GP-SF-SS scheme D | GP-SF-SS scheme E | GP-SF-SS scheme F | GP-SF-SS scheme G | GP-SF-SS scheme H |
|--|----------------------|----------------------|----------------------|----------------------|----------------------|----------------------|----------------------|----------------------|
| RMS motor voltage (PU) | 0.9433 | 0.9255 | 0.9255 | 0.9307 | 0.9426 | 0.9267 | 0.9360 | 0.9439 |
| RMS motor current (PU) | 0.7381 | 0.6974 | 0.7504 | 0.6655 | 0.7413 | 0.7308 | 0.6966 | 0.7152 |
| Maximum transient voltage over/under shoot (PU) | 0.0963 | 0.0948 | 0.0893 | 0.0922 | 0.0872 | 0.0886 | 0.0946 | 0.0931 |
| Maximum transient current over/under shoot (PU) | 0.0859 | 0.0919 | 0.0908 | 0.0957 | 0.0889 | 0.0865 | 0.0910 | 0.0965 |
| System efficiency | 0.8600 | 0.8684 | 0.8863 | 0.8962 | 0.8528 | 0.8733 | 0.8943 | 0.8603 |
| NMSE_V $\times 10^{-1}$ | 0.3769 | 0.9310 | 0.9132 | 0.2972 | 0.7992 | 0.3404 | 0.8021 | 0.4641 |
| NMSE_ $\omega_m \times 10^{-1}$ | 0.6436 | 0.5793 | 0.5509 | 0.1301 | 0.4771 | 0.1291 | 0.1325 | 0.5180 |
| NMSE_I $\times 10^{-1}$ | 0.5613 | 0.9268 | 0.7721 | 0.2488 | 0.6421 | 0.7495 | 0.2426 | 0.6112 |
| THDv_bus L (%) | 6.5757 | 6.8160 | 9.2780 | 8.7515 | 6.3297 | 9.1557 | 7.3576 | 6.6441 |
| THDi_bus L (%) | 8.0879 | 9.5562 | 7.6951 | 8.0894 | 8.6950 | 6.0297 | 9.2242 | 9.4264 |
| THDv_bus M (%) | 6.0975 | 6.3986 | 7.4541 | 9.7252 | 8.3935 | 8.5866 | 7.7680 | 9.2297 |
| THDi_bus M (%) | 9.1725 | 8.0970 | 6.3755 | 7.1521 | 8.3271 | 6.7217 | 8.8283 | 8.1229 |
| Motor power factor | 0.8685 | 0.8854 | 0.8832 | 0.8548 | 0.8980 | 0.8905 | 0.8527 | 0.8914 |
| Reduction in KWh consumption (%) | 12.8652 | 12.9883 | 13.9106 | 13.5067 | 12.6772 | 12.7328 | 12.8655 | 13.5720 |

Table 23: System dynamic behavior comparison using the SOGA based tuned variable structure sliding mode controller

| Items | GP-SF-SS scheme A | GP-SF-SS scheme B | GP-SF-SS scheme C | GP-SF-SS scheme D | GP-SF-SS scheme E | GP-SF-SS scheme F | GP-SF-SS scheme G | GP-SF-SS scheme H |
|--|----------------------|----------------------|----------------------|----------------------|----------------------|----------------------|----------------------|----------------------|
| RMS motor voltage (PU) | 0.9897 | 0.9892 | 0.9767 | 0.9843 | 0.9841 | 0.9822 | 0.9781 | 0.9889 |
| RMS motor current (PU) | 0.6286 | 0.6361 | 0.6417 | 0.6410 | 0.6589 | 0.5812 | 0.6079 | 0.6501 |
| Maximum transient voltage over/under shoot (PU) | 0.0425 | 0.0400 | 0.0480 | 0.0450 | 0.0349 | 0.0394 | 0.0235 | 0.0369 |
| Maximum transient current over/under shoot (PU) | 0.0345 | 0.0459 | 0.0456 | 0.0350 | 0.0437 | 0.0401 | 0.0219 | 0.0255 |
| System efficiency | 0.9360 | 0.9250 | 0.9644 | 0.9418 | 0.9236 | 0.9585 | 0.9505 | 0.9572 |
| NMSE_V $\times 10^{-2}$ | 0.9052 | 0.5126 | 0.7802 | 0.6428 | 0.1495 | 0.1789 | 0.5138 | 0.4751 |
| NMSE_ $\omega_m \times 10^{-2}$ | 0.9566 | 0.5780 | 0.9161 | 0.2047 | 0.2551 | 0.4279 | 0.6962 | 0.9476 |
| NMSE_I $\times 10^{-2}$ | 0.1561 | 0.1892 | 0.1810 | 0.6909 | 0.8941 | 0.1720 | 0.6173 | 0.3063 |
| THDv_bus L (%) | 5.3814 | 3.0527 | 3.1587 | 4.4393 | 3.8467 | 3.0609 | 5.2676 | 3.2121 |
| THDi_bus L (%) | 5.8074 | 4.0206 | 4.7807 | 4.4807 | 5.3266 | 4.4048 | 5.0903 | 5.0312 |
| THDv_bus M (%) | 4.5868 | 3.2134 | 4.4250 | 5.3862 | 4.3253 | 5.2276 | 4.4124 | 4.9892 |
| THDi_bus M (%) | 3.5953 | 3.7997 | 4.3836 | 4.1535 | 5.0078 | 3.9306 | 3.1589 | 5.2204 |
| Motor power factor | 0.9440 | 0.9549 | 0.9364 | 0.9168 | 0.9173 | 0.9583 | 0.9151 | 0.9569 |
| Reduction in KWh consumption (%) | 16.4575 | 17.3265 | 16.6721 | 17.9670 | 17.4947 | 16.8581 | 17.5310 | 16.5667 |

Table 24: System dynamic behavior comparison using a selected solution from the MOGA Pareto front based tuned variable structure sliding mode controller

| Items | GP-SF-SS scheme A | GP-SF-SS scheme B | GP-SF-SS scheme C | GP-SF-SS scheme D | GP-SF-SS scheme E | GP-SF-SS scheme F | GP-SF-SS scheme G | GP-SF-SS scheme H |
|--|----------------------|----------------------|----------------------|----------------------|----------------------|----------------------|----------------------|----------------------|
| RMS motor voltage (PU) | 0.9893 | 0.9899 | 0.9848 | 0.9864 | 0.9775 | 0.9847 | 0.9897 | 0.9933 |
| RMS motor current (PU) | 0.6394 | 0.5993 | 0.6342 | 0.6344 | 0.6394 | 0.5965 | 0.6373 | 0.5953 |
| Maximum transient voltage over/under shoot (PU) | 0.0401 | 0.0425 | 0.0315 | 0.0464 | 0.0315 | 0.0235 | 0.0418 | 0.0485 |
| Maximum transient current over/under shoot (PU) | 0.0262 | 0.0334 | 0.0245 | 0.0344 | 0.0460 | 0.0327 | 0.0289 | 0.0317 |
| System efficiency | 0.9429 | 0.9439 | 0.9378 | 0.9619 | 0.9303 | 0.9225 | 0.9171 | 0.9465 |
| NMSE_V $\times 10^{-2}$ | 0.9433 | 0.4550 | 0.5516 | 0.5471 | 0.6182 | 0.4256 | 0.2076 | 0.6312 |
| NMSE_ $\omega_m \times 10^{-2}$ | 0.5618 | 0.5446 | 0.2318 | 0.3872 | 0.5468 | 0.7479 | 0.7313 | 0.7201 |
| NMSE_I $\times 10^{-2}$ | 0.4695 | 0.6063 | 0.3295 | 0.6326 | 0.6434 | 0.8820 | 0.6294 | 0.9610 |
| THDv_bus L (%) | 3.3714 | 5.5126 | 5.3215 | 5.1804 | 5.3135 | 4.9511 | 4.7887 | 4.0627 |
| THDi_bus L (%) | 5.1991 | 5.0793 | 5.6082 | 3.3219 | 5.5356 | 4.7045 | 3.0560 | 3.6958 |
| THDv_bus M (%) | 4.4394 | 4.2025 | 5.2826 | 5.5403 | 4.4735 | 4.1239 | 5.6535 | 3.8214 |
| THDi_bus M (%) | 5.2254 | 5.3110 | 5.0673 | 3.1500 | 4.7562 | 3.9698 | 4.6729 | 5.6042 |
| Motor power factor | 0.9623 | 0.9236 | 0.9438 | 0.9373 | 0.9591 | 0.9522 | 0.9357 | 0.9122 |
| Reduction in KWh consumption (%) | 17.7936 | 16.0550 | 17.5783 | 17.9888 | 18.0277 | 17.6206 | 16.9121 | 17.0328 |

algorithms and traditional controllers with constant controller gains results, ANN controller and FLC, it is quite apparent that the GA and PSO tuning algorithms highly improved the system dynamic performance from a

general power quality point of view. The GA and PSO tuning algorithms had a great impact on Motor RMS voltage (PU) is improved from 0.8782 (without the GP-SF-SS device), 0.9433 (constant gains controller), 0.9414

Table 25: System dynamic behavior comparison using the SOPSO based tuned variable structure sliding mode controller

| Items | GP-SF-SS scheme A | GP-SF-SS scheme B | GP-SF-SS scheme C | GP-SF-SS scheme D | GP-SF-SS scheme E | GP-SF-SS scheme F | GP-SF-SS scheme G | GP-SF-SS scheme H |
|--|----------------------|----------------------|----------------------|----------------------|----------------------|----------------------|----------------------|----------------------|
| RMS motor voltage (PU) | 0.9806 | 0.9802 | 0.9927 | 0.9798 | 0.9915 | 0.9936 | 0.9798 | 0.9799 |
| RMS motor current (PU) | 0.5816 | 0.6537 | 0.6359 | 0.6304 | 0.6020 | 0.6540 | 0.6037 | 0.6478 |
| Maximum transient voltage over/under shoot (PU) | 0.0276 | 0.0263 | 0.0396 | 0.0219 | 0.0312 | 0.0295 | 0.0231 | 0.0245 |
| Maximum transient Current over/under shoot (PU) | 0.0333 | 0.0446 | 0.0461 | 0.0225 | 0.0421 | 0.0454 | 0.0421 | 0.0484 |
| System efficiency | 0.9567 | 0.9450 | 0.9449 | 0.9626 | 0.9275 | 0.9454 | 0.9401 | 0.9581 |
| NMSE _V $\times 10^{-2}$ | 0.8955 | 0.1152 | 0.9075 | 0.3170 | 0.9514 | 0.7139 | 0.7336 | 0.8753 |
| NMSE _{ω_m} $\times 10^{-2}$ | 0.4872 | 0.9507 | 0.7797 | 0.5850 | 0.2811 | 0.5647 | 0.1954 | 0.4885 |
| NMSE _I $\times 10^{-2}$ | 0.3756 | 0.7838 | 0.7896 | 0.5872 | 0.7103 | 0.1617 | 0.3679 | 0.1525 |
| THD _v bus L (%) | 4.2650 | 3.4415 | 4.7792 | 5.1551 | 3.8153 | 4.5126 | 3.9054 | 3.5358 |
| THDi _{bus} L (%) | 5.5612 | 3.1049 | 3.8194 | 3.5532 | 4.7433 | 3.6139 | 5.8433 | 3.0693 |
| THDv _{bus} M (%) | 4.6731 | 4.9615 | 5.1879 | 5.5603 | 5.7558 | 5.5833 | 3.5268 | 5.7888 |
| THDi _{bus} M (%) | 3.7393 | 3.4340 | 3.9875 | 5.0950 | 3.1176 | 4.5609 | 4.6010 | 4.9156 |
| Motor power factor | 0.9444 | 0.9592 | 0.9498 | 0.9226 | 0.9176 | 0.9511 | 0.9523 | 0.9267 |
| Reduction in KWh consumption (%) | 16.9575 | 17.1734 | 17.6314 | 16.1444 | 17.2443 | 16.1263 | 16.8650 | 16.6417 |

Table 26: System dynamic behavior comparison using a selected solution from the MOPSO pareto front based tuned variable structure sliding mode controller

| Items | GP-SF-SS scheme A | GP-SF-SS scheme B | GP-SF-SS scheme C | GP-SF-SS scheme D | GP-SF-SS scheme E | GP-SF-SS scheme F | GP-SF-SS scheme G | GP-SF-SS scheme H |
|--|----------------------|----------------------|----------------------|----------------------|----------------------|----------------------|----------------------|----------------------|
| RMS motor voltage (PU) | 0.9760 | 0.9766 | 0.9881 | 0.9789 | 0.9923 | 0.9786 | 0.9785 | 0.9954 |
| RMS motor current (PU) | 0.6490 | 0.6400 | 0.5918 | 0.5886 | 0.5813 | 0.6059 | 0.6535 | 0.6687 |
| Maximum transient voltage over/under shoot (PU) | 0.0488 | 0.0354 | 0.0446 | 0.0397 | 0.0304 | 0.0402 | 0.0318 | 0.0480 |
| Maximum transient current over/under shoot (PU) | 0.0354 | 0.0244 | 0.0406 | 0.0362 | 0.0280 | 0.0420 | 0.0238 | 0.0487 |
| System efficiency | 0.9561 | 0.9371 | 0.9299 | 0.9407 | 0.9417 | 0.9610 | 0.9264 | 0.9276 |
| NMSE _V $\times 10^{-2}$ | 0.8868 | 0.3567 | 0.8480 | 0.4443 | 0.4895 | 0.4691 | 0.9470 | 0.6252 |
| NMSE _{ω_m} $\times 10^{-2}$ | 0.2801 | 0.6030 | 0.9367 | 0.6884 | 0.1285 | 0.4599 | 0.6357 | 0.3357 |
| NMSE _I $\times 10^{-2}$ | 0.8297 | 0.3605 | 0.3022 | 0.3046 | 0.3535 | 0.8193 | 0.5832 | 0.5447 |
| THDv _{bus} L (%) | 3.8253 | 3.9468 | 4.3685 | 3.6609 | 5.7422 | 3.8885 | 5.2245 | 5.5537 |
| THDi _{bus} L (%) | 5.2151 | 4.2433 | 4.2551 | 3.6561 | 3.0591 | 4.0850 | 5.3932 | 3.8313 |
| THDv _{bus} M (%) | 4.2222 | 4.1980 | 4.1197 | 5.4412 | 5.3492 | 5.6062 | 5.3860 | 5.4766 |
| THDi _{bus} M (%) | 5.6939 | 3.0614 | 3.1751 | 5.1101 | 4.8191 | 5.6545 | 4.3254 | 4.4722 |
| Motor power factor | 0.9518 | 0.9198 | 0.9470 | 0.9244 | 0.9505 | 0.9256 | 0.9368 | 0.9574 |
| Reduction in KWh consumption (%) | 17.1977 | 17.5629 | 17.0965 | 17.3205 | 16.4476 | 16.7930 | 17.6094 | 17.4021 |

(ANN controller) and 0.9525 (FLC) to around 0.9897 (SOGA based tuned controller), 0.9893 (MOGA based tuned controller), 0.9806 (SOPSO) based tuned controller and 0.9760 (MOPSO based tuned controller). Motor RMS current (PU) is reduced from 0.8576 (without the GP-SF-SS device), 0.7381 (constant gains controller), 0.7269 (ANN controller) and 0.7158 (FLC) to around 0.6286 (SOGA based tuned controller), 0.6394 (MOGA based tuned controller), 0.5816 (SOPSO) based tuned controller and 0.6490 (MOPSO based tuned controller).

Maximum transient motor voltage over/Under shoot (PU) is reduced from 0.1597 (without the GP-SF-SS device), 0.0963 (constant gains controller), 0.0888 (ANN controller) and 0.0949 (FLC) to around 0.0425 (SOGA based tuned controller), 0.0401 (MOGA based tuned controller), 0.0276 (SOPSO) based tuned controller and 0.0488 (MOPSO based tuned controller). Maximum transient motor current-over/under shoot (PU) is reduced from 0.1775 (without the GP-SF-SS device), 0.0859 (constant gains controller), 0.0859 (ANN controller) and

0.0928 (FLC) to around 0.0345 (SOGA based tuned controller), 0.0262 (MOGA based tuned controller), 0.0333 (SOPSO) based tuned controller and 0.0354 (MOPSO based tuned controller). The system efficiency is improved from 0.8145 (without the GP-SF-SS device), 0.8600 (constant gains controller), 0.9012 (ANN controller) and 0.8788 (FLC) to around 0.9360 (SOGA based tuned controller), 0.9429 (MOGA based tuned controller), 0.9567 (SOPSO) based tuned controller and 0.9561 (MOPSO based tuned controller).

The Normalized Mean Square Error (NMSE-V) of the Motor voltage is reduced from 0.329 (without the GP-SF-SS device), 0.0376 (constant gains controller), 0.0337 (ANN controller) and 0.04076 (FLC) to around 0.0905 (SOGA based tuned controller), 0.00943 (MOGA based tuned controller), 0.008955 (SOPSO) based tuned controller and 0.008868 (MOPSO based tuned controller). In addition the (NMSE- ω_m) of the SPIM motor is reduced from 0.5093 (without the GP-SF-SS device), 0.06436 (constant gains controller), 0.06218 (ANN controller) and

Table 27: System dynamic behavior comparison using the constant parameters zonal activation or target practice controller

| Items | GP-SF-SS scheme A | GP-SF-SS scheme B | GP-SF-SS scheme C | GP-SF-SS scheme D | GP-SF-SS scheme E | GP-SF-SS scheme F | GP-SF-SS scheme G | GP-SF-SS scheme H |
|--|----------------------|----------------------|----------------------|----------------------|----------------------|----------------------|----------------------|----------------------|
| RMS motor voltage (PU) | 0.9382 | 0.9352 | 0.9344 | 0.9360 | 0.9368 | 0.9427 | 0.9286 | 0.9261 |
| RMS motor current (PU) | 0.7499 | 0.7172 | 0.6760 | 0.6870 | 0.6697 | 0.7015 | 0.6930 | 0.6987 |
| Maximum transient voltage over/under shoot (PU) | 0.0959 | 0.0919 | 0.0929 | 0.0942 | 0.0870 | 0.0858 | 0.0917 | 0.0859 |
| Maximum transient Current over/under shoot (PU) | 0.0907 | 0.0879 | 0.0944 | 0.0925 | 0.0860 | 0.0955 | 0.0941 | 0.0957 |
| System efficiency | 0.8673 | 0.8920 | 0.8574 | 0.8639 | 0.8778 | 0.8982 | 0.8826 | 0.8742 |
| NMSE_V $\times 10^{-1}$ | 0.6263 | 0.6762 | 0.6123 | 0.8988 | 0.5377 | 0.8272 | 0.8963 | 0.6289 |
| NMSE_ $\omega_m \times 10^{-1}$ | 0.8417 | 0.2866 | 0.5197 | 0.4371 | 0.4737 | 0.5362 | 0.1873 | 0.6084 |
| NMSE_I $\times 10^{-1}$ | 0.1299 | 0.1159 | 0.5846 | 0.2074 | 0.7075 | 0.7526 | 0.3250 | 0.3244 |
| THDi_bus L (%) | 6.6196 | 9.5629 | 6.7957 | 6.0542 | 8.6596 | 7.5567 | 7.4748 | 9.4791 |
| THDi_bus L (%) | 9.6328 | 7.8362 | 6.0898 | 9.1605 | 6.2415 | 6.3669 | 8.6885 | 6.5851 |
| THDi_bus M (%) | 6.2423 | 6.2644 | 8.7887 | 6.1509 | 8.6849 | 6.8685 | 8.4157 | 7.9866 |
| THDi_bus M (%) | 8.2256 | 7.1214 | 9.4389 | 6.3763 | 7.1414 | 9.1679 | 9.8268 | 6.2814 |
| Motor power factor | 0.8950 | 0.8888 | 0.8753 | 0.8769 | 0.8987 | 0.8861 | 0.8596 | 0.8631 |
| Reduction in KWh consumption (%) | 12.8356 | 12.2520 | 13.3622 | 13.9313 | 13.2306 | 13.0419 | 12.7971 | 13.0469 |

0.07776 (FLC) to around 0.09566 (SOGA based tuned controller), 0.005618 (MOGA based tuned controller), 0.004872 (SOPSO) based tuned controller and 0.002801 (MOPSO based tuned controller).

The Normalized (NMSE-I) of the Motor current is reduced from 0.2398 (without the GP-SF-SS device), 0.05613 (constant gains controller), 0.02170 (ANN controller) and 0.04893 (FLC) to around 0.01561 (SOGA based tuned controller), 0.004695 (MOGA based tuned controller), 0.003756 (SOPSO) based tuned controller and 0.008297 (MOPSO based tuned controller). Total Harmonic Distortion THD (%) of the supply voltage is reduced from 17.486 (without the GP-SF-SS device), 6.5757 (constant gains controller), 8.0866 (ANN controller) and 8.4756 (FLC) to around 5.3814 (SOGA based tuned controller), 3.3714 (MOGA based tuned controller), 4.2650 (SOPSO) based tuned controller and 3.8253 (MOPSO based tuned controller).

THD (%) of the supply current is reduced from 19.475 (without the GP-SF-SS device), 8.0879 (constant gains controller), 8.8441 (ANN controller) and 7.5479 (FLC) to around 5.8074 (SOGA based tuned controller), 5.1991 (MOGA based tuned controller), 5.5612 (SOPSO) based tuned controller and 5.2151 (MOPSO based tuned controller).

THD (%) of the motor voltage is reduced from 16.456 (without the GP-SF-SS device), 6.0975 (constant gains controller), 7.7610 (ANN controller) and 6.2888 (FLC) to around 4.5868 (SOGA based tuned controller), 4.4394 (MOGA based tuned controller), 4.6731 (SOPSO based tuned controller) and 4.2222 (MOPSO based tuned controller). THD (%) of the motor current is reduced from 18.465 (without the GP-SF-SS device), 9.1725 (constant gains controller), 8.4061 (ANN controller) and 9.3727 (FLC) to around 3.5953 (SOGA based tuned controller),

5.2254 (MOGA based tuned controller), 3.7393 (SOPSO based tuned controller) and 5.6939 (MOPSO based tuned controller). Motor power factor is improved from 0.7516 (without the GP-SF-SS device), 0.8685 (constant gains controller), 0.8909 (ANN controller) and 0.8837 (FLC) to around 0.9440 (SOGA based tuned controller), 0.9623 (MOGA based tuned controller), 0.9444 (SOPSO based tuned controller) and 0.9518 (MOPSO based tuned controller). Reduction in KWh Consumption (%) is reduced from 0.000 (without the GP-SF-SS device), 12.8652 (constant gains controller), 12.6386 (ANN controller) and 12.2319 (FLC) to around 16.2051 (SOGA based tuned controller), 16.0151 (MOGA based tuned controller), 16.8778 (SOPSO) based tuned controller and 17.4786 (MOPSO based tuned controller).

Self tuned zonal activation or target practice controller:

Table 27 shows the system behavior using traditional controllers with constant controller gains for the (GP-SF-SS) eight schemes. In addition, Table 28 shows system behavior comparison using the SOGA based the self tuned zonal activation or target practice controller and Table 29 shows the system behavior comparison using the MOGA based the self tuned zonal activation or target practice controller.

Finally, Table 30 and 31 show system behavior comparison using the SOPSO and MOPSO, respectively based the self tuned zonal activation or target practice controller.

Comparing the system dynamic response results of the two study cases, with GA and PSO tuning algorithms and traditional controllers with constant controller gains results, ANN controller and FLC, it is quite apparent that the GA and PSO tuning algorithms highly improved the system dynamic performance from a

Table 28: System dynamic behavior comparison using the SOGA based tuned zonal activation or target practice controller

| Items | GP-SF-SS scheme A | GP-SF-SS scheme B | GP-SF-SS scheme C | GP-SF-SS scheme D | GP-SF-SS scheme E | GP-SF-SS scheme F | GP-SF-SS scheme G | GP-SF-SS scheme H |
|--|----------------------|----------------------|----------------------|----------------------|----------------------|----------------------|----------------------|----------------------|
| RMS motor voltage (PU) | 0.9844 | 0.9928 | 0.9942 | 0.9804 | 0.9783 | 0.9929 | 0.9799 | 0.9882 |
| RMS motor current (PU) | 0.5857 | 0.6038 | 0.6700 | 0.5991 | 0.6249 | 0.6061 | 0.6405 | 0.6662 |
| Maximum transient voltage over/under shoot (PU) | 0.0432 | 0.0488 | 0.0417 | 0.0436 | 0.0285 | 0.0273 | 0.0292 | 0.0417 |
| Maximum transient current over/under shoot (PU) | 0.0490 | 0.0396 | 0.0370 | 0.0454 | 0.0442 | 0.0404 | 0.0405 | 0.0447 |
| System efficiency | 0.9255 | 0.9443 | 0.9356 | 0.9341 | 0.9337 | 0.9498 | 0.9173 | 0.9320 |
| NMSE_V $\times 10^{-2}$ | 0.9344 | 0.4085 | 0.5162 | 0.8464 | 0.2071 | 0.4482 | 0.8398 | 0.7426 |
| NMSE_ $\omega_m \times 10^{-2}$ | 0.7623 | 0.3127 | 0.7577 | 0.3099 | 0.5050 | 0.1420 | 0.5591 | 0.4524 |
| NMSE_I $\times 10^{-2}$ | 0.8792 | 0.2581 | 0.1329 | 0.6171 | 0.5983 | 0.6088 | 0.4031 | 0.5892 |
| THDv_bus L (%) | 3.8914 | 4.3280 | 5.3682 | 3.8706 | 5.0285 | 3.2328 | 5.1433 | 4.3478 |
| THDi_bus L (%) | 5.2460 | 3.5087 | 3.6048 | 4.3353 | 3.2326 | 4.7089 | 3.5619 | 5.6653 |
| THDv_bus M (%) | 3.0758 | 4.4593 | 5.4804 | 5.2800 | 5.2819 | 3.5764 | 5.0420 | 3.6299 |
| THDi_bus M (%) | 4.7253 | 3.1828 | 3.2255 | 4.8194 | 5.5000 | 4.2307 | 5.0251 | 3.2203 |
| Motor power factor | 0.9378 | 0.9483 | 0.9311 | 0.9332 | 0.9392 | 0.9143 | 0.9645 | 0.9283 |
| Reduction in KWh consumption (%) | 16.1557 | 18.0242 | 17.2037 | 16.8814 | 17.0676 | 16.7003 | 16.9005 | 16.4818 |

Table 29: System dynamic behavior comparison using a selected solution from the MOGA Pareto front based tuned zonal activation or target practice controller

| Items | GP-SF-SS scheme A | GP-SF-SS scheme B | GP-SF-SS scheme C | GP-SF-SS scheme D | GP-SF-SS scheme E | GP-SF-SS scheme F | GP-SF-SS scheme G | GP-SF-SS scheme H |
|--|----------------------|----------------------|----------------------|----------------------|----------------------|----------------------|----------------------|----------------------|
| RMS motor voltage (PU) | 0.9948 | 0.9886 | 0.9928 | 0.9752 | 0.9778 | 0.9918 | 0.9838 | 0.9933 |
| RMS motor current (PU) | 0.6338 | 0.6654 | 0.6060 | 0.6600 | 0.5891 | 0.5859 | 0.6011 | 0.6640 |
| Maximum transient voltage over/under shoot (PU) | 0.0292 | 0.0270 | 0.0474 | 0.0253 | 0.0222 | 0.0321 | 0.0413 | 0.0466 |
| Maximum transient current over/under shoot (PU) | 0.0384 | 0.0262 | 0.0307 | 0.0283 | 0.0221 | 0.0329 | 0.0399 | 0.0242 |
| System efficiency | 0.9250 | 0.9612 | 0.9347 | 0.9145 | 0.9599 | 0.9638 | 0.9468 | 0.9505 |
| NMSE_V $\times 10^{-2}$ | 0.4511 | 0.9186 | 0.8596 | 0.9551 | 0.4457 | 0.8968 | 0.5022 | 0.6763 |
| NMSE_ $\omega_m \times 10^{-2}$ | 0.5567 | 0.9504 | 0.8794 | 0.6495 | 0.4077 | 0.3728 | 0.8807 | 0.2028 |
| NMSE_I $\times 10^{-2}$ | 0.3647 | 0.8383 | 0.7341 | 0.6602 | 0.3407 | 0.7330 | 0.8730 | 0.5469 |
| THDv_bus L (%) | 4.5209 | 4.4647 | 3.6651 | 5.6658 | 4.4858 | 4.3206 | 5.2183 | 5.0969 |
| THDi_bus L (%) | 3.6205 | 5.4286 | 5.1228 | 4.1673 | 3.8845 | 4.3628 | 3.4311 | 4.4198 |
| THDv_bus M (%) | 5.4651 | 5.0247 | 5.8447 | 5.3287 | 5.2339 | 5.1812 | 5.5810 | 3.3135 |
| THDi_bus M (%) | 4.0933 | 5.1371 | 4.2741 | 3.3043 | 5.8288 | 4.5383 | 3.4023 | 3.3931 |
| Motor power factor | 0.9299 | 0.9129 | 0.9527 | 0.9362 | 0.9142 | 0.9171 | 0.9627 | 0.9442 |
| Reduction in KWh consumption (%) | 16.3008 | 16.0484 | 17.8331 | 16.4275 | 16.6290 | 17.3628 | 16.6000 | 16.9739 |

general power quality point of view. The GA and PSO tuning algorithms had a great impact on Motor RMS voltage (PU) is improved from 0.8782 (without the GP-SF-SS device), 0.9382 (constant gains controller), 0.9414 (ANN controller) and 0.9525 (FLC) to around 0.9844 (SOGA based tuned controller), 0.9948 (MOGA based tuned controller), 0.9901 (SOPSO) based tuned controller and 0.9851 (MOPSO based tuned controller).

Motor RMS current (PU) is reduced from 0.8576 (without the GP-SF-SS device), 0.7499 (constant gains controller), 0.7269 (ANN controller) and 0.7158 (FLC) to around 0.5857 (SOGA based tuned controller), 0.6338 (MOGA based tuned controller), 0.6310 (SOPSO) based tuned controller and 0.6306 (MOPSO based tuned controller). Maximum Transient Motor Voltage Over/Under Shoot (PU) is reduced from 0.1597 (without the GP-SF-SS device), 0.0959 (constant gains controller), 0.0888 (ANN controller) and 0.0949 (FLC) to around 0.0432

(SOGA based tuned controller), 0.0292 (MOGA based tuned controller), 0.0477 (SOPSO) based tuned controller and 0.0264 (MOPSO based tuned controller). Maximum Transient Motor Current-Over/Under Shoot (PU) is reduced from 0.1775 (without the GP-SF-SS device), 0.0907 (constant gains controller), 0.0859 (ANN controller) and 0.0928 (FLC) to around 0.0490 (SOGA based tuned controller), 0.0384 (MOGA based tuned controller), 0.0271 (SOPSO) based tuned controller and 0.0392 (MOPSO based tuned controller).

The system efficiency is improved from 0.8145 (without the GP-SF-SS device), 0.8673 (constant gains controller), 0.9012 (ANN controller) and 0.8788 (FLC) to around 0.9255 (SOGA based tuned controller), 0.9250 (MOGA based tuned controller), 0.9263 (SOPSO) based tuned controller and 0.9162 (MOPSO based tuned controller). Moreover, the Normalized Mean Square Error (NMSE-V) of the motor voltage is reduced from 0.3293

Table 30: System dynamic behavior comparison using the SOPSO based tuned zonal activation or target practice controller

| Items | GP-SF-SS scheme A | GP-SF-SS scheme B | GP-SF-SS scheme C | GP-SF-SS scheme D | GP-SF-SS scheme E | GP-SF-SS scheme F | GP-SF-SS scheme G | GP-SF-SS scheme H |
|--|----------------------|----------------------|----------------------|----------------------|----------------------|----------------------|----------------------|----------------------|
| RMS motor voltage (PU) | 0.9901 | 0.9891 | 0.9821 | 0.9784 | 0.9782 | 0.9789 | 0.9837 | 0.9925 |
| RMS motor current (PU) | 0.6310 | 0.5910 | 0.6270 | 0.5905 | 0.6493 | 0.6138 | 0.6541 | 0.5842 |
| Maximum transient Voltage over/under shoot (PU) | 0.0477 | 0.0327 | 0.0361 | 0.0244 | 0.0225 | 0.0263 | 0.0453 | 0.0463 |
| Maximum transient current Over/under shoot (PU) | 0.0271 | 0.0494 | 0.0417 | 0.0461 | 0.0352 | 0.0357 | 0.0299 | 0.0236 |
| System efficiency | 0.9263 | 0.9343 | 0.9490 | 0.9553 | 0.9557 | 0.9333 | 0.9465 | 0.9200 |
| NMSE_V $\times 10^{-2}$ | 0.5837 | 0.8633 | 0.8423 | 0.6233 | 0.5233 | 0.1221 | 0.3497 | 0.6017 |
| NMSE_ $\omega_m \times 10^{-2}$ | 0.8182 | 0.7129 | 0.4035 | 0.4548 | 0.5716 | 0.2737 | 0.4827 | 0.4605 |
| NMSE_I $\times 10^{-2}$ | 0.2873 | 0.3622 | 0.3304 | 0.3785 | 0.5799 | 0.8206 | 0.3657 | 0.8602 |
| THDv_bus L (%) | 4.9241 | 3.9995 | 5.7948 | 4.0228 | 3.0770 | 5.3202 | 5.8011 | 3.9037 |
| THDi_bus L (%) | 5.8456 | 4.9748 | 5.7395 | 5.2148 | 3.0239 | 3.9422 | 4.5605 | 3.8886 |
| THDv_bus M (%) | 4.4285 | 3.3007 | 4.5897 | 4.2539 | 3.5344 | 3.4568 | 5.6623 | 3.4072 |
| THDi_bus M (%) | 5.1721 | 5.2724 | 3.9094 | 3.6887 | 4.4201 | 4.9596 | 5.6931 | 4.2641 |
| Motor power factor | 0.9174 | 0.9293 | 0.9257 | 0.9325 | 0.9595 | 0.9526 | 0.9248 | 0.9360 |
| Reduction in KWh consumption (%) | 17.0819 | 17.8053 | 16.3745 | 18.0068 | 16.5738 | 16.5351 | 17.7964 | 17.5163 |

Table 31: System dynamic behavior comparison using a selected solution from the MOPSO Pareto front based tuned zonal activation or target practice controller

| Items | GP-SF-SS scheme A | GP-SF-SS scheme B | GP-SF-SS scheme C | GP-SF-SS scheme D | GP-SF-SS scheme E | GP-SF-SS scheme F | GP-SF-SS scheme G | GP-SF-SS scheme H |
|--|----------------------|----------------------|----------------------|----------------------|----------------------|----------------------|----------------------|----------------------|
| RMS motor voltage (PU) | 0.9851 | 0.9917 | 0.9844 | 0.9844 | 0.9842 | 0.9835 | 0.9935 | 0.9751 |
| RMS motor current (PU) | 0.6306 | 0.6087 | 0.6137 | 0.6581 | 0.6135 | 0.5866 | 0.5980 | 0.5845 |
| Maximum transient voltage over/under shoot (PU) | 0.0264 | 0.0306 | 0.0227 | 0.0318 | 0.0226 | 0.0439 | 0.0496 | 0.0249 |
| Maximum transient current over/under shoot (PU) | 0.0392 | 0.0255 | 0.0305 | 0.0256 | 0.0281 | 0.0329 | 0.0256 | 0.0286 |
| System efficiency | 0.9162 | 0.9279 | 0.9214 | 0.9499 | 0.9538 | 0.9295 | 0.9534 | 0.9531 |
| NMSE_V $\times 10^{-2}$ | 0.7559 | 0.3893 | 0.3321 | 0.7382 | 0.4850 | 0.3784 | 0.8828 | 0.7048 |
| NMSE_ $\omega_m \times 10^{-2}$ | 0.7575 | 0.3393 | 0.6333 | 0.2588 | 0.2414 | 0.6953 | 0.2978 | 0.7634 |
| NMSE_I $\times 10^{-2}$ | 0.1690 | 0.3168 | 0.4140 | 0.6303 | 0.4641 | 0.6375 | 0.4803 | 0.4667 |
| THDv_bus L (%) | 4.7073 | 4.3480 | 5.0503 | 5.4506 | 3.5467 | 4.3294 | 5.5762 | 3.0844 |
| THDi_bus L (%) | 5.7041 | 4.9754 | 4.7624 | 5.5527 | 3.0573 | 3.8728 | 5.7509 | 3.3106 |
| THDv_bus M (%) | 4.7636 | 3.7811 | 5.8248 | 5.1719 | 4.3853 | 5.6947 | 4.0420 | 3.2605 |
| THDi_bus M (%) | 3.6998 | 4.4071 | 4.2197 | 5.2719 | 5.1806 | 3.6974 | 4.8178 | 3.6766 |
| Motor power factor | 0.9133 | 0.9289 | 0.9146 | 0.9315 | 0.9322 | 0.9297 | 0.9592 | 0.9245 |
| Reduction in KWh consumption (%) | 16.7740 | 17.4464 | 17.1304 | 16.9247 | 17.4298 | 17.2816 | 17.6327 | 17.9605 |

(without the GP-SF-SS device), 0.06263 (constant gains controller), 0.03378 (ANN controller) and 0.04076 (FLC) to around 0.009344 (SOGA based tuned controller), 0.004511 (MOGA based tuned controller), 0.005837 (SOPSO) based tuned controller and 0.007559 (MOPSO based tuned controller). In addition the NMSE- ω_m of the SPIM motor is reduced from 0.5093 (without the GP-SF-SS device), 0.08417 (constant gains controller), 0.06218 (ANN controller) and 0.07776 (FLC) to around 0.007623 (SOGA based tuned controller), 0.005567 (MOGA based tuned controller), 0.8182 (SOPSO) based tuned controller and 0.007575 (MOPSO based tuned controller). The NMSE-I of the Motor current is reduced from 0.2398 (without the GP-SF-SS device), 0.01299 (constant gains controller), 0.02170 (ANN controller) and 0.04893 (FLC) to around 0.008792 (SOGA based tuned controller), 0.003647 (MOGA based tuned controller), 0.002873 (SOPSO) based tuned controller and 0.001690 (MOPSO based tuned controller). Total Harmonic Distortion (THD) (%) of the

supply voltage is reduced from 17.486 (without the GP-SF-SS device), 6.6196 (constant gains controller), 8.0866 (ANN controller) and 8.4756 (FLC) to around 3.8914 (SOGA based tuned controller), 4.5209 (MOGA based tuned controller), 4.9241 (SOPSO) based tuned controller and 4.7073 (MOPSO based tuned controller). THD (%) of the supply current is reduced from 19.475 (without the GP-SF-SS device), 9.6328 (constant gains controller), 8.8441 (ANN controller) and 7.5479 (FLC) to around 5.2460 (SOGA based tuned controller), 3.6205 (MOGA based tuned controller), 5.8456 (SOPSO) based tuned controller and 5.7041 (MOPSO based tuned controller).

THD (%) of the motor voltage is reduced from 16.456 (without the GP-SF-SS device), 6.2423 (constant gains controller), 7.7610 (ANN controller) and 6.2888 (FLC) to around 3.0758 (SOGA based tuned controller), 5.4651 (MOGA based tuned controller), 4.4285 (SOPSO) based tuned controller and 4.7636 (MOPSO based tuned controller). THD (%) of the motor current is reduced from

18.465 (without the GP-SF-SS device), 8.2256 (constant gains controller), 8.4061 (ANN controller) and 9.3727 (FLC) to around 4.7253 (SOGA based tuned controller), 4.0933 (MOGA based tuned controller), 5.1721 (SOPSO) based tuned controller and 3.6998 (MOPSO based tuned controller). Motor power factor is improved from 0.7516 (without the GP-SF-SS device), 0.8950 (constant gains controller), 0.8909 (ANN controller) and 0.8837 (FLC) to around 0.9378 (SOGA based tuned controller), 0.9299 (MOGA based tuned controller), 0.9174 (SOPSO) based tuned controller and 0.9133 (MOPSO based tuned controller).

Reduction in KWh Consumption (%) is reduced from 0.000 (without the GP-SF-SS device), 13.8356 (constant gains controller), 13.6386 (ANN controller) and 13.2319 (FLC) to around 16.2601 (SOGA based tuned controller), 16.7016 (MOGA based tuned controller), 16.8207 (SOPSO) based tuned controller and 17.4587 (MOPSO based tuned controller).

Self tuned tan-sigmoid incremental integral action controller: Table 32 shows the system behavior using traditional controllers with constant controller gains for the (GP-SF-SS) eight schemes. In addition, Table 33 shows system behavior comparison using the SOGA based the self tuned tan-sigmoid incremental integral action controller and Table 34 shows the system behavior comparison using the MOGA based the self tuned tan-sigmoid incremental integral action controller.

Finally, Tables 35 and 36 show system behavior comparison using the SOPSO and MOPSO, respectively based the self tuned tan-sigmoid incremental integral action controller. Comparing the system dynamic response results of the two study cases, with GA and PSO tuning algorithms and traditional controllers with

constant controller gains results, ANN controller and FLC, it is quite apparent that the GA and PSO tuning algorithms highly improved the system dynamic performance from a general power quality point of view. The GA and PSO tuning algorithms had a great impact on Motor RMS voltage (PU) is improved from 0.8782 (without the GP-SF-SS device), 0.9339 (constant gains controller), 0.9414 (ANN controller) and 0.9525 (FLC) to around 0.9878 (SOGA based tuned controller), 0.9923 (MOGA based tuned controller), 0.9798 (SOPSO) based tuned controller and 0.9831 (MOPSO based tuned controller). Motor RMS current (PU) is reduced from 0.8576 (without the GP-SF-SS device), 0.7141 (constant gains controller), 0.7269 (ANN controller) and 0.7158 (FLC) to around 0.5918 (SOGA based tuned controller), 0.6672 (MOGA based tuned controller), 0.6000 (SOPSO) based tuned controller and 0.6567 (MOPSO based tuned controller). Maximum Transient Motor Voltage Over/Under Shoot (PU) is reduced from 0.1597 (without the (GP-SF-SS) device), 0.0941 (constant gains controller), 0.0888 (ANN controller) and 0.0949 (FLC) to around 0.0485 (SOGA based tuned controller), 0.0380 (MOGA based tuned controller), 0.0484 (SOPSO) based tuned controller and 0.0482 (MOPSO based tuned controller). Maximum Transient Motor Current-Over/Under Shoot (PU) is reduced from 0.1775 (without the GP-SF-SS device), 0.0945 (constant gains controller), 0.0859 (ANN controller) and 0.0928 (FLC) to around 0.0221 (SOGA based tuned controller), 0.0434 (MOGA based tuned controller), 0.0293 (SOPSO) based tuned controller and 0.0279 (MOPSO based tuned controller). The system efficiency is improved from 0.8145 (without the GP-SF-SS device), 0.8585 (constant gains controller), 0.9012 (ANN controller) and 0.8788 (FLC) to around 0.9514 (SOGA based tuned controller), 0.9399

Table 32: System dynamic behavior comparison using the constant parameters tan-sigmoid incremental integral action controller

| Items | GP-SF-SS scheme A | GP-SF-SS scheme B | GP-SF-SS scheme C | GP-SF-SS scheme D | GP-SF-SS scheme E | GP-SF-SS scheme F | GP-SF-SS scheme G | GP-SF-SS scheme H |
|--|----------------------|----------------------|----------------------|----------------------|----------------------|----------------------|----------------------|----------------------|
| RMS motor voltage (PU) | 0.9339 | 0.9265 | 0.9458 | 0.9445 | 0.9545 | 0.9416 | 0.9370 | 0.9310 |
| RMS motor current (PU) | 0.7141 | 0.6575 | 0.6830 | 0.7139 | 0.6684 | 0.7152 | 0.6758 | 0.7117 |
| Maximum transient voltage over/under shoot (PU) | 0.0941 | 0.0899 | 0.0894 | 0.0913 | 0.0920 | 0.0942 | 0.0943 | 0.0911 |
| Maximum transient current over/under shoot (PU) | 0.0945 | 0.0909 | 0.0880 | 0.0921 | 0.0931 | 0.0932 | 0.0961 | 0.0942 |
| System efficiency | 0.8585 | 0.8803 | 0.8965 | 0.8646 | 0.8530 | 0.8597 | 0.8771 | 0.8985 |
| NMSE _V $\times 10^{-1}$ | 0.7225 | 0.8596 | 0.3356 | 0.1378 | 0.6607 | 0.8153 | 0.7761 | 0.5173 |
| NMSE _{ω_m} $\times 10^{-1}$ | 0.8313 | 0.3188 | 0.4275 | 0.9348 | 0.5120 | 0.5665 | 0.1580 | 0.6427 |
| NMSE _I $\times 10^{-1}$ | 0.6793 | 0.7598 | 0.6881 | 0.3909 | 0.9516 | 0.5489 | 0.8092 | 0.4484 |
| THDv _{bus L} (%) | 9.7466 | 9.5541 | 9.6917 | 8.1775 | 9.6603 | 7.2400 | 7.0397 | 6.2557 |
| THDi _{bus L} (%) | 7.2956 | 7.1412 | 7.5625 | 6.1524 | 7.1222 | 6.8625 | 8.1881 | 9.3524 |
| THDv _{bus M} (%) | 6.9979 | 8.2872 | 8.0226 | 6.5162 | 6.0363 | 7.2690 | 7.4028 | 9.8268 |
| THDi _{bus M} (%) | 9.6199 | 7.6837 | 9.6028 | 7.9236 | 9.7389 | 9.6877 | 8.7807 | 8.5021 |
| Motor power factor | 0.8977 | 0.9048 | 0.8921 | 0.8989 | 0.8714 | 0.8899 | 0.8670 | 0.8938 |
| Reduction in KWh consumption (%) | 13.1976 | 12.8086 | 12.0070 | 12.3581 | 12.8105 | 13.9594 | 13.4968 | 12.5835 |

Table 33: System dynamic behavior comparison using the SOGA based tuned tan-sigmoid incremental integral action controller

| Items | GP-SF-SS scheme A | GP-SF-SS scheme B | GP-SF-SS scheme C | GP-SF-SS scheme D | GP-SF-SS scheme E | GP-SF-SS scheme F | GP-SF-SS scheme G | GP-SF-SS scheme H |
|--|----------------------|----------------------|----------------------|----------------------|----------------------|----------------------|----------------------|----------------------|
| RMS motor voltage (PU) | 0.9878 | 0.9900 | 0.9827 | 0.9752 | 0.9836 | 0.9905 | 0.9913 | 0.9939 |
| RMS motor current (PU) | 0.5918 | 0.6647 | 0.6432 | 0.6563 | 0.5988 | 0.6210 | 0.5873 | 0.6566 |
| Maximum transient voltage over/under shoot (PU) | 0.0485 | 0.0408 | 0.0234 | 0.0385 | 0.0328 | 0.0278 | 0.0269 | 0.0240 |
| Maximum transient current over/under shoot (PU) | 0.0221 | 0.0438 | 0.0224 | 0.0463 | 0.0317 | 0.0419 | 0.0488 | 0.0262 |
| System efficiency | 0.9514 | 0.9378 | 0.9464 | 0.9141 | 0.9296 | 0.9349 | 0.9171 | 0.9480 |
| NMSE_V $\times 10^{-2}$ | 0.5229 | 0.7285 | 0.6060 | 0.3016 | 0.3046 | 0.4150 | 0.6596 | 0.6604 |
| NMSE_ $\omega_m \times 10^{-2}$ | 0.1563 | 0.9586 | 0.4427 | 0.3670 | 0.3230 | 0.1548 | 0.5847 | 0.6571 |
| NMSE_I $\times 10^{-2}$ | 0.2935 | 0.3050 | 0.1686 | 0.5785 | 0.4108 | 0.1625 | 0.6638 | 0.9420 |
| THDv_bus L (%) | 5.3448 | 5.3765 | 4.8314 | 3.4636 | 5.2365 | 5.0901 | 4.6188 | 5.0674 |
| THDi_bus L (%) | 3.2508 | 5.4138 | 5.0533 | 5.4832 | 5.4882 | 5.1754 | 4.9150 | 5.5726 |
| THDv_bus M (%) | 5.3376 | 3.2178 | 5.7244 | 3.9192 | 3.0366 | 5.1708 | 3.8947 | 5.0445 |
| THDi_bus M (%) | 5.2257 | 4.7685 | 4.8578 | 5.1605 | 3.4399 | 4.7170 | 5.5630 | 3.5081 |
| Motor power factor | 0.9164 | 0.9375 | 0.9567 | 0.9366 | 0.9437 | 0.9229 | 0.9393 | 0.9202 |
| Reduction in KWh consumption (%) | 16.7165 | 16.6108 | 16.7149 | 17.1051 | 17.4957 | 16.6504 | 17.7210 | 17.1739 |

Table 34: System dynamic behavior comparison using a selected solution from the MOGA Pareto front based tuned tan-sigmoid incremental integral action controller

| Items | GP-SF-SS scheme A | GP-SF-SS scheme B | GP-SF-SS scheme C | GP-SF-SS scheme D | GP-SF-SS scheme E | GP-SF-SS scheme F | GP-SF-SS scheme G | GP-SF-SS scheme H |
|--|----------------------|----------------------|----------------------|----------------------|----------------------|----------------------|----------------------|----------------------|
| RMS motor voltage (PU) | 0.9923 | 0.9825 | 0.9877 | 0.9900 | 0.9790 | 0.9935 | 0.9867 | 0.9880 |
| RMS motor current (PU) | 0.6672 | 0.6120 | 0.5844 | 0.6480 | 0.6605 | 0.6058 | 0.6026 | 0.6639 |
| Maximum transient voltage over/under shoot (PU) | 0.0380 | 0.0463 | 0.0427 | 0.0324 | 0.0420 | 0.0264 | 0.0485 | 0.0273 |
| Maximum transient current over/under shoot (PU) | 0.0434 | 0.0389 | 0.0264 | 0.0227 | 0.0299 | 0.0489 | 0.0483 | 0.0282 |
| System efficiency | 0.9399 | 0.9300 | 0.9155 | 0.9259 | 0.9647 | 0.9323 | 0.9536 | 0.9580 |
| NMSE_V $\times 10^{-2}$ | 0.5330 | 0.4638 | 0.9481 | 0.5785 | 0.6903 | 0.5463 | 0.8194 | 0.8086 |
| NMSE_ $\omega_m \times 10^{-2}$ | 0.2997 | 0.1899 | 0.4980 | 0.7655 | 0.3363 | 0.9166 | 0.5075 | 0.5294 |
| NMSE_I $\times 10^{-2}$ | 0.7327 | 0.8908 | 0.5843 | 0.4930 | 0.7583 | 0.7018 | 0.6255 | 0.2162 |
| THDv_bus L (%) | 4.0008 | 3.5197 | 3.2138 | 3.8968 | 3.9685 | 4.0856 | 5.7145 | 5.0560 |
| THDi_bus L (%) | 4.4022 | 4.4996 | 5.2333 | 4.6937 | 3.3793 | 3.3321 | 4.8964 | 5.8414 |
| THDv_bus M (%) | 3.0317 | 3.6635 | 5.7888 | 5.4573 | 3.0625 | 4.3955 | 4.1994 | 5.2075 |
| THDi_bus M (%) | 5.3838 | 5.7651 | 3.4035 | 3.7316 | 5.5952 | 4.9348 | 4.7840 | 4.4703 |
| Motor power factor | 0.9501 | 0.9617 | 0.9123 | 0.9428 | 0.9414 | 0.9485 | 0.9523 | 0.9556 |
| Reduction in KWh consumption (%) | 17.7517 | 17.2255 | 17.0292 | 17.8450 | 17.6869 | 17.3294 | 17.6795 | 17.3604 |

(MOGA based tuned controller), 0.9287 (SOPSO) based tuned controller and 0.9592 (MOPSO based tuned controller). Moreover, the Normalized Mean Square Error (NMSE-V) of the Motor voltage is reduced from 0.3293 (without the GP-SF-SS device), 0.07225 (constant gains controller), 0.03378 (ANN controller) and 0.04076 (FLC) to around 0.005229 (SOGA based tuned controller), 0.005330 (MOGA based tuned controller), 0.004453 (SOPSO) based tuned controller and 0.002398 (MOPSO based tuned controller). In addition the (NMSE- ω_m) of the SPIM motor is reduced from 0.5093 (without the (GP-SF-SS) device), 0.08313 (constant gains controller), 0.06218 (ANN controller) and 0.07776 (FLC) to around 0.001563 (SOGA based tuned controller), 0.002997 (MOGA based tuned controller), 0.3387 (SOPSO) based tuned controller and 0.008440 (MOPSO based tuned controller).

The NMSE-I of the motor current is reduced from 0.2398 (without the GP-SF-SS device), 0.06793 (constant gains controller), 0.02170 (ANN controller) and 0.04893

(FLC) to around 0.002935 (SOGA based tuned controller), 0.007327 (MOGA based tuned controller), 0.3279 (SOPSO) based tuned controller and 0.006582 (MOPSO based tuned controller).

Total Harmonic Distortion (THD) (%) of the supply voltage is reduced from 17.486 (without the GP-SF-SS device), 9.7466 (constant gains controller), 8.0866 (ANN controller) and 8.4756 (FLC) to around 5.3448 (SOGA based tuned controller), 4.0008 (MOGA based tuned controller), 4.1346 (SOPSO) based tuned controller and 5.0450 (MOPSO based tuned controller). THD (%) of the supply current is reduced from 19.475 (without the GP-SF-SS device), 7.2956 (constant gains controller), 8.8441 (ANN controller) and 7.5479 (FLC) to around 3.2508 (SOGA based tuned controller), 4.4022 (MOGA based tuned controller), 5.8108 (SOPSO) based tuned controller and 3.2818 (MOPSO based tuned controller). THD (%) of the motor voltage is reduced from 16.456 (without the GP-SF-SS device), 6.9979 (constant gains controller), 7.7610

Table 35: System dynamic behavior comparison using the SOPSO based tuned tan-sigmoid incremental integral action controller

| Items | GP-SF-SS scheme A | GP-SF-SS scheme B | GP-SF-SS scheme C | GP-SF-SS scheme D | GP-SF-SS scheme E | GP-SF-SS scheme F | GP-SF-SS scheme G | GP-SF-SS scheme H |
|--|----------------------|----------------------|----------------------|----------------------|----------------------|----------------------|----------------------|----------------------|
| RMS motor voltage (PU) | 0.9798 | 0.9863 | 0.9941 | 0.9819 | 0.9884 | 0.9830 | 0.9879 | 0.9893 |
| RMS motor current (PU) | 0.6000 | 0.6433 | 0.6270 | 0.6640 | 0.6442 | 0.6005 | 0.6205 | 0.5955 |
| Maximum transient voltage over/under shoot (PU) | 0.0484 | 0.0255 | 0.0238 | 0.0253 | 0.0265 | 0.0472 | 0.0256 | 0.0390 |
| Maximum transient current over/under shoot (PU) | 0.0293 | 0.0280 | 0.0417 | 0.0371 | 0.0480 | 0.0310 | 0.0415 | 0.0481 |
| System efficiency | 0.9287 | 0.9221 | 0.9242 | 0.9235 | 0.9161 | 0.9184 | 0.9404 | 0.9484 |
| NMSE _V $\times 10^{-2}$ | 0.4453 | 0.6888 | 0.7994 | 0.1934 | 0.3481 | 0.1419 | 0.4995 | 0.5662 |
| NMSE _{ω_m} $\times 10^{-2}$ | 0.3387 | 0.1995 | 0.5803 | 0.9102 | 0.2344 | 0.5724 | 0.2868 | 0.6031 |
| NMSE _I $\times 10^{-2}$ | 0.3279 | 0.6662 | 0.1176 | 0.1213 | 0.7383 | 0.1976 | 0.7731 | 0.7481 |
| THDv _{bus L} (%) | 4.1346 | 5.7415 | 3.1070 | 5.7188 | 5.0420 | 4.8502 | 4.2849 | 3.5157 |
| THDi _{bus L} (%) | 5.8108 | 5.5253 | 4.1667 | 4.7953 | 4.1119 | 5.4194 | 4.5117 | 5.3050 |
| THDv _{bus M} (%) | 3.7638 | 4.0936 | 3.9757 | 3.9115 | 5.7001 | 4.5352 | 5.0069 | 5.4963 |
| THDi _{bus M} (%) | 5.1561 | 3.6952 | 5.6887 | 3.2725 | 4.5574 | 5.5767 | 5.4575 | 4.8076 |
| Motor power factor | 0.9483 | 0.9636 | 0.9267 | 0.9211 | 0.9608 | 0.9257 | 0.9318 | 0.9461 |
| Reduction in KWh consumption (%) | 16.4160 | 17.4049 | 16.6372 | 17.1205 | 16.3299 | 17.4366 | 16.7901 | 17.7645 |

Table 36: System dynamic behavior comparison using a selected solution from the MOPSO Pareto front based tuned tan-sigmoid incremental integral action controller

| Items | GP-SF-SS scheme A | GP-SF-SS scheme B | GP-SF-SS scheme C | GP-SF-SS scheme D | GP-SF-SS scheme E | GP-SF-SS scheme F | GP-SF-SS scheme G | GP-SF-SS scheme H |
|--|----------------------|----------------------|----------------------|----------------------|----------------------|----------------------|----------------------|----------------------|
| RMS motor voltage (PU) | 0.9831 | 0.9835 | 0.9884 | 0.9922 | 0.9826 | 0.9837 | 0.9872 | 0.9866 |
| RMS motor current (PU) | 0.6567 | 0.6484 | 0.6655 | 0.6302 | 0.5813 | 0.6337 | 0.6535 | 0.6679 |
| Maximum transient voltage over/under shoot (PU) | 0.0482 | 0.0445 | 0.0477 | 0.0305 | 0.0293 | 0.0368 | 0.0264 | 0.0277 |
| Maximum transient current over/under shoot (PU) | 0.0279 | 0.0400 | 0.0233 | 0.0282 | 0.0404 | 0.0305 | 0.0304 | 0.0419 |
| System efficiency | 0.9592 | 0.9645 | 0.9331 | 0.9300 | 0.9287 | 0.9312 | 0.9446 | 0.9436 |
| NMSE _V $\times 10^{-2}$ | 0.2398 | 0.1248 | 0.1557 | 0.4391 | 0.4864 | 0.1424 | 0.8244 | 0.7792 |
| NMSE _{ω_m} $\times 10^{-2}$ | 0.8440 | 0.7200 | 0.6191 | 0.7520 | 0.2874 | 0.1927 | 0.3002 | 0.2484 |
| NMSE _I $\times 10^{-2}$ | 0.6582 | 0.6585 | 0.3243 | 0.2198 | 0.8071 | 0.6359 | 0.5505 | 0.1174 |
| THDv _{bus L} (%) | 5.0450 | 3.1221 | 5.7919 | 4.4286 | 5.0034 | 5.2930 | 4.4829 | 4.4434 |
| THDi _{bus L} (%) | 3.2818 | 4.7248 | 5.3759 | 3.8518 | 4.3383 | 3.1506 | 3.2643 | 4.4729 |
| THDv _{bus M} (%) | 4.4262 | 3.0417 | 3.9160 | 5.1100 | 5.2568 | 4.1538 | 4.1527 | 3.7336 |
| THDi _{bus M} (%) | 4.8837 | 3.0255 | 5.7988 | 4.1878 | 4.0048 | 4.9113 | 4.2765 | 5.3969 |
| Motor power factor | 0.9318 | 0.9392 | 0.9594 | 0.9459 | 0.9227 | 0.9155 | 0.9544 | 0.9343 |
| Reduction in KWh consumption (%) | 17.4029 | 16.7924 | 17.7075 | 17.0419 | 17.4600 | 16.8923 | 16.6409 | 16.4083 |

(ANN controller) and 6.2888 (FLC) to around 5.3376 (SOGA based tuned controller), 3.0317 (MOGA based tuned controller), 3.7638 (SOPSO) based tuned controller and 4.4262 (MOPSO based tuned controller). THD (%) of the motor current is reduced from 18.465 (without the GP-SF-SS device), 9.6199 (constant gains controller), 8.4061 (ANN controller) and 9.3727 (FLC) to around 5.2257 (SOGA based tuned controller), 5.3838 (MOGA based tuned controller), 5.1561 (SOPSO) based tuned controller and 4.8837 (MOPSO based tuned controller). Motor power factor is improved from 0.7516 (without the GP-SF-SS device), 0.8977 (constant gains controller), 0.8909 (ANN controller) and 0.8837 (FLC) to around 0.9164 (SOGA based tuned controller), 0.9501 (MOGA based tuned controller), 0.9483 (SOPSO) based tuned controller and 0.9318 (MOPSO based tuned controller).

Reduction in KWh Consumption (%) is reduced from 0.000 (without the GP-SF-SS device), 12.1976 (constant gains controller), 13.6386 (ANN controller) and 13.2319

(FLC) to around 17.9799 (SOGA based tuned controller), 17.6391 (MOGA based tuned controller), 17.5938 (SOPSO) based tuned controller and 17.8238 (MOPSO based tuned controller).

Self tuned multi-stage incremental action controller:

Table 37 shows the system behavior using traditional controllers with constant controller gains for the (GP-SF-SS) eight schemes. In addition, Table 38 shows system behavior comparison using the SOGA based the self tuned multi-stage incremental action controller and Table 39 shows the system behavior comparison using the MOGA based the self tuned multi-stage incremental action controller. Finally, Table 40 and 41 show system behavior comparison using the SOPSO and MOPSO respectively based the self tuned multi-stage incremental action controller. Comparing the system dynamic response results of the two study cases with GA and PSO tuning algorithms and traditional controllers with

Table 37: System dynamic behavior comparison using the constant parameters multi-stage incremental action controller

| Items | GP-SF-SS scheme A | GP-SF-SS scheme B | GP-SF-SS scheme C | GP-SF-SS scheme D | GP-SF-SS scheme E | GP-SF-SS scheme F | GP-SF-SS scheme G | GP-SF-SS scheme H |
|--|----------------------|----------------------|----------------------|----------------------|----------------------|----------------------|----------------------|----------------------|
| RMS motor voltage (PU) | 0.9465 | 0.9403 | 0.9483 | 0.9397 | 0.9306 | 0.9460 | 0.9545 | 0.9492 |
| RMS motor current (PU) | 0.7031 | 0.6988 | 0.7068 | 0.7489 | 0.6859 | 0.6922 | 0.6823 | 0.6932 |
| Maximum transient voltage over/under shoot (PU) | 0.0938 | 0.0952 | 0.0966 | 0.0913 | 0.0927 | 0.0944 | 0.0907 | 0.0915 |
| Maximum transient current over/under shoot (PU) | 0.0877 | 0.0872 | 0.0882 | 0.0869 | 0.0873 | 0.0908 | 0.0944 | 0.0889 |
| System efficiency | 0.8628 | 0.8747 | 0.8853 | 0.8816 | 0.8649 | 0.8867 | 0.8589 | 0.8791 |
| NMSE _V $\times 10^{-1}$ | 0.1334 | 0.8238 | 0.2414 | 0.8787 | 0.8119 | 0.5822 | 0.9541 | 0.5921 |
| NMSE _{ω_m} $\times 10^{-1}$ | 0.9611 | 0.9203 | 0.2588 | 0.4302 | 0.4102 | 0.8110 | 0.7654 | 0.6572 |
| NMSE _I $\times 10^{-1}$ | 0.7236 | 0.8603 | 0.8733 | 0.8893 | 0.6823 | 0.6743 | 0.1716 | 0.6206 |
| THDv _{bus L} (%) | 9.3237 | 6.1402 | 7.4224 | 6.3810 | 7.3028 | 6.0499 | 9.1435 | 6.1176 |
| THDi _{bus L} (%) | 7.6456 | 6.1512 | 8.6122 | 7.2772 | 8.1657 | 7.6479 | 6.5964 | 6.2682 |
| THDv _{bus M} (%) | 8.3815 | 8.4296 | 6.6980 | 7.5833 | 8.7248 | 7.6670 | 6.8293 | 8.2841 |
| THDi _{bus M} (%) | 9.2265 | 9.4221 | 9.4118 | 9.7077 | 8.9679 | 7.4303 | 6.2827 | 6.4387 |
| Motor power factor | 0.8664 | 0.8831 | 0.8661 | 0.8935 | 0.8598 | 0.8929 | 0.8795 | 0.8830 |
| Reduction in KWh consumption (%) | 12.0813 | 12.6022 | 12.9933 | 13.1296 | 12.4333 | 13.6200 | 13.0986 | 12.3687 |

Table 38: System dynamic behavior comparison using the SOGA based tuned multi-stage incremental action controller

| Items | GP-SF-SS scheme A | GP-SF-SS scheme B | GP-SF-SS scheme C | GP-SF-SS scheme D | GP-SF-SS scheme E | GP-SF-SS scheme F | GP-SF-SS scheme G | GP-SF-SS scheme H |
|--|----------------------|----------------------|----------------------|----------------------|----------------------|----------------------|----------------------|----------------------|
| RMS motor voltage (PU) | 0.9894 | 0.9849 | 0.9773 | 0.9886 | 0.9825 | 0.9779 | 0.9866 | 0.9919 |
| RMS motor current (PU) | 0.6446 | 0.6312 | 0.6215 | 0.6201 | 0.5879 | 0.6199 | 0.6130 | 0.6072 |
| Maximum transient voltage over/under shoot (PU) | 0.0300 | 0.0246 | 0.0329 | 0.0311 | 0.0481 | 0.0452 | 0.0290 | 0.0231 |
| Maximum transient current over/under shoot (PU) | 0.0220 | 0.0378 | 0.0425 | 0.0443 | 0.0396 | 0.0288 | 0.0259 | 0.0400 |
| System efficiency | 0.9221 | 0.9475 | 0.9324 | 0.9156 | 0.9480 | 0.9573 | 0.9170 | 0.9327 |
| NMSE _V $\times 10^{-2}$ | 0.7376 | 0.5544 | 0.8761 | 0.8761 | 0.4977 | 0.4506 | 0.6239 | 0.9361 |
| NMSE _{ω_m} $\times 10^{-2}$ | 0.8525 | 0.7383 | 0.4283 | 0.8241 | 0.5473 | 0.8922 | 0.2278 | 0.4722 |
| NMSE _I $\times 10^{-2}$ | 0.8973 | 0.8664 | 0.7651 | 0.1978 | 0.4379 | 0.2272 | 0.8348 | 0.1598 |
| THDv _{bus L} (%) | 5.2884 | 3.6051 | 5.2068 | 5.4897 | 5.3050 | 5.1615 | 5.5799 | 4.2124 |
| THDi _{bus L} (%) | 3.8367 | 5.0997 | 4.4273 | 3.1765 | 3.5628 | 5.0708 | 5.7752 | 5.0140 |
| THDv _{bus M} (%) | 4.6016 | 5.2352 | 3.4199 | 4.5988 | 3.6028 | 5.4552 | 3.7496 | 3.8070 |
| THDi _{bus M} (%) | 5.7616 | 5.3605 | 3.3849 | 5.4036 | 5.2543 | 3.9970 | 5.1102 | 3.1901 |
| Motor power factor | 0.9648 | 0.9176 | 0.9361 | 0.9189 | 0.9492 | 0.9281 | 0.9153 | 0.9211 |
| Reduction in KWh consumption (%) | 16.9674 | 16.8716 | 17.7366 | 17.0871 | 16.4346 | 17.3845 | 17.7203 | 16.0644 |

Table 39: System dynamic behavior comparison using a selected solution from the MOGA Pareto front based tuned Multi-Stage Incremental action controller

| Items | GP-SF-SS scheme A | GP-SF-SS scheme B | GP-SF-SS scheme C | GP-SF-SS scheme D | GP-SF-SS scheme E | GP-SF-SS scheme F | GP-SF-SS scheme G | GP-SF-SS scheme H |
|--|----------------------|----------------------|----------------------|----------------------|----------------------|----------------------|----------------------|----------------------|
| RMS motor voltage (PU) | 0.9888 | 0.9955 | 0.9947 | 0.9762 | 0.9824 | 0.9862 | 0.9804 | 0.9872 |
| RMS motor current (PU) | 0.6226 | 0.6613 | 0.6206 | 0.6524 | 0.6546 | 0.5950 | 0.6155 | 0.6269 |
| Maximum transient voltage over/under shoot (PU) | 0.0274 | 0.0406 | 0.0476 | 0.0314 | 0.0384 | 0.0390 | 0.0220 | 0.0492 |
| Maximum transient current over/under shoot (PU) | 0.0469 | 0.0411 | 0.0341 | 0.0414 | 0.0388 | 0.0302 | 0.0457 | 0.0250 |
| System efficiency | 0.9344 | 0.9149 | 0.9542 | 0.9416 | 0.9528 | 0.9647 | 0.9166 | 0.9502 |
| NMSE _V $\times 10^{-2}$ | 0.4401 | 0.3441 | 0.7284 | 0.5516 | 0.5401 | 0.2528 | 0.6967 | 0.6146 |
| NMSE _{ω_m} $\times 10^{-2}$ | 0.5495 | 0.6575 | 0.6114 | 0.1795 | 0.9326 | 0.1501 | 0.5793 | 0.8413 |
| NMSE _I $\times 10^{-2}$ | 0.2884 | 0.1171 | 0.4845 | 0.2851 | 0.1622 | 0.8887 | 0.9037 | 0.8336 |
| THDv _{bus L} (%) | 4.9745 | 4.4705 | 5.8253 | 3.5424 | 4.6025 | 4.3991 | 4.1459 | 4.4155 |
| THDi _{bus L} (%) | 5.2901 | 4.2462 | 3.7039 | 4.8165 | 4.0602 | 4.2419 | 3.8756 | 4.2440 |
| THDv _{bus M} (%) | 5.3575 | 3.9766 | 3.5799 | 4.4642 | 3.6154 | 4.6619 | 5.7909 | 4.3428 |
| THDi _{bus M} (%) | 3.2045 | 3.3622 | 3.1048 | 5.4684 | 4.1931 | 5.2613 | 5.3305 | 4.1397 |
| Motor power factor | 0.9551 | 0.9377 | 0.9180 | 0.9195 | 0.9535 | 0.9261 | 0.9414 | 0.9191 |
| Reduction in KWh consumption (%) | 16.4267 | 17.2462 | 16.5753 | 16.4269 | 16.0555 | 17.5355 | 16.9251 | 17.9098 |

constant controller gains results, ANN controller and FLC, it is quite apparent that the GA and PSO tuning algorithms highly improved the system dynamic performance from a general power quality point of view.

The GA and PSO tuning algorithms had a great impact on motor RMS voltage (PU) is improved from 0.8782 (without the GP-SF-SS device), 0.9465 (constant gains controller), 0.9414 (ANN controller) and 0.9525 (FLC) to around

Table 40: System dynamic behavior comparison using the SOPSO based tuned multi-stage incremental action controller

| Items | GP-SF-SS scheme A | GP-SF-SS scheme B | GP-SF-SS scheme C | GP-SF-SS scheme D | GP-SF-SS scheme E | GP-SF-SS scheme F | GP-SF-SS scheme G | GP-SF-SS scheme H |
|--|----------------------|----------------------|----------------------|----------------------|----------------------|----------------------|----------------------|----------------------|
| RMS motor voltage (PU) | 0.9760 | 0.9867 | 0.9894 | 0.9947 | 0.9904 | 0.9902 | 0.9839 | 0.9880 |
| RMS motor current (PU) | 0.5813 | 0.6398 | 0.6452 | 0.6053 | 0.6036 | 0.6438 | 0.6505 | 0.6688 |
| Maximum transient voltage over/under shoot (PU) | 0.0296 | 0.0373 | 0.0354 | 0.0483 | 0.0283 | 0.0352 | 0.0365 | 0.0439 |
| Maximum transient current over/Under shoot (PU) | 0.0272 | 0.0472 | 0.0475 | 0.0222 | 0.0432 | 0.0482 | 0.0445 | 0.0476 |
| System efficiency | 0.9638 | 0.9342 | 0.9637 | 0.9394 | 0.9407 | 0.9320 | 0.9570 | 0.9408 |
| NMSE _V $\times 10^{-2}$ | 0.4588 | 0.3869 | 0.6361 | 0.6242 | 0.9130 | 0.3472 | 0.8454 | 0.5022 |
| NMSE _{ω_m} $\times 10^{-2}$ | 0.6239 | 0.7875 | 0.6591 | 0.7100 | 0.6362 | 0.6990 | 0.7834 | 0.9236 |
| NMSE _I $\times 10^{-2}$ | 0.8869 | 0.8738 | 0.6364 | 0.2293 | 0.8519 | 0.4789 | 0.7844 | 0.9172 |
| THD _v _bus L (%) | 4.9696 | 3.9434 | 5.6327 | 5.1629 | 4.1561 | 3.5764 | 4.1538 | 3.4587 |
| THDi _{bus} L (%) | 3.7954 | 5.6413 | 3.6857 | 3.3838 | 4.1887 | 4.8167 | 3.5352 | 4.1621 |
| THDv _{bus} M (%) | 4.5814 | 3.6308 | 4.9037 | 3.8953 | 4.3503 | 4.4522 | 4.9685 | 3.5672 |
| THDi _{bus} M (%) | 3.7586 | 3.6731 | 4.5067 | 4.6073 | 5.3577 | 3.8376 | 3.7365 | 3.7012 |
| Motor power factor | 0.9598 | 0.9397 | 0.9474 | 0.9478 | 0.9625 | 0.9450 | 0.9362 | 0.9463 |
| Reduction in KWh consumption (%) | 16.8547 | 17.8326 | 16.1417 | 16.7385 | 17.6698 | 16.0446 | 16.3056 | 16.4348 |

Table 41: System dynamic behavior comparison using a selected solution from the MOPSO Pareto front based tuned multi-stage incremental ction ontroller

| Items | GP-SF-SS scheme A | GP-SF-SS scheme B | GP-SF-SS scheme C | GP-SF-SS scheme D | GP-SF-SS scheme E | GP-SF-SS scheme F | GP-SF-SS scheme G | GP-SF-SS scheme H |
|--|----------------------|----------------------|----------------------|----------------------|----------------------|----------------------|----------------------|----------------------|
| RMS motor voltage (PU) | 0.9915 | 0.9767 | 0.9944 | 0.9938 | 0.9873 | 0.9802 | 0.9929 | 0.9855 |
| RMS motor current (PU) | 0.6057 | 0.6155 | 0.6253 | 0.6450 | 0.6076 | 0.5901 | 0.6199 | 0.6220 |
| Maximum transient voltage over/under shoot (PU) | 0.0281 | 0.0471 | 0.0221 | 0.0382 | 0.0369 | 0.0400 | 0.0306 | 0.0283 |
| Maximum transient current over/under shoot (PU) | 0.0334 | 0.0302 | 0.0406 | 0.0480 | 0.0314 | 0.0375 | 0.0252 | 0.0266 |
| System efficiency | 0.9271 | 0.9238 | 0.9433 | 0.9418 | 0.9578 | 0.9235 | 0.9279 | 0.9430 |
| NMSE _V $\times 10^{-2}$ | 0.7217 | 0.4314 | 0.6061 | 0.8761 | 0.7558 | 0.1252 | 0.5398 | 0.7257 |
| NMSE _{ω_m} $\times 10^{-2}$ | 0.3437 | 0.7327 | 0.7851 | 0.8464 | 0.1876 | 0.2789 | 0.9443 | 0.8082 |
| NMSE _I $\times 10^{-2}$ | 0.7074 | 0.2361 | 0.7185 | 0.5610 | 0.8967 | 0.2983 | 0.5994 | 0.2509 |
| THDv _{bus} L (%) | 3.1842 | 3.8447 | 4.9337 | 5.7144 | 3.1357 | 5.3452 | 3.6542 | 5.8488 |
| THDi _{bus} L (%) | 5.2700 | 3.0767 | 5.7271 | 5.4394 | 5.8110 | 3.7308 | 4.3863 | 3.9398 |
| THDv _{bus} M (%) | 3.8515 | 3.2479 | 5.6469 | 3.4935 | 4.1156 | 4.3962 | 5.3149 | 4.1691 |
| THDi _{bus} M (%) | 5.6710 | 4.4670 | 3.6193 | 4.2127 | 5.3676 | 3.4247 | 3.9314 | 5.3348 |
| Motor power factor | 0.9394 | 0.9193 | 0.9286 | 0.9576 | 0.9349 | 0.9150 | 0.9589 | 0.9255 |
| Reduction in KWh consumption (%) | 17.2697 | 17.6268 | 17.8896 | 17.5181 | 16.3812 | 16.8454 | 17.9172 | 17.8797 |

0.9894 (SOGA based tuned controller), 0.9888 (MOGA based tuned controller), 0.9760 (SOPSO) based tuned controller and 0.9915 (MOPSO based tuned controller). Motor RMS current (PU) is reduced from 0.8576 (without the GP-SF-SS device), 0.7031 (constant gains controller), 0.7269 (ANN controller) and 0.7158 (FLC) to around 0.6446 (SOGA based tuned controller), 0.6226 (MOGA based tuned controller), 0.5813 (SOPSO) based tuned controller and 0.6057 (MOPSO based tuned controller). Maximum Transient Motor Voltage Over/Under Shoot (PU) is reduced from 0.1597 (without the (GP-SF-SS) device), 0.0938 (constant gains controller), 0.0888 (ANN controller) and 0.0949 (FLC) to around 0.0300 (SOGA based tuned controller), 0.0274 (MOGA based tuned controller), 0.0296 (SOPSO) based tuned controller and 0.0281 (MOPSO based tuned controller). Maximum transient motor current-over/under shoot (PU) is reduced from 0.1775 (without the GP-SF-SS device), 0.0877 (constant gains controller), 0.0859 (ANN controller) and 0.0928 (FLC) to around 0.0220 (SOGA based tuned controller), 0.0469 (MOGA based

tuned controller), 0.0272 (SOPSO) based tuned controller and 0.0334 (MOPSO based tuned controller). The system efficiency is improved from 0.8145 (without the GP-SF-SS device), 0.8628 (constant gains controller), 0.9012 (ANN controller) and 0.8788 (FLC) to around 0.9221 (SOGA based tuned controller), 0.9344 (MOGA based tuned controller), 0.9638 (SOPSO) based tuned controller and 0.9271 (MOPSO based tuned controller). Moreover, the Normalized Mean Square Error (NMSE-V) of the Motor voltage is reduced from 0.3293 (without the GP-SF-SS device), 0.01334 (constant gains controller), 0.03378 (ANN controller) and 0.04076 (FLC) to around 0.007376 (SOGA based tuned controller), 0.004401 (MOGA based tuned controller), 0.004588 (SOPSO) based tuned controller and 0.007217 (MOPSO based tuned controller). In addition, the (NMSE- ω_m) of the SPIM motor is reduced from 0.5093 (without the GP-SF-SS device), 0.09611 (constant gains controller), 0.06218 (ANN controller) and 0.07776 (FLC) to around 0.008525 (SOGA based tuned controller), 0.005495 (MOGA based tuned controller), 0.006239 (SOPSO) based

tuned controller and 0.003437 (MOPSO based tuned controller). The (NMSE-I) of the Motor current is reduced from 0.2398 (without the GP-SF-SS device), 0.07236 (constant gains controller), 0.02170 (ANN controller) and 0.04893 (FLC) to around 0.008973 (SOGA based tuned controller), 0.002884 (MOGA based tuned controller), 0.008869 (SOPSO) based tuned controller and 0.007074 (MOPSO based tuned controller).

Total Harmonic Distortion THD (%) of the supply voltage is reduced from 17.486 (without the GP-SF-SS device), 9.3237 (constant gains controller), 8.0866 (ANN controller) and 8.4756 (FLC) to around 5.2884 (SOGA based tuned controller), 4.9745 (MOGA based tuned controller), 4.9696 (SOPSO) based tuned controller and 3.1842 (MOPSO based tuned controller). THD (%) of the supply current is reduced from 19.475 (without the GP-SF-SS device), 7.6456 (constant gains controller), 8.8441 (ANN controller) and 7.5479 (FLC) to around 3.8367 (SOGA based tuned controller), 5.2901 (MOGA based tuned controller), 3.7954 (SOPSO) based tuned controller and 5.2700 (MOPSO based tuned controller). THD (%) of the motor voltage is reduced from 16.456 (without the GP-SF-SS device), 8.3815 (constant gains controller), 7.7610 (ANN controller) and 6.2888 (FLC) to around 4.6016 (SOGA based tuned controller), 5.3575 (MOGA based tuned controller), 4.5814 (SOPSO) based tuned controller and 3.8515 (MOPSO based tuned controller). THD (%) of the motor current is reduced from 18.465 (without the GP-SF-SS device), 9.2265 (constant gains controller), 8.4061 (ANN controller) and 9.3727 (FLC) to around 5.7616 (SOGA based tuned controller), 3.2045 (MOGA based tuned controller), 3.7586 (SOPSO) based tuned controller and 5.6710 (MOPSO based tuned controller). Motor power factor is improved from 0.7516 (without the GP-SF-SS device), 0.8664 (constant gains controller), 0.8909 (ANN controller) and 0.8837 (FLC) to around 0.9648 (SOGA based tuned controller), 0.9551 (MOGA based tuned controller), 0.9598 (SOPSO) based tuned controller and 0.9394 (MOPSO based tuned controller).

Reduction in KWh Consumption (%) is reduced from 0.000 (without the GP-SF-SS device), 12.0813 (constant gains controller), 12.6386 (ANN controller) and 12.2319 (FLC) to around 16.0901 (SOGA based tuned controller), 17.6541 (MOGA based tuned controller), 16.6020 (SOPSO) based tuned controller and 17.6654 (MOPSO based tuned controller).

CONCLUSION

The study presents a family of novel low cost Green Plug electricity saving device/Smart Filter/Soft Starter (GP-SF-SS) devices developed by the First researcher and

equipped with a dynamic online error driven optimally tuned controller using a dynamic online error driven optimally tuned controllers.

The GP-SF-SS are a small low cost energy conservation devices in the form add-on dynamic switched capacitor filter compensator schemes for low horse power motors used in household appliances, washers, dryers, fans, water pumps, ventilation systems, air-conditioners and other cyclical motorized loads used in dispersing machines, actuators and small converters with induction motor size up to 5 KVA. The GP-SF-SS device uses a smart dynamic error driven tracking controller to ensure combined functions of speed reference tracking and efficient utilization. This ensures of reduced electricity consumption, efficient operation, reduced motor losses, motor extended life span, enhanced AC supply operation with minimal voltage and current excursions, harmonics, voltage sags, inrush currents and severe excursions that cause voltage flickering, notching and spikes.

The GP-SF-SS devices family can be used with all types of small horse power motors with speed control up to 5 KVA with billions of small motors used in multitude of applications that consumes over 50-60% of total electrical energy generated in the world. The GP-SF-SS device can save 10-20% of the electricity cost of operating the small motor over the estimated motor life span of 7-10 years. This translate into millions of dollars in daily electricity savings, reduced electrical utility overloading conditions, blackouts, brownouts and enhanced secure and reliable operation with additional sizable power capacity release due to reduced electric demand and feeder losses.

APPENDIX

SPIM: Nominal Power = 0.25 HP, Nominal voltage = 110 V, Nominal frequency = 60 HZ, Main Winding Stator: $R_s = 2.02 \text{ Ohm}$, $L_{ls} = 7.4 \text{ mH}$, Main winding rotor: $R_r' = 4.12 \text{ ohm}$, $L_{lr}' = 5.6 \text{ mH}$, Main winding mutual inductance: $L_{ms} = 0.177 \text{ H}$, Auxilary Winding Stator: $R_s = 7.14 \text{ Ohm}$, $L_{ls} = 8.54 \text{ mH}$, Inertia: $J = 0.0146$, Pairs of poles: $P = 2$, ratio of turns: 1.18, Capacitor start: $R_{st} = 2.15 \text{ ohm}$, $C_{st} = 255 \text{ }\mu\text{F}$, Capacitor Run: $R_{ru} = 18 \text{ ohm}$, $C_{ru} = 21.1 \text{ }\mu\text{F}$.
 GPFC-Scheme A: $R_f = 0.2 \text{ }\Omega$, $L_f = 2 \text{ mH}$, $C_f = 35 \text{ }\mu\text{F}$, $C_p = 100 \text{ }\mu\text{F}$,
 GPFC-Scheme B: $R_f = 0.3 \text{ }\Omega$, $L_f = 5 \text{ mH}$, $C_f = 45 \text{ }\mu\text{F}$, $C_p = 120 \text{ }\mu\text{F}$,
 GPFC-Scheme C: $R_f = 0.25 \text{ }\Omega$, $L_f = 3 \text{ mH}$, $C_f = 25 \text{ }\mu\text{F}$, $C_p = 90 \text{ }\mu\text{F}$,
 GPFC-Scheme D: $R_f = 0.25 \text{ }\Omega$, $L_f = 4 \text{ mH}$, $C_f = 55 \text{ }\mu\text{F}$, $C_s = 25 \text{ }\mu\text{F}$,
 GPFC-Scheme E: $C_f = 65 \text{ }\mu\text{F}$, $C_s = 35 \text{ }\mu\text{F}$,

GPFC-Scheme F: $R_1 = 0.3 \Omega$, $L_1 = 5 \text{ mH}$, $C_1 = 75 \mu\text{F}$, $R_2 = 0.2 \Omega$, $L_2 = 3 \text{ mH}$, $C_2 = 100 \mu\text{F}$,
 GPFC-Scheme G: $R_1 = 0.5 \Omega$, $L_1 = 3 \text{ mH}$, $C_1 = 85 \mu\text{F}$,
 GPFC-Scheme H: $R_1 = 0.4 \Omega$, $C_1 = 85 \mu\text{F}$, $R_2 = 0.3 \Omega$, $L_2 = 4 \text{ mH}$, $C_2 = 120 \mu\text{F}$,
 Control Weightings Scaling: $\gamma_{vs} = 0.86$, $\gamma_{is} = 0.45$, $\gamma_{ps} = 0.25$, $\gamma_{vm} = 0.92$, $\gamma_{im} = 0.54$, $\gamma_{pm} = 0.24$,
 Tuned conventional PID controller Gains: $10 \leq K_p \leq 200$, $1 \leq K_i \leq 20$, $0.1 \leq K_d \leq 10$,
 Tuned modified PID controller-I Gains: $50 \leq K_p \leq 300$, $1 \leq K_i \leq 10$, $0.1 \leq K_d \leq 5$, $1 \leq K_{es} \leq 50$,
 Tuned modified PID controller-II Gains: $50 \leq K_p \leq 300$, $1 \leq K_i \leq 10$, $0.1 \leq K_d \leq 5$, $1 \leq K_{es} \leq 100$,
 Tuned Variable structure sliding mode controller VSC/SMC/B-B Gains: $1 \leq \beta_{0s} \leq 10$, $1 \leq \beta_{1s} \leq 50$, $0.01 \leq K_{\alpha s} \leq 1$,
 Tuned Zonal Activation or Target Practice Controller Gains: $1 \leq \beta_{0s} \leq 10$, $0 \leq \beta_{1s} \leq 50$, $0.01 \leq K_{\alpha s} \leq 1$,
 Tuned Tan-sigmoid Incremental Integral Action Controller Gains: $1 \leq \beta_{0s} \leq 5$, $50 \leq K_{0s} \leq 200$,
 Tuned Multi-Stage Incremental Action Controller Gains: $1 \leq \gamma_{1s} \leq 100$, $1 \leq \gamma_{2s} \leq 100$, $1 \leq \gamma_{3s} \leq 100$, $1 \leq \gamma_{4s} \leq 100$

REFERENCES

- Berizzi, A., M. Innorta and P. Marannino, 2001. Multiobjective optimization techniques applied to modern power systems. IEEE Power Eng. Soc. Winter Meeting, 3: 1503-1508.
- Coello, C.A.C. and M.S. Lechuga, 2002. MOPSO: A proposal for multiple objective particle swarm optimization. Proceedings of the 2002 Congress on Evolutionary Computation part of the 2002 IEEE World Congress on Computational Intelligence, May, 12-17, Hawaii, pp: 1051-1056.
- Davis, L., 1991. Handbooks of Genetic Algorithm. Van Nostrand Reinhold Co., New York.
- De Rossiter Correa, M.B., C.B. Jacobina, E.R.C. da Silva and A.M.N. Lima, 2004. Vector control strategies for single-phase induction motor drive systems. IEEE Trans. Ind. Electr., 51: 1073-1080.
- Deb, K., A. Pratap, S. Agarwal and T. Meyarivan, 2002. A fast and elitist multiobjective genetic algorithm: NSGA-II. IEEE Tran. Evol. Comput., 6: 182-197.
- Kennedy, J. and R. Eberhart, 1995. Particle swarm optimization. Proc. IEEE Int. Conf. Neural Networks, 4: 1942-1948.
- Mademlis, C., I. Kioskeridis and T. Theodoulidis, 2005. Optimization of single-phase induction Motors-part I: Maximum energy efficiency control. IEEE Trans. Energy Convers., 20: 187-195.
- Neri, A.L., A.C.C. Lyra and Y. Burian, 2005. New topology supply for the single-phase induction motor: A simple soft starter. Power Tech, 2005 IEEE Russia, pp: 1-8.
- Ngatchou, P., A. Zarei and A. El-Sharkawi, 2005. Pareto multi objective optimization. Proceedings of the 13th International Conference on Intelligent Systems Application to Power Systems, Nov. 6-10, Arlington, VA., pp: 84-91.
- Poirier, E., M. Ghribi and A. Kaddouri, 2001. Losses minimization control of induction motor drives based on genetic algorithms. Electric Machines Drives Conf., 2001: 475-478.
- Sharaf, A.M. and A. Aljankawey, 2006. Voltage stabilization using a facts modulated power filter. IEEE Int. Symp. Ind. Electronics, 3: 1937-1942.
- Sharaf, A.M. and P. Kreidi, 2002. Dynamic compensation using switched/modulated power filters. Can. Conf. Electrical Comput. Eng., 1: 230-235.
- Sharaf, A.M. and R. Chalet, 1998. A low cost on-off modulated power filter for single phase motorized loads. IEEE Can. Conf. Electrical Comput. Eng., 2: 862-865.
- Sharaf, A.M., C. Guo and H. Huang, 2000. A smart PWM switched power filter for single phase nonlinear loads. Can. Conf. Electrical Comput. Eng., 2: 932-935.
- Sharaf, A.M., Guo, C. and H. Huang, 1998. A smart PWM-modulated power filter for single phase motorized loads. IEEE Can. Conf. Electrical Comput. Eng., 2: 778-781.
- Shenoy, T.P. and J.S. Nirody, 2006. Design and development of a high performance electronic starter for single-phase induction motors. Proceedings of the International Conference on Power Electronics, Dec. 1-5, Drives and Energy Systems, pp: 12-15.
- Shi, Y. and R.C. Eberhart, 1999. Empirical study of particle swarm optimization. Proceeding of the IEEE International Conference on Evolutionary Computer, July 6-9, Washington, DC., USA., pp: 1945-1950.
- Srinivas, N. and K. Deb, 1994. Multiobjective optimization using nondominated sorting in genetic algorithms. Evolut. Comput., 2: 221-248.
- Zahedi, B. and S. Vaez-Zadeh, 2009. Efficiency optimization control of single-phase induction motor drives. IEEE Trans. Power Electr., 24: 1062-1070.